Diplomarbeit

Dynamics of Intraabdominal and Intrauterine Pressures During Amnioreduction

eingereicht von

Maximilian Philipp Pohl, B.Sc.

zur Erlangung des akademischen Grades

Doktor der gesamten Heilkunde

(Dr. med. univ.)

an der

Medizinischen Universität Graz

ausgeführt am

Lehrstuhl für Physiologie

unter der Anleitung von

ao. Prof. Dr. Daniel Schneditz & Dr. med. univ. Patrick Greimel

Graz, am 8.5.2021

Eidesstattliche Erklärung

Ich erkläre ehrenwörtlich, dass ich die vorliegende Arbeit selbstständig und ohne fremde Hilfe verfasst habe, andere als die angegebenen Quellen nicht verwendet habe und die den benutzten Quellen wörtlich oder inhaltlich entnommenen Stellen als solche kenntlich gemacht habe.

Graz, am 8.5.2021 Maximilian Pohl eh

Contents

Abbreviations

AA arterio-arterial

ACS abdominal compartment syndrome

ANP atrial natriuretic peptide

AV arterio-venous

BAP brachial arterial pressure

BMI body mass index

BNP brain natriuretic peptide

DVP deepest vertical pocket

FLA fetoscopic laser ablation

HR heartrate

IAH intraabdominal hypertension

IAP intraabdominal pressure

IUP intrauterine pressure

IVP intravesical pressure

MAP mean arterial pressure

PPP placental perfusion pressure

RAS renin-angiotensin system

RTF return to flow

TTTS twin-twin transfusion syndrom

VV veno-venous

WSACS World Society of Abdominal Compartment Syndrome

List of Figures

List of Tables

Abstract

Background Continuous uterine pressure recordings outside labour are rare since they require an invasive procedure which is morally difficult to justify. This work presents the findings of continuous uterine and abdominal pressure recordings during therapeutic amnioreductions.

Methods Stepwise amnioreduction following the fetoscopic laser ablation (FLA) treatment of a twin-twin transfusion syndrom (TTTS) enabled the measurements of the intrauterine pressure (IUP). Hands off phases, conducted after each step, allowed recordings free from external interferences. Additionally, the placental perfusion pressure (PPP) was derived by non-invasive haemodynamic measurements. Overall, the maternal dynamics of five patients were recorded and four were included in the analysis ($n = 4$) .

Results Strong uterine contractions with a maximum intrauterine pressure up to 63.8 mmHg were recorded. Simultaneously, the intraabdominal pressure fell in a number of instances. During uterine contractions the placental perfusion pressure decreased and thereby reduced foetal oxygenation.

Respirational pressure changes in the abdominal cavity revealed a pressure transmission of 88 % on the uterus. On average we found the uterine transmural elastance to be $2.8\,\mathrm{mmHg}\cdot\mathrm{l}^{-1}$.

Conclusion The fall in intraabdominal pressure during uterine contractions suggests that the observed contractions lower the placental volume to reduce the negative effects of the placental steal phenomenon following amnioreduction.

The low placental perfusion pressure levels and the related foetal oxygenation should be further investigated and remembered during amnioreductions to guarantee a stable foetal oxygenation.

The high pressure transmission shows that an elevated intraabdominal pressure has a strong effect on the intrauterine pressure and we assume this result applies to all pregnancies.

This thesis uncovers some unknown dynamics during amnioreduction which will become more relevant in the future since the number of therapeutic amnioreductions will increase with rising twin pregnancies.

Zusammenfassung

Hintergrund In dieser Arbeit werden die Ergebnisse kontinuierlicher Uterus- und Abdominaldruckmessungen während therapeutischer Amnioreduktionen vorgestellt, welche außerhalb der Geburt moralisch schwer zu rechtfertigen sind, da sie einen invasiven Zugang erfordern.

Methoden Die schrittweise Amnioreduktion mittels Laserablation nach der Behandlung des Fetofetalen Transfusionssyndroms ermöglichte die Messungen des intrauterinen Druckes. Hands-off-Phasen, die nach jedem Schritt durchgeführt wurden, erlaubten Messungen frei von externen Störfaktoren. Durch zusätzliche, nichtinvasive hämodynamische Messungen wurde der plazentare Perfusionsdruck abgeleitet. Insgesamt wurden die mütterlichen Dynamiken von fünf Patientinnen erfasst, von welchen vier für die Datenauswertung dieser Arbeit herangezogen wurden ($n = 4$).

Ergebnisse Es wurden starke Gebärmutterkontraktionen mit intrauterinen Drücken von bis zu 63,8 mmHg aufgezeichnet. Häufig fiel simultan der intraabdominelle Druck. Während der Uteruskontraktionen nahm der plazentare Perfusionsdruck ab und reduzierte dadurch die fetale Sauerstoffversorgung.

Durch die Atmung verursachte Druckschwankungen in der Bauchhöhle zeigten eine Übertragungsrate von durchschnittlich 88 % auf die Gebärmutter. Die transmurale Elastanz der Gebärmutter war im Durchschnitt $2,8\,\mathrm{mmHg} \cdot \mathrm{l}^{-1}$.

Schlussfolgerung Die Senkungen des intraabdominellen Druckes während der Gebärmutterkontraktionen deuten darauf hin, dass das Plazentavolumen durch Kontraktionen reduziert wird, um nach einer Amnioreduktion die negativen Auswirkungen des plazentaren Steal-Phänomens zu reduzieren.

Die niedrigen plazentaren Perfusionsdrücke und die damit verbundene reduzierte fetale Sauerstoffversorung sollten weiter erforscht und zukünftig berücksichtigt werden, um während und nach Amnioreduktionen eine stabile Sauerstoffversorgung des Feten gewährleisten zu können. Die hohe Drucküübertragungsrate zeigt, dass ein erhöhter intraabdomineller Druck einen starken Einfluss auf die uterinen Druckverhältnisse hat. Wir nehmen an, dass dieses Ergebnis auf alle Schwangerschaften zutrifft.

Diese Arbeit zeigt unbekannte Dynamiken während der Amnioreduktion auf, die in Zukunft an Bedeutung gewinnen werden, da die Häufigkeit therapeutischer Amnioreduktionen durch die zunehmende Anzahl von Zwillingsschwangerschaften ansteigen wird.

1 Introduction

This work provides new insights into the dynamics and physiological mechanisms of the utero-placental interplay outside labour. Measurements of haemodynamics and the uterine and abdominal pressure help to enlighten the protective purpose of non-labour uterine contractions and interactions between the uterine and abdominal cavity during amnioreduction. The procedure provides direct contact with the amniotic fluid without an additional invasive procedure. The intrauterine fetoscopic laser ablation (FLA) treatment of the twin-twin transfusion syndrom (TTTS) at the Department of Obstetrics and Gynaecology of the Medical University of Graz was followed by a stepwise amnioreduction. Between the amnioreduction steps we performed prolonged hands off phases which allowed pressure recordings free from external influences.

The twin-twin transfusion syndrom is a severe complication of monochorionic multiple gestations. Due to a harmful inter-twin transfusion of blood via placental anastomoses one of the foetuses turns into a 'receiver' the other becomes a 'donor'.

1.1 Twin-twin Transfusion Syndrome

Although the outcome has improved significantly due to better therapy methods, intrauterine and neonatal morbidity and mortality rates for both twins affected by twin-twin transfusion syndrom remain high (Lewi et al., 2008; Baxi and Walsh, 2010). The fetoscopic laser ablation of the superficial anastomoses changed decisively the outcomes from an overall foetal mortality rate ranging between 70% to 100% for untreated cases to a survival rate of 91.8% for at least one foetus and 69.5% for both foetuses (Berghella and Kaufmann, 2001; Fieni et al., 2004; Gul et al., 2003; Diehl et al., 2017).

While 9% of monochorionic diamniotic twin pregnancies developed a twin-twin transfusion syndrom, 3.8% of monochorionic monoamniotic twin pregnancies established the same pathology (Lewi et al., 2008; Umur, van Gemert, Martin J. C., and Nikkels, 2003).

During the last century the average maternal age at gestation has risen steadily in industrialised countries and the use of fertility treatments has become more popular, both leading to higher twin birth rates. The number of monozygotic twin pregnancies, of which about two thirds were monochorionic, was associated with assisted reproductive technologies (Aston, Peterson, and Carrell, 2008). As both the use of reproductive technologies and the average maternal age are most likely to increase the incidence numbers of twin-twin transfusion syndroms will rise further. Therefore, the treatment and understanding of twin-twin transfusion

syndroms will gain more importance.

Placental anastomoses between foetal circulations exist in almost all (96%) monochorionic twin placentas and usually do not cause net inter-twin transfusion (Denbow et al., 2000; Umur, van Gemert, Martin J. C., and Nikkels, 2003). Post-delivery placental studies classified three types of anastomoses (Denbow et al., 2000; Lopriore et al., 2008; Hack et al., 2008):

- arterio-venous (AV)
- arterio-arterial (AA)
- veno-venous (VV)

Most frequent are AV anastomoses in monochorionic diamniotic placentas. They are deep connections within the cotyledon between a twin's chorionic artery and a vein of the co-twin. An AV anastomosis allows unidirectional flow between the two circulations and is usually balanced by an AV anastomosis running the opposite direction.
Anastomoses of the AA and VV type develop superficially on the chorionic plate and allow bidirectional blood flow. The actual net flow direction depends upon the hydrostatic pressure differences between the two twin circulations.
A protective effect on the development of a twin-twin transfusion syndrom have AA anastomoses whereas VV anastomoses lower the chance of perinatal survival. AA anastomoses are less present in placentas which develop a TTTS.
Only in some of the unaffected placentas AV anastomoses are present. In contrast, all placentas affected by a twin-twin transfusion syndrom have AV anastomoses, suggesting that this type of anastomoses may promote the development of the syndrome (Denbow et al., 2000; Lopriore et al., 2008; Hack et al., 2008).

Following the flow imbalances the receiver develops hypervolemia, the donor hypovolemia. Consequently the receiver develops polyuria and the donor oliguria.
The receiver's hypervolemia increases the atrial pressure and leads to a release of atrial natriuretic peptide (ANP) and brain natriuretic peptide (BNP). The two hormones' natriuretic and vasodilatory effect reinforce polyuria, trying to compensate the receivers' hypervolemia (Bajoria, Ward, and Chatterjee, 2002). However, at the same time the donor's hypovolemia intensifies and his renin and angiotensin-II levels rise. Unfortunately renin and angiotensin-II reach the receiver via anastomoses. In addition, plasma endothelin-1 level increase in the re-

ceiver (Bajoria, Sullivan, and Nicholas M. Fisk, 1999). The activation of the renin-angiotensin system (RAS) and the rise in endothelin-1 hormone levels intensify the receiver's hypertension and provoke cardiac hypertrophy, cardiomegaly and cardiac dysfunction (Simpson et al., 1998; Lougheed et al., 2001).
The donor's oliguria, caused by high renin and angiotensin-II levels, results in anhydramnios which presents itself as the 'stuck twin' phenotype.

The twin-twin transfusion syndrom is classified into five stages, depending on sonographic and clinical parameters (Table 1). Depending on the stage the survival rate for one or two foetuses changes (Rubén A. Quintero et al., 1999).

Table 1: Staging of the twin-twin transfusion syndrom

Stage	**Ultrasound Parameter**	**Categorical Criteria**
I	Maximal vertical pocket (MVP) of amniotic fluid	Polyhydramnios-oligohydramnios sequence: Polyhydramnios (MVP>8 cm) in recipient sac and oligohydramnios (MVP<2 cm) in donor sac
II	Foetal bladder	Nonvisualization of foetal bladder in donor twin during a 60 min lasting observation
III	Umbilical artery, ductus venosus, and umbilical vein Doppler waveforms	Absent or reversed umbilical artery diastolic flow, reversed ductus venosus a-wave flow, pulsatile umbilical vein flow
IV	Foetal hydrops	Hydrops in one or both twins
V	Absent foetal cardiac activity	Foetal demise in one or both twins

Adapted from Simpson, 2013 based on Rubén A. Quintero et al., 1999

1.1.1 Models of the Twin-twin Transfusion Syndrome

Due to lack of animal models the pathophysiological mechanisms causing TTTS remains unknown to date. Mathematical models have been developed with the aim to identify the factors which play into the syndrome's progress. The first differential equation model made up of two identical foetoplacental units was limited in its initial setup, as the two foetoplacental units were suddenly connected at 27 weeks of gestation by anastomoses. The model simulated the flow of volume between the two circulations with various combinations of directions and numbers of anastomoses until they reached a steady state (Talbert et al., 1996). The group around Van der Wijngaard designed five consecutively improved models. These consisted of two parts: Firstly, foetoplacental and amniotic fluid development of uncon-

nected, normal, physiologic twins and secondly, the dynamics following a foetofoetal blood transfusion. They showed that the TTTS stages (Table 1) correlated with an advancement of the syndrome and uncovered a number of different findings summarised in table 2 (van den Wijngaard, Jeroen P. H. M., Umur, Michael G. Ross, et al., 2008).

Table 2: Overview of twin-twin transfusion syndrom models

Model	**Setup**	**Parameters**	**Findings**
I	Two identical foetoplacental units with 1kg foetuses of 27 weeks' maturity abruptly connected by AV anastomoses with pulsatile circulation	Interrelated hemodynamic, osmotic and metabolic physiological variables; Direction and number of arteriovenous anastomoses	Severe TTTS cases can be explained by unidirectional transfusion; asymmetric bidirectional transfusion can lead to moderate manifestations of TTTS
II	Two part model: 1. dynamic foetoplacental/ anastomotic growth and unequal placental sharing (neglecting size of placenta) 2. Consequences of foetofoetal transfusion	Foetal blood volume, types of anastomoses, non-pulsating arterial circulation	Anastomotic blood flow has to increase faster than foetal physiologic growth
III	Identical to II	Identical to II and additional amniotic fluid	Maturity of gestation at TTTS's discovery does not correlate with its severity
IV	Identical to II	Identical to III and additional arterial and venous blood volume, interstitial and intracellular fluids	For advanced TTTS cases the hydropic recipient twin tries to reduce its polyhydramnios and indicates the severity of the intertwin transfusion progress
V	Identical to II	Identical to IV and additional the RAS system, hematocrit and arterial walls and a pulsatile arterial circulation	Abnormal umbilical arterial flow pulsations (TTTS stage III) occur earlier and more frequently in the donor than in the recipient

Models by: **I:** Talbert et al., 1996, **II:** van Gemert and Sterenborg, 1998, **III:** Umur, van Gemert, Martin J. C., Michael G. Ross, et al., 2001, **IV:** van den Wijngaard, Jeroen P. H. M., Umur, Krediet, et al., 2005, **V:** van den Wijngaard, Jeroen P. H. M., Westerhof, et al., 2007

The model by Umur et al. uses a superficial estimate of the uterine compliance, based on physiological amniotic volumes and constant amniotic pressures during gestation. Also the

work van den Wijngaard, Jeroen P. H. M., Umur, Krediet, et al., 2005 requires a uterine compliance estimate.

None of the models includes the IAP implying that the authors assume it has no lasting effect on the foetuses and the twin-twin transfusion syndrom progress. Although the purpose of these models is to simulate the twin-twin transfusion syndrom and the outcome of the foetuses, non of these models factors determining the maternal health. These limitations provide opportunities for further improvements.

For the setup of this work most relevant is the prediction by Van den Wijngaard's group that amnioreduction in the hydropic recipient could lead to a deterioration of the hydrops and the cardiovascular status. The model suggests limiting amnioreduction and opting for laser therapy as the superior treatment in cases in which the gestation is still early (van den Wijngaard, Jeroen P. H. M., Michael G. Ross, et al., 2005).

1.2 Intraabdominal Pressure

The intraabdominal pressure is defined as a steady state pressure within the abdominal cavity (Malbrain, Manu L. N. G. et al., 2006). It depends on the walls enclosing the cavity, its content and, more specifically, on both volume and elasticity of the content. Consequently, a gravid uterus affects IAP, as do several other factors: the body mass index (BMI) and the sagittal abdominal diameter and respiration, since pressure rises with inspiration and falls with expiration (Sugermann et al., 1997).

As the content of the abdomen is virtually fluid and relatively non-compressive (apart from the gravid uterus), intraabdominal pressure follows Pascal's law:

$$P = \frac{F}{A} \tag{1}$$

where P is the pressure, F the force exerted onto the cavity and A the cavity's surface area. The law states that, relative to the reference height, the pressure is equal throughout the cavity and can be measured at any point.

Physiologically the intraabdominal pressure ranges around 5-7 mmHg for general patients and around 9-14 mmHg for obese patients (Keulenaer et al., 2009). In a prospective cohort study of 77 patients the average IAP was 6.5 mmHg (Sanchez et al., 2001).

In recent years elevated IAP levels have attracted considerable attention, especially for critically ill patients, since its effect on the body is large and frequently neglected. For the purpose of defining standards and abnormalities concerning IAP the World Society of Abdominal Compartment Syndrome (WSACS) has been formed. The society defined intraabdominal

hypertension (IAH) as an increased IAP level above 12 mmHg. The abdominal compartment syndrome (ACS) is defined as an IAP level $\geq$ 20 mmHg which often leads to organ malfunction (Malbrain, Manu L. N. G. et al., 2006).

1.2.1 Pregnancy and Intraabdominal Pressure

The interaction between pregnancy and the intraabdominal pressure has been rigorously inspected (Paramore, 1913). Paramore found that it rises in pregnancy and suggested a link between preeclampsia and intraabdominal hypertension.

The intraabdominal hypertension in pregnancy has received more attention in recent years and the original link with pre-eclampsia has been revived (Chun and Kirkpatrick, 2012; Sawchuck and Wittmann, 2014). The first systematic intraabdominal pressure recordings during pregnancy in line with the official guidelines were conducted in groups of term women undergoing an elective caesarean section with spinal anaesthesia. The measurements took place before and after the caesarean section. The median intraabdominal pressure fell from 22 mmHg to 16 mmHg (Al-Khan et al., 2011) and from 10.9 mmHg to 7.4 mmHg (Chun, Baghirzada, et al., 2012). These results show that pregnancy increases intraabdominal pressure into intraabdominal hypertension regions. However, no data exists for earlier pregnancy stages. The physiologic intraabdominal pressure during pregnancy resumes unknown although current guidelines group pregnancy and obese together as chronic intraabdominal hypertension cases (Malbrain, Manu L. N. G. et al., 2006). Neither the effect of the enlarged uterus on the intraabdominal pressure has been analysed nor the relationship between the intraabdominal pressure and the immobile and constricted bladder during pregnancy (Chun and Kirkpatrick, 2012). The weight of the gravid uterus might falsely increase the intraabdominal pressure results obtained via the intra-vesicular method (Chun, Baghirzada, et al., 2012). It also remains unknown whether the type of abdominal tissue, i.e. abdominal fat or uteral muscle, has an impact on the intraabdominal pressure.

The influence of the intraabdominal pressure on uterus and foetus is still untested. Only animal studies showed that a rise in the intraabdominal pressure directly increases the intrauterine pressure which in turn compresses the foetal urinary system and has effects on the foetal development (Attah and Hutson, 1993; Tanyel, 2000). The direct relationship between the intraabdominal pressure and the intrauterine pressure within rabbits at 20 days of gestation was (Karnak et al., 2008):

$$IUP = IAP * 0.8 + 2.0 \tag{2}$$

1.2.2 Measuring Methods

There are a number of different techniques which allow a reliable measurement of the IAP (Malbrain, Manu L. N. G., 2004). They divide into the two main categories direct and indirect measuring methods. Direct measurements require physical contact with the abdominal cavity and need an invasive route inside the abdomen. Indirect measure techniques use a hollow organ or vascular structure within the abdomen. Their wall acts as a membrane transducing the abdominal pressure. For this purpose, intragastric, intracolonic, intrarectal, intravesical and inferior vena cava catheters are available (Malbrain, Manu L. N. G., 2004). The standard method set by the WSACS is the measurement via the intra-vesical route (Malbrain, Manu L. N. G. et al., 2006). This method provides a precise approximation of the IAP with transurethral catheters (Yol et al., 1998).

The WSACS defined the following routine setup, enabling comparability and reproducibility between patients: patients should be in complete supine position, as an elevated body and head both increase the IAP (this requirement implies that the abdomen does not behave as a perfect fluid). Since respiration influences the IAP the measurement should take place at the end of expiration. Transducers should be zeroed at the level of the midaxillary line. Less than 25 ml of saline should be instilled into the bladder for priming to guarantee a fluid column between bladder wall and transducer, as larger volumes artificially increase the IAP (Malbrain, Manu L. N. G. et al., 2006; Keulenaer et al., 2009).

1.3 Intrauterine Pressure

Intrauterine pressure is defined as the pressure within amniotic volume inside the uterus and is identical to the more commonly used term intraamniotic pressure. However, in this work it has been renamed for better distinction to IUP as the abbreviation for intraamniotic pressure would be the same as for Intraabdominal pressure. Although recordings of IUP measurements have already existed for a long time, concrete knowledge about IUP other than during labour is very limited, since invasive measures without a combined therapy are not morally permissible. To date, most of the IUP work is related with uterine activity during or shortly before labour.

The theoretical framework of the pressure within the uterus shows that it follows Pascal's law, although the area of the cavity is not constant (Coren and A. I. Csapo, 1963). However, for measurement purposes it is important to sustain an equal pressure throughout the uterus and allow a measurement within the cavity at any point.

Muscular surrounding of the amniotic sac is elastic and the pressure depends heavily on its

activity and elasticity. It can be modelled by Laplace's law of pressure in spheroids (Coren and A. I. Csapo, 1963; Sideris and Nicolaides, 1990). As the pregnant uterus increases in size due to the rise in amniotic fluid and foetal size the radius of the spheroid expands. Simultaneously, the wall of the uterus thins. Due to hormonal effects the elasticity of the wall increases at the same time and the wall tension is either constant or decreases, complicating the model. These associations are simplified within Laplace's law of pressure in spheroids:

$$P = 2 * W * \frac{T}{R} \tag{3}$$

where P is the pressure, W is the wall thickness, T is the tension and R is the radius of the uterus.

Physiological ranges of the IUP are still unknown as they vary strongly between existing studies, especially the dynamics during the course of pregnancy. There are contradicting data regarding whether the IUP falls or rises during pregnancy.

Studies suggesting rises are A. Csapo, 1970; Nicolini et al., 1989; Weiner et al., 1989; N. M. Fisk et al., 1992.

Nicolini et al., 1989 recorded an increase in 36 patients ($P < 0.01$) and explained this by a higher myometrical fibre tension caused by the stretch of the expanding uterus. However, as the determination coefficient was relatively low ($r^2 = 0.23$), the conclusion focussed on the range for the intrauterine pressure between 1 and 14 mmHg for normal amniotic fluid volume levels.

In another study the mean IUP was 11.4±4 mmHg and the intrauterine pressure correlated with the gestational age (Weiner et al., 1989).

In addition described N. M. Fisk et al., 1992 the same positive relationship and provide a reference range for different pregnancy stages. Similar to Nicolini et al., 1989 their relationship between normal singleton pregnancie's intrauterine pressure and gestational age has a weak coefficient of determination ($r^2 = 0.19$).

Sideris and Nicolaides, 1990, by contrast, observed in 200 patients that the usual mean IUP falls exponentially from 9 mmHg at 10 weeks to 5 mmHg at 30 weeks of gestation. After this gestational stage the pressure reached a plateau until labour.

The intrauterine pressure for twin pregnancies was comparable to singleton pregnancies' (N. M. Fisk et al., 1992). Although the two amniotic sacks of twins are separated the intrauterine pressures were similar high, since the membrane separating the two amniotic cavities is virtually tension free (R. A. Quintero et al., 1998; Hartung, Chaoui, and Bollmann, 2000).

As well as the weak effect of gestational age on the physiological intrauterine pressure, other factors such as amniotic fluid volume, deepest pool, maternal age or parity, showed to be insignificant as main determination factors, too (N. M. Fisk et al., 1992).

1.3.1 Amniotic Fluid Volume and Intrauterine Pressure

Drainage or infusion of amniotic fluid provides a good opportunity to measure the intrauterine pressure as the catheter creates a direct transabdominal access into the amniotic cavity. This method has been used for existing research.

The intrauterine pressure correlated with the amniotic fluid volume and fell as a consequence of amniodrainage with a larger impact on patients with prior elevated intrauterine pressures. Polyhydramniotic patients had higher IUPs and the opposite applied to oligohydramniotic patients. Contrary, an amnioinfusion lead to a rise in IUP (Nicholas M. Fisk et al., 1990; Nicolini et al., 1989). Based on this link the study concluded that monitoring IUP during amnioinfusion or amnioreduction might be advantageous (Nicholas M. Fisk et al., 1990).

Patients with a twin-twin transfusion syndrom had an elevated mean IUP and the therapeutic amniodrainage lowered it to a physiological level (Garry et al., 1998). However, the pressure change due to amnioreduction may have had a negative impact on the foetal status. The therapeutically induced reduction in IUP may have been followed by a flow of blood into the chorioangioma due to a reduction in vascular impedance and thereby caused a deterioration of the high-output cardiac failure (Jones et al., 2012).

1.3.2 Measuring Methods

Presumably one reason for limited intrauterine pressure knowledge is the range of different measurement methods and procedures, making findings incomparable (M. G. Ross and Brace, 2001). Existing works used for example the level of the foetal heart, the top of the abdomen or the tip of the needle for zeroing of the transducer (Nicolini et al., 1989; Weiner et al., 1989; N. M. Fisk et al., 1992; Sideris and Nicolaides, 1990).

Yet non of the three methods is suitable to compare IUP results across different groups. They are partly even inadequate to compare the measurements of the same patient at different gestation dates within the same study, as the position of the foetus' heart and the level of abdomen change during pregnancy.

Faber and Barbera, 1992 suggest that the most suitable level for zeroing the transducer is at the surface supporting the supine patient, making measurements comparable. However, attempts at establishing uniform measuring conventions have not been successful so far.

1.4 Interplay between Intrauterine Pressure and Intraabdominal Pressure

Limited research exists on the link between IAP and IUP. However, a patent has been granted for the measurement of the IUP pressure via the intra-vesical route (R. H. Neal and R. C. Neal, 2002). Although no results have been published yet, this device suggests that the inventors assume a strong and direct relationship between IAP and IUP.

1.5 Aim

This work intends to provide a clearer understanding of the interactions between the intraabdominal pressure and the intrauterine pressure for humans and will clarify the relations with the progress of the amnioreduction. It will produce sequential continuous pressure recordings of the IAP and the IUP allowing the analysis of the dynamics between them. The results could provide the basis for further models and will help explain the physiology of contractions.

This work will simultaneously examine the course of the mean arterial pressure (MAP). The MAP in combination with the IAP and IUP will give details about the placental perfusion pressure PPP during amnioreduction. All variables will be further processed, visualised and statistically analysed.

2 Methods and Materials

This prospective non-therapeutic pilot study recorded non-invasively and continuously the intraabdominal pressure, the intrauterine pressure, the mean arterial pressure and the heartrate. Measurements were conducted during endoscopic intrauterine intervention to treat TTTS. All measurements did not require further procedures other than those of the TTTS treatment. Therefore, there was no additional risk for participants associated with this work. The detailed manual instructions for the measurements are described in German in section 6.3 and the full equipment list is in section 6.2.

2.1 Study Population and Recruiting Criteria

Twin-twin transfusion syndrom patients were recruited by the outpatient clinic of the Department of Obstetrics and Gynaecology of the Medical University of Graz for a fetoscopic intrauterine treatment. Approximately twenty patients were expected to be treated per year. Inclusion criteria were: [1] female sex, [2] over 18 years old, [3] an ongoing monochorionic-diamniotic twin pregnancy with a TTTS in stage I and [4] a given informed consent.
Prior to the treatment patients received profound patient information, providing details about the intervention and the measurements planned. Emergency cases of TTTS treatment were not part of this work since the measurements required a sufficient amount of preparation.

2.2 Parameters

The following general parameters were obtained at the date of the intervention: maternal age, gestational age, normal and current weight, length, BMI, gravida, Quintero stage and the total volume of amnioreduction.
The measured variables were IAP, IUP, MAP, HR and the uterine volume prior and post amnioreduction.

2.3 Chronological Sequence

The figure 1 stylises the chronological order of the clinical procedure. Preparations had to be finished prior to the FLA phase. Following the FLA the amniotic volume was estimated and the IUP transducer connected with the trocar. After zeroing the transducers the amnioreduction was conducted step-by-step and the results were ultrasonically evaluated until the target was reached and the amnioreduction completed. Following each amnioreduction step a 'hands-off' phase was conducted for about one minute. Only during these amniotic fluid

constant phases was the direct connection between the transducer and the uterus necessary for the IUP measurement established and a meaningful recording of both IAP and IUP possible. The complete procedure was terminated by a final ultrasonic assessment of the amniotic volume.

FIGURE 1: TIMELINE OF THE CLINICAL INTERVENTION

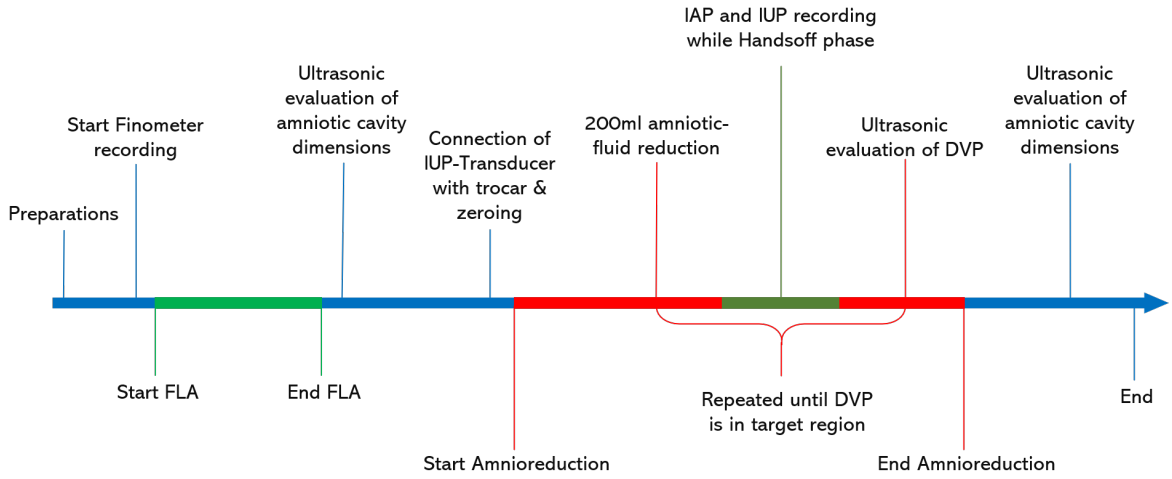

Fetoscopic laser ablation (FLA), intraabdominal pressure (IAP), intrauterine pressure (IUP), deepest vertical pocket (DVP)

2.4 Physical Setup

The preparations for the technical equipment followed a fixed procedure (see section 6.3 for details).

The isolating transformer ERT 230/230/4G (*Thalheimer Transformatorenwerke GmbH, 09380 Thalheim, Germany*) connected with the grounding of the operation theatres provided the electricity for the equipment. Thereby, this setup produced a potential equalisation to stop any possible leakage current, which could have occurred otherwise, since the patients were electroconductive and connected simultaneously to several different electric devices. The usage of the normal PC for data recording made the isolating transformer indispensable.

2.5 Amnioreduction

After the FLA the amnioreduction took place in a step-by-step routine. It was split into 200 ml steps and the amniotic fluid was removed with a 50 ml syringe. While the syringe was used, the three-way valve connected the syringe with the uterus. During the hands-off phases the valve was set to connect the transducer with the uterus and nobody touched the patient and no ultrasonic measurements took place to guarantee pressure recordings independent of external influences.

Previous TTTS treatments by the Fetal Treatment Center at the Medical University Graz showed that large amnioreduction steps were associated with more maternal complications. The trade off between fewer maternal complications with minute small steps and the procedures duration with larger steps was solved with 200 ml amnioreduction steps.

This step-by-step amnioreduction was repeated until the deepest vertical pocket (DVP) of the receiver reached the target treatment region of 6-8 cm.

During the recordings comments were added to mark the start ('hands off x ml') and end ('end') of a hands-off phase.

FIGURE 2: DATA RECORD EXAMPLE

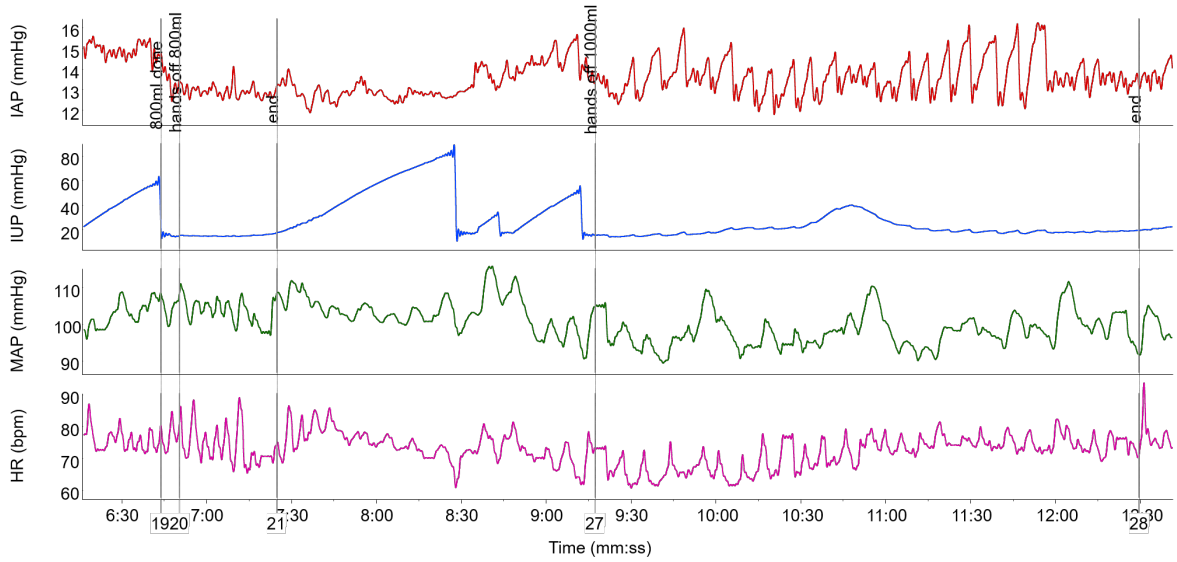

The graphic shows a section of a recording from minute 6:30 to 12:30. The comments are indicated by vertical lines and the comment number is located along the time axis. Intraabdominal pressure (IAP), intrauterine pressure (IUP), mean arterial pressure (MAP), heartrate (HR) (Extract from patient C, recorded at 20Hz)

Figure 2 shows an example of the data recordings during removal of the amniotic fluid with the subsequent hands-off phase. The IUP includes three steep peaks between comment 20 and 27, caused by the continuous flow.

2.6 Intraabdominal Pressure

The IAP was measured via a intravesical Foley catheter which did not require additional invasive procedures or equipment.

At the beginning the urinary bladder was emptied by inserting a catheter. The catheter was connected with a CA-0200 intraabdominal monitoring set (*Biometrix BV, Overbroek 10 6247 EN, Gronsveld, The Netherlands*). 50 ml of sterile saline solution freeflex® K929525 (*Fre-*

senius Kabi Deutschland GmbH, Germany) was filled into the bladder and a BP transducer (*BP Transducer, Utah Medical Products Inc®, Midvale, UT, USA*) was connected with the intraabdominal monitoring set. These parts were linked by a tubing flushed with saline. Although small bubbles do not have a relevant effect all lines including transducers were flushed completely (J. J. d. Waele et al., 2004).

The BP transducer was secured onto a transducer clamp on midaxillary level for zeroing and pressure recordings. Patients were in a supine position throughout the procedure.

Although urine does not clot the tubing or transducer a continuous flow with 300 mmHg pressure was installed to the anaesthesia's transducer to which the BP transducer was fastened. The continuous flow cleared any clots coming from the urinary bladder.

BP transducer have a sufficient pressure operation range from -50 mmHg to +300 mmHg and provide an accuracy of 5uV/V/mmHg or ±2%.

2.7 Intrauterine Pressure

The intrauterine pressure was measured via the fetoscopic trocar used for the TTTS treatment. Following the FLA the flushed and sterile tubing was connected with a BP transducer (the identical model used for IAP measurements). The transducer was fastened on the transducer clamp and zeroed on midaxillary height. Since the IAP transducer was fixed on the same level the two simultaneous pressure recordings are comparable.

Identical to the IAP setup we attached a continuous flow with 300 mmHg pressure to the transducer of the anaesthesia to which the BP transducer was fastened.

2.8 Haemodynamics

The hemodynamics were measured with a Finometer® Model 1 (*Finapres Medical Systems BV, Arnhem, The Netherlands*). This device allows non-invasive recordings of the arterial blood pressure on a beat-to-beat basis and calculations of the stroke volume and total peripheral resistance.

The principle of the basic non-invasive blood pressure measurement is a so called plethysmanometer (Penaz, 1976). It consists of a finger cuff with a balloon under pressure on the side facing the finger. The pressure is adjustable with a pneumatic mechanism. In addition, it uses a photoplethysmograph, which measures the change in blood volume within the finger via light absorption, which is comparable to pulse oximetry.

The inflatable balloon exerts a pressure onto the finger. However, unlike the pulse oximeter it is continuously adjusted throughout the cardiac cycle so that it equals the arterial wall

pressure within the finger and the diameter of the finger arteries remains constant. As the blood pressure increases during the systole, the induced arterial volume rise is measured by the photoplethysmograph. The pneumatic pressure inside the balloon is instantly adapted to keep the volume constant. The same mechanism is used vice versa for a decrease in blood pressure.

If the blood volume in the finger stays constant and the photoplethysmograph does not detect pulsations any longer, then the pressure of the finger cuff equals the arterial wall pressure and the arterial walls in the finger are 'unloaded'. It follows that the pressure exerted on the arterial walls, i.e. the blood pressure in the finger, equals the pressure within the balloon. The pressure is then continuously recorded and measured in mmHg.

Finding the volume at which the arteries are unloaded is a complex task as not only the blood pressure but also the vascular muscle tone affect the state. As the smooth muscle tone and stress are subject to constant changes, the correct unloaded volume of the finger has to be revised frequently. This is achieved by the *'Physiocal'* ® algorithm (K. H. Wesseling, De Wit, et al., 1995). It calibrates the finger's vascular physiology by analysing the plethysmogram during calibration periods at which the balloons pressure is kept steady. This procedure is repeated frequently throughout measurements of the Finometer depending on the quality of the signal.

The digital arterial pressure is not equal to the invasive brachial arterial pressure (BAP) with significant differences due to the pressure gradient and the pulse wave distortion (P. Gizdulich and Wasseling, 1990). The pulse wave distortion deviations caused by wave reflections in progressively narrowing arteries have been successfully removed with a frequency dependent model (Paolo Gizdulich, Prentza, and Karel H. Wesseling, 1997). The pressure gradient problem caused by the flow in the resistive vascular tree has been solved by a level correction equation (Bos et al., 1996). In combination these two allow a reliable mathematical reconstruction of the brachial arterial pressure on the basis of the digital arterial pressure.

In addition to both correction methods the recordings of the digital arterial pressure is calibrated automatically by the Finometer with an upper-arm cuff return to flow (RTF) measurement. Comparable to the Riva-Rocci method with a sphygmomanometer and pulsation detection of the systolic pressure at the radial artery, the RTF pressure is equal to the arm cuff pressure when the arm cuff deflates and the first pressure pulse reaches the finger cuff. This technique allows an individual calibration and the resulting reconstructed BAP fulfils the requirements of the Association for the Advancement of Medical Instrumentation (Guelen et al., 2008). These requirements state that the mean and standard deviation of the obtained

results must be below ± 5 mmHg and ± 8 mmHg of the true BAP.

As the hydrostatic difference between the heart level and the finger cuff has a significant effect upon the measurements, the Finometer includes a hydrostatic height correction module. The double-ended device is fixed onto the finger cuff as well as the arm cuff on the right atrial level. The hydrostatic difference is constantly measured and used to adjust the blood pressure to heart level measurements.

As an alternative to the insufficient thermodilution method, the Finometer computes reliable the cardiac output continuously and based solely on the non-invasive data. The original method used constant aortic properties and is called 'pulse-contour analysis'. However, these aortic properties are not constant and to give full considerations 'Modelflow' has been developed with a nonlinear, three-element Windkessel model for more accurate calculations. The Finometer uses the 'Modelflow' method to derive the aortic flow from the arterial pressure. This model, illustrated in figure 3, computes the aortic flow from the aortic impedance, arterial compliance and systemic vascular resistance. The aortic impedance and compliance are approximated values based on population averages of 65 autopsied thoracic and abdominal aortas (Langewouters, K. H. Wesseling, and Goedhard, 1984). For this approximation the Finometer uses the age, height, weight and gender of the patient for its calculations. The systemic vascular resistance is calculated from the mean pressure and mean aortic flow (K. H. Wesseling, Jansen, et al., 1993).

Figure 3: Three element model

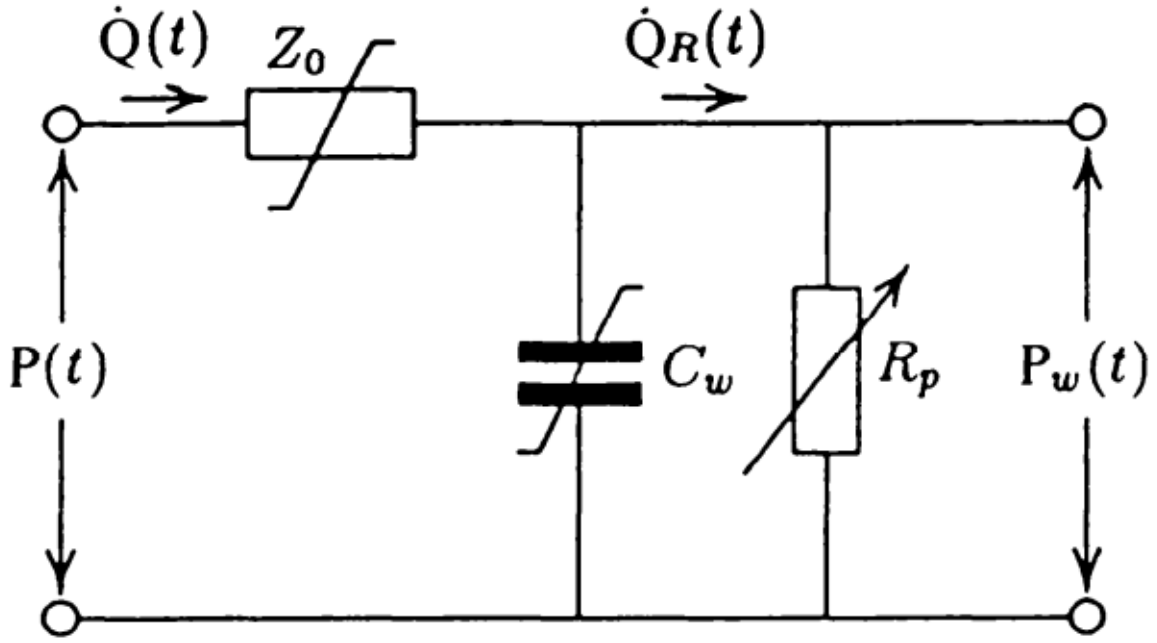

The original diagram of K. H. Wesseling, Jansen, et al., 1993 showing the three-element Windkesselmodel to derive the aortic flow. It is an electrical analogue of the aortic Windkessel with C_w standing for the arterial compliance, Z_o for the aortic impedance, R_p for the peripheral vascular resistance, $\dot{Q}(t)$ for the cardiac output, $P(t)$ for the pressure waveform and $P_w(t)$ for the pressure within the windkessel

Windkessels are able to model the output of pulsating arterial blood flow entering vascular organs. Originally, Windkessels were used by German firefighters on their fire trucks to turn the pulsating water flow, generated manually by firefighters, into a steady flow of water. The pulsatile water flow was damped by tanks filled partly with air and water.

For this work the Finometer provided the two variables, MAP and HR, via the Analog Signal I/O signal converter (*Finapres Medical Systems BV, Arnhem, The Netherlands*) in two separate channels, approximated automatically in a staircase manner. Both signals are updated every second plus the time of the last beat.

The RTF calibration of the Finometer was done at the beginning of the intervention and deactivated for the rest of the amnioreduction as the position of the operation table was not adjusted.

The installation of the Finometer took place prior to the fetoscopic laser ablation. Before the sterile operation sheet covered the patient the arm/finger cuff and height adjustment tools were installed to ensure good access. To guarantee correct calculations the Finometer required the input of the patient's gender, height, weight and age. The Finometer had a fixed presetting to ensure the same settings were applied to each patient.

2.9 Recordings

LabChart Version 7 (*AD Instruments Pty Ltd., Dunedin 9016, New Zealand*) recorded continuously the pressure measurements and haemodynamics on the computer. The two BP Amps (*AD Instruments Pty Ltd., Dunedin 9016, New Zealand*) converted the analogue signals from the BP Transducer and the Analog Signal I/O Signal Converter to digital signals. The PowerLab 4/20 device transferred them to the PC. The PowerLab 4/20 device has an accuracy of ±2 mV for a range of ±10 V. In combination with the BP Amp and BP transducer this provides an accuracy of ±0.2 mmHg.

The sampling rate for all channels was 20 Hz and the following settings were used for each channel:

Channel 1: IAP: 1 V = 89.5937 mmHg

Channel 2: IUP: 1 V = 89.6330 mmHg

Channel 3: MAP: 1 mmHg (1 V = 100 mmHg)

Channel 4: HR: Beats per minute (bpm) (1 V = 100 beats per minute)

For channels 1 and 2 the conversion rate was automatically set by the manufacturer and the value was unique to each BP Amp device.

The setup allowed the simultaneous measurement of HR, MAP, IUP and IAP in one recording and was tested thoroughly prior to the measurements to guarantee its reliability.

2.10 Definitions and Analysis of Recordings

Variables and technical terms were standardised to ensure a repeatable data analysis and result presentation.

LabChart automatically selected the datapoints between the comments 'hands off x ml' and 'end' and returned the predefined values into the so-called 'Data Pad View'. For each patient it created a table and a text file with the results and selected variables.

2.10.1 Minimum and Maximum Values

Minimum pressure values of each hands-off phase were important as singular indicators as these were assumed to be the temporary baseline pressures free from uterine contractions. Maximum pressure values were also depicted for each hands-off phase.

2.10.2 Changes in Intraabdominal and Intrauterine Pressure

The difference between the IAP/IUP minimum of the first and the IAP/IUP minimum of the last hands-off phase was defined as $\Delta IAP/\Delta IUP$ and it is referred to as the change in IAP/IUP.

2.10.3 Temporary Uterine Contractions

The difference between a minimum and maximum IUP within the same hands-off phase was defined as δIUP_{cont} and is called temporary uterine contraction.

2.10.4 Temporary Uterine Contractions Duration

$tIUP_{cont}$ was defined as the time duration of a uterine contraction after an amnioreduction. If the temporary amplitude was not completely recorded the time was extrapolated as following: the time period between the maximum IUP value of the amplitude and the point where IUP was at its baseline level was doubled.
In several hands-off phases it was not feasible to set a meaningful beginning and end of an amplitude. Therefore, only for amplitudes larger than 15mmHg the time period was measured. This value was set after manual analysis of the recordings.

2.10.5 Respirational Intraabdominal and Intrauterine Pressure Changes

For the two compartments δIAP_{resp} and δIUP_{resp} was defined as the average IAP and IUP amplitudes of at least five consecutive respiratory cycles during a hands-off phase. These cyclic changes are exemplified in figure 5 and 13. The cycle measurement tool of LabChart was able to identify the cycles and added markers to the channels at the cyclic maxima.
During the selected time periods for the cyclic analysis the two pressure recordings were supposed to have a relative constant baseline pressure as great variations would have affected the correlation and the cyclic measurement tool, making the identification of the maxima less accurate.
The cyclic measurement tool was used with the following processing settings: before the cycle detection auto-levelling normalized the recording with a window width of 20 s and an assumed noise of 1 mmHg. Cycle peaks were detected if the peak deviated more than 0.6 standard deviations. The minimum cycle period was set to 2 s. The peak search window had a width of 30 s.

2.10.6 Duration of Respirational Intraabdominal and Intrauterine Pressure Changes

$tIAP_{resp}$ and $tIUP_{resp}$ were the average time periods of at least five consecutive respiratory IAP and IUP amplitudes. The time periods were measured on a 'peak-to-peak' basis between two maxima.

2.10.7 Current Amnioreduction Volume

The current volume of amniotic fluid extracted rose in 200 ml steps and was the current number of amnioreduction steps ($x_{current}$) multiplied by 200.

$$V_{current\_fluid} = 200 * x_{current} \tag{4}$$

2.10.8 Total Amnioreduction Volume

The total amniotic fluid extracted was called 'amnioreduction' and was the number of all amnioreduction steps conducted during an intervention (x_{total}) multiplied by 200.

$$V_{total\_fluid} = 200 * x_{total} \tag{5}$$

2.10.9 Fractional Amnioreduction

The total amnioreduction varied and to enable comparisons between the studies the fractional amnioreduction was used.

$$V_{fraction\_fluid} = \frac{V_{currentl\_fluid}}{V_{total\_fluid}} \tag{6}$$

2.10.10 Amniotic Volume

The amniotic volume was an estimate based on the total volume of the uterus measured ultrasonographically with a Voluson E10 (*GE Healthcare, USA*) prior and post amnioreduction. The two outer layers of the myometrium were used as boundaries to obtain the anterior-posterior, cranio-caudal and transverse diameter. These values were used to calculate the amniotic volume with the equation for ellipsoids:

$$V = \frac{4}{3}\pi * \frac{a}{2} * \frac{b}{2} * \frac{c}{2} \tag{7}$$

where V is the volume, a the anterior-posterior diameter, b the cranio-caudal diameter and c the transverse diameter. This estimated volume included a large share of substances apart

from the amniotic fluid, such as the uterus, the foetuses and the placenta. However, all of them contain a large proportion of water and we therefore assumed the total mass to be homogeneous and to have fluid like compression characteristics.

2.10.11 Current Amniotic Volume

The current amniotic volume was defined as the amniotic volume reduced by the current amnioreduction volume.

$$V_{current} = V - V_{current\_fluid} \tag{8}$$

2.10.12 Elastance

In general the elastance is calculated with the change in pressure over the change in volume.

$$E = \frac{\Delta P}{\Delta V} \tag{9}$$

However, to make use of all data points available from each patient we used regression coefficients of the IUP values and the difference between IUP and IAP values against the amniotic volume as the measure for elastance. Minimum IAP and IUP values from each hands-off phase were used since these were assumed to be free of any contraction.

2.10.13 Placental Perfusion Pressure

The placental perfusion pressure was defined as the difference between mean arterial pressure and intrauterine pressure.

$$PPP = MAP - IUP \tag{10}$$

2.11 Processing of Recordings

The amount of noise within the IUP and IAP channels, created with the settings from section 2.9 and exemplified in figure 4, was significant. Digital filters were applied to the pressure recordings to reduce the high frequency noise, since these allow removal or adjustment post data acquisition without changing the raw data. For the analysis filtered recordings were used.

Figure 4: Example of a hands-off phase

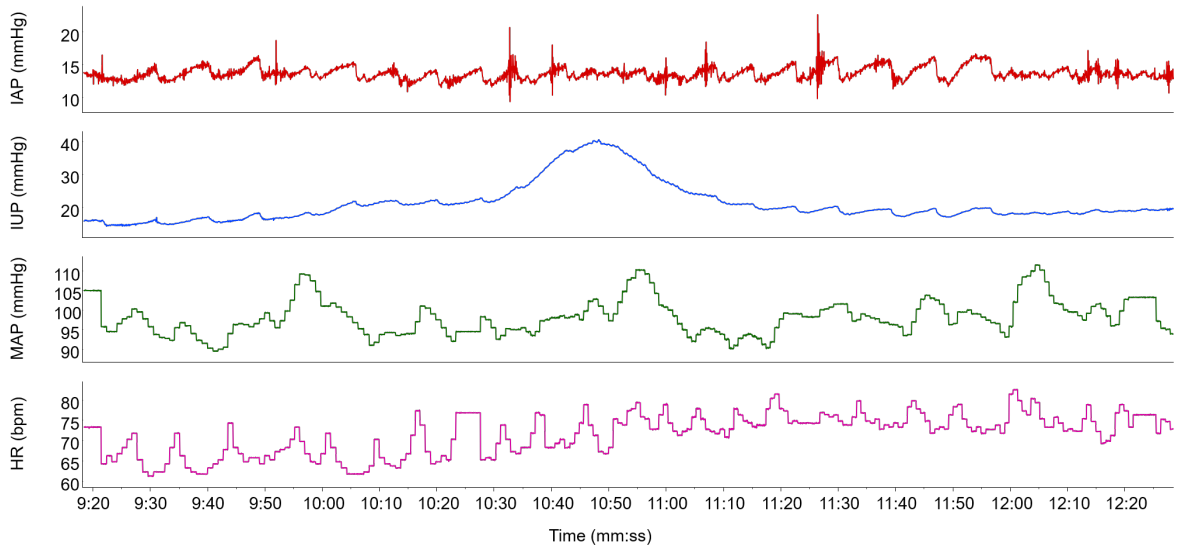

Raw data recording of a typical hands-off phase (Detail from figure 2). It shows very high frequency oscillations in the IAP channel, which are noise. Slower oscillations are present in all channels and an additional very low frequency oscillation in the IUP recording. Intraabdominal pressure (IAP), intrauterine pressure (IUP), mean arterial pressure (MAP), heartrate (HR) (Extract from patient C, recorded at 20 Hz)

2.11.1 Respiratory Dynamics

For the analysis of respirational dynamics independent of the amnioreduction progress a 1 Hz low pass filter was applied with the result exemplified in figure 5. The filter reduced the noise by blocking all frequencies above 1 Hz. The cycle detection tool of LabChart Version 7 automatically detected the cycles. For the analysis only time periods with a constant baseline intrauterine pressure were used. Pressure changes within the frequency ranges of the heart beat and the arterial pulse from mother and foetuses were neglected.

Figure 5: Example of a hands-off phase with a 1 Hz low pass filter

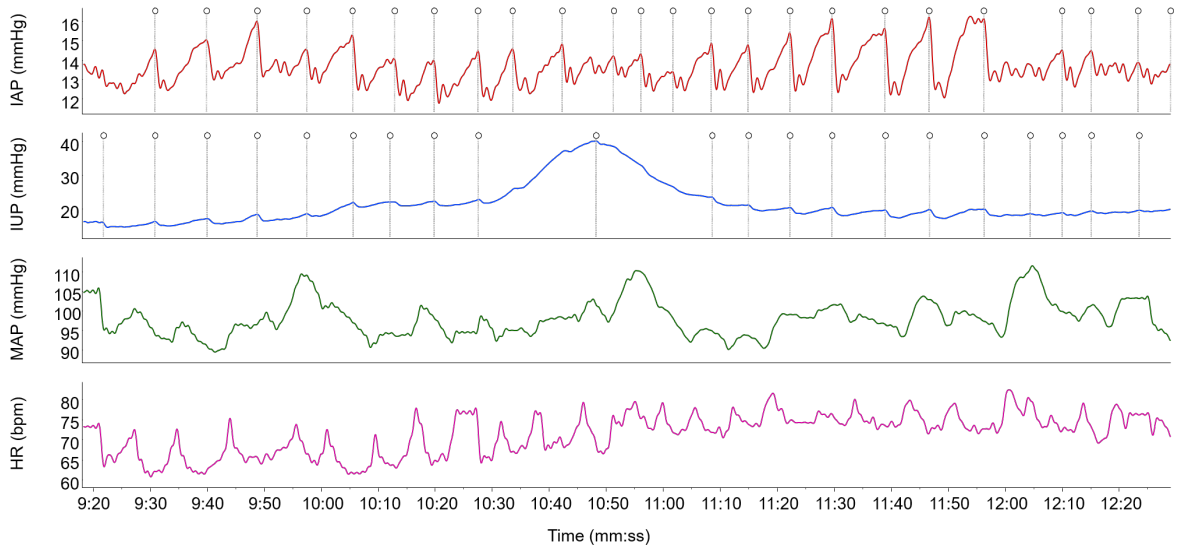

1 Hz low pass filter recording of a typical hands-off phase produced by amnioreduction (Detail from figure 2). The cyclic markers (circles) above the grid are added automically at the cyclic maxima. Intraabdominal pressure (IAP), intrauterine pressure (IUP), mean arterial pressure (MAP), heartrate (HR) (Extract from patient C, recorded at 20 Hz)

2.11.2 Contractile Interplay

For the analysis of the contractile pressure interplay a 0.1 Hz low pass filter was applied since the longest respiratory period observed had a 8.4 s duration, equalling a frequency of 0.12 Hz (see table 5). This filter neglected all respiratory changes such that solely the contractile long wave changes were remaining. The results are exemplified in figure 6.

Figure 6: Extract with a 0.1 Hz low pass filter

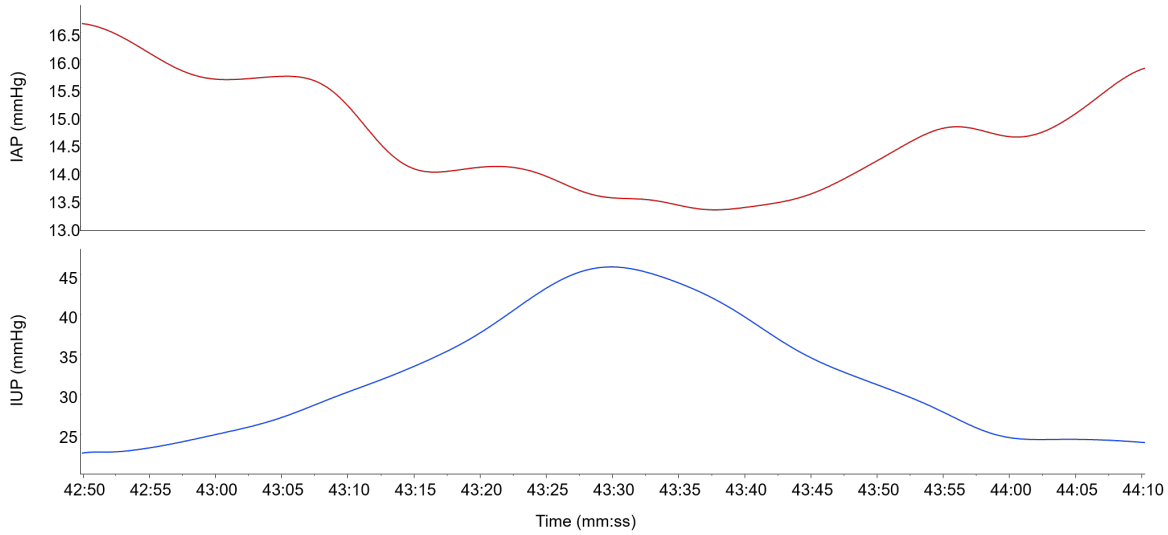

The graph exemplifies a typical long wave extract following amnioreduction with a 0.1 Hz low pass filter. Intraabdominal pressure (IAP), intrauterine pressure (IUP) (Extract from patient E, recorded at 20 Hz)

2.12 Statistical Methods

The general analysis was done by describing the mean pressures and comparing the prior and post amnioreduction values. Variables are summarised as means (± SD) or medians (range). All statistical analyses were performed with Stata (*Stata Corporation LP, Statistical Software: Release 12, College Station, USA*). The results were tested for normal distribution with the Shapiro Wilk test. Differences in means were tested for statistical significance with a Student's t-test for which a probability level of $P < 0.05$ was defined as significant. Linear regressions were used to analyse the relationships between the different pressures. Coefficients were tested for a significant difference from 0 with a 2-tailed t-test.

2.13 Ethical Approval

Prior to clinical measurements the ethical committee of the Medical University of Graz, Austria, has accepted and approved the study (registered at the Office for Human Research Protections of the US Departments of Health and Human Services, IRB00002556) under license 30-035 ex 17/18. Participants' data was saved and processed anonymously and access to the data was strictly restricted. Written informed consent was obtained from each patient. All measurements were in accordance with the declaration of Helsinki.

3 Results

3.1 Overview

Overall recordings were made of five patients who had a severe twin-twin transfusion syndrom and who had to undergo a fetoscopic laser ablation and amniodrainage at the Department of Obstetrics and Gynaecology of the Medical University of Graz. Patients were recruited between October 2018 and January 2020 and four recordings were successful and one recording was incomplete. The recordings of patient D had technical difficulties, since the tubes were snapped off below the operation sheet making a correcting during the operation impossible. Therefore, the analysis of this work is based on four patients.

The total interventions lasted in average for about one and a half hours and the amnioreduction between 30 to 60 minutes.

Of all patients included in the analysis the mean age was 26.3 years (23-29) and the mean BMI was 24.1 (19.7-29.1). At the time of measurement the gestational age was in average 20 weeks and 3 days. Two patients had a Quintero stage I and two a Quintero stage III TTTS. The median amnioreduction was 1500 ml (1400-3000 ml).

Table 3: Patient characteristics

ID	A	B	C	D	E	Median
Age (years)	26	23	27	34	29	27 (23-34)
Weight before pregnancy (kg)	70.0	48.0	42.0	62.0	79.0	62 (42.0-79.0)
Weight* (kg)	77.0	53.0	48.0	70.0	90.0	70.0 (48.0-90.0)
Height (cm)	166.0	164.0	156.0	172.0	176.0	166.0 (156.0-176.0)
Body Mass Index (kg/m^2)	27.9	19.7	19.7	23.7	29.1	23.7 (19.7-29.1)
Gestational Age* (weeks)	19w6d	20w6d	19w5d	19w3d	24w1d	19w6d (19w3d-24w1d)
Gravida/Para**	G1/P0	G1/P0	G2/P1	G3/P1	G1/P0	
Quintero Stage* (weeks)	III	III	I	III	I	
Uterine Volume (prior) (ml)	2560	2649	3583	1309	6909	2649 (1309-6909)
Uterine Volume (post) (ml)	1271	2175	2462	647	3124	2175 (647-3124)
Amnioreduction (ml)	1400	1400	1600	1000	3000	1400 (1000-3000)
Placental Thickness, prior (mm)	10	11	10	28	16	11 (10-28)
Placental Thickness, post (mm)	20	24	28	41	24	24 (20-41)

*At the date of intervention

**Gx/Py = Gravida (number of pregnancies)x / Para (number of births of viable offspring)y

Figure 7 exemplifies the typical course of an IUP recording. The first row shows the compressed recording across the complete intervention and the separation between the fetoscopic laser ablation and amnioreduction phase. Each row below is an extract of the previous one.

The second row makes the steep increases in the intrauterine pressure during the amnioreduction visible and the third extract shows a typical hands-off phase with the oscillating details expanded during a relative contraction free phase in the last diagram. The last diagram shows the circular markers above the grid added by the cyclic measurement tool to identify the cyclic maxima.

Maximum and minimum values during a hands-off phase are also illustrated in the third row, with the resulting δIUP. It also exemplifies $tIUP_{cont}$. The last row shows the cyclical analysis with a singular $tIUP_{resp}$ interval and a singular δIUP_{resp} highlighted.

Figure 7: Example of a complete intrauterine pressure recording

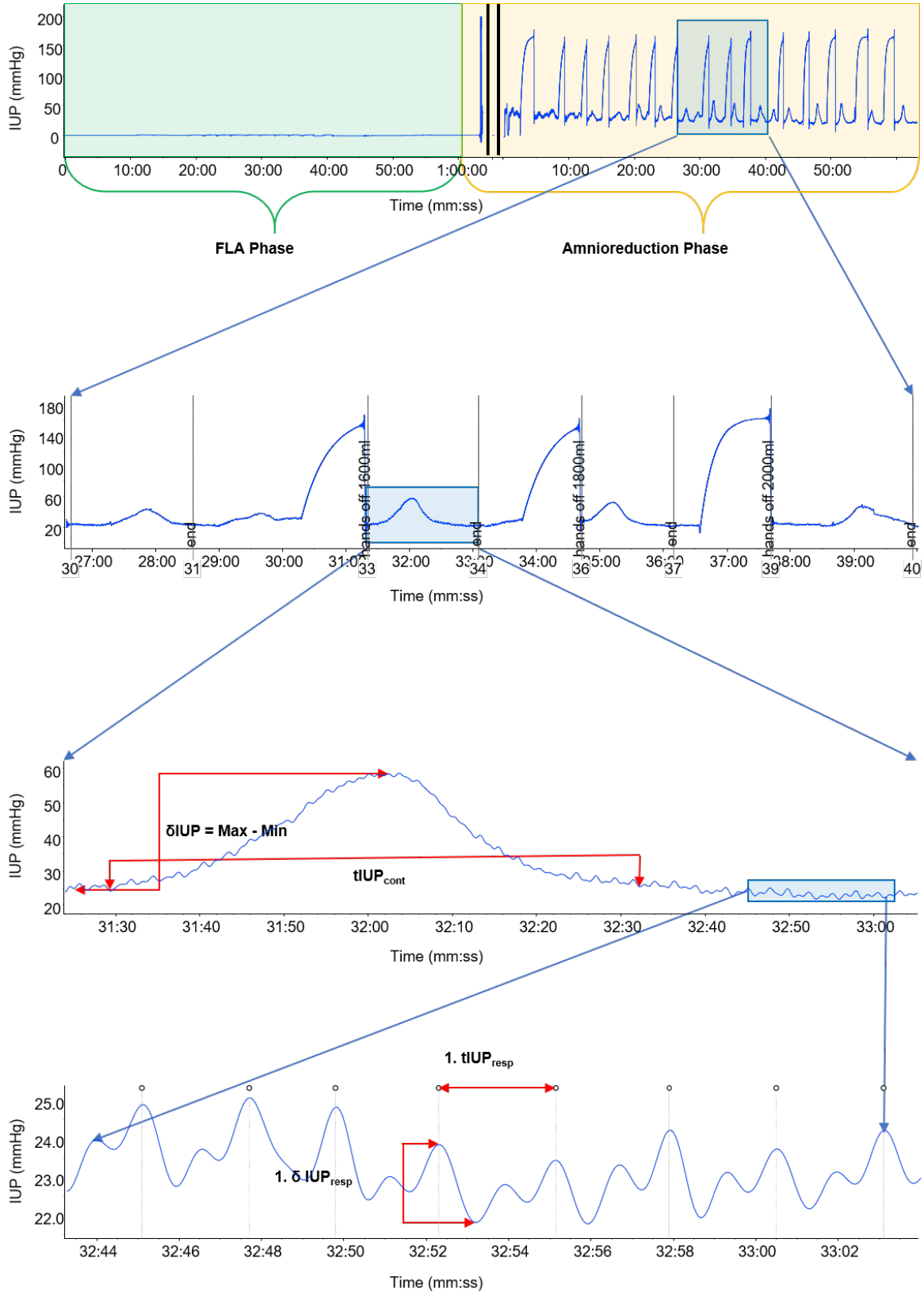

The graphic shows the dissection of an entire intrauterine pressure recording with the obtained variables exemplified and highlighted. The last row includes the automatically added cyclic markers (circles) above the grid. Intrauterine pressure (IUP), fetoscopic laser ablation (FLA) (Extract from patient E, recorded at 20 Hz)

3.2 Pressure Changes across Amnioreduction

Table 4: Summary of pressure changes across amnioreduction for all patients

Patient	A	B	C	E	Mean	SD
Amnioreduction (ml)	1400	1400	1600	3000	1850	
Pre IUP	26.9	21.8	18.2	32.2	24.8	5.3
Post IUP	15.1	10.9	12.0	16.4	13.6	2.2
ΔIUP	11.8	11.0	6.1	15.7	11.2*	3.4
Pre IAP	9.1	12.3	16.5	15.6	13.4	2.9
Post IAP	5.1	7.0	11.1	13.7	9.2	3.4
ΔIAP	4.0	5.3	5.4	1.9	4.2*	1.4
Pre PPP	40.6	46.7	73.2	55.7	54.0	12.3
Post PPP	25.1	43.3	80.6	66.1	53.8	21.2
ΔPPP	15.5	3.4	-7.4	-10.4	0.2	10.2

Based on minimum values during hands-off phases
Pre/Post values were measured before/after amnioreduction
* For a significance level of $P < 0.05$

Minimum intrauterine pressure values continuously decreased as the amnioreduction progressed, as illustrated in figure 8. The mean start pressure almost halved from 24.8±5.3 mmHg prior amnioreduction to 13.6±2.2 post amnioreduction ($P < 0.011$). The intrauterine pressure change between the start and end of the amnioreduction was on average 11.2 mmHg (see table 4).

Figure 8: Falling minimum intrauterine pressure in relation to the progress of amnioreduction

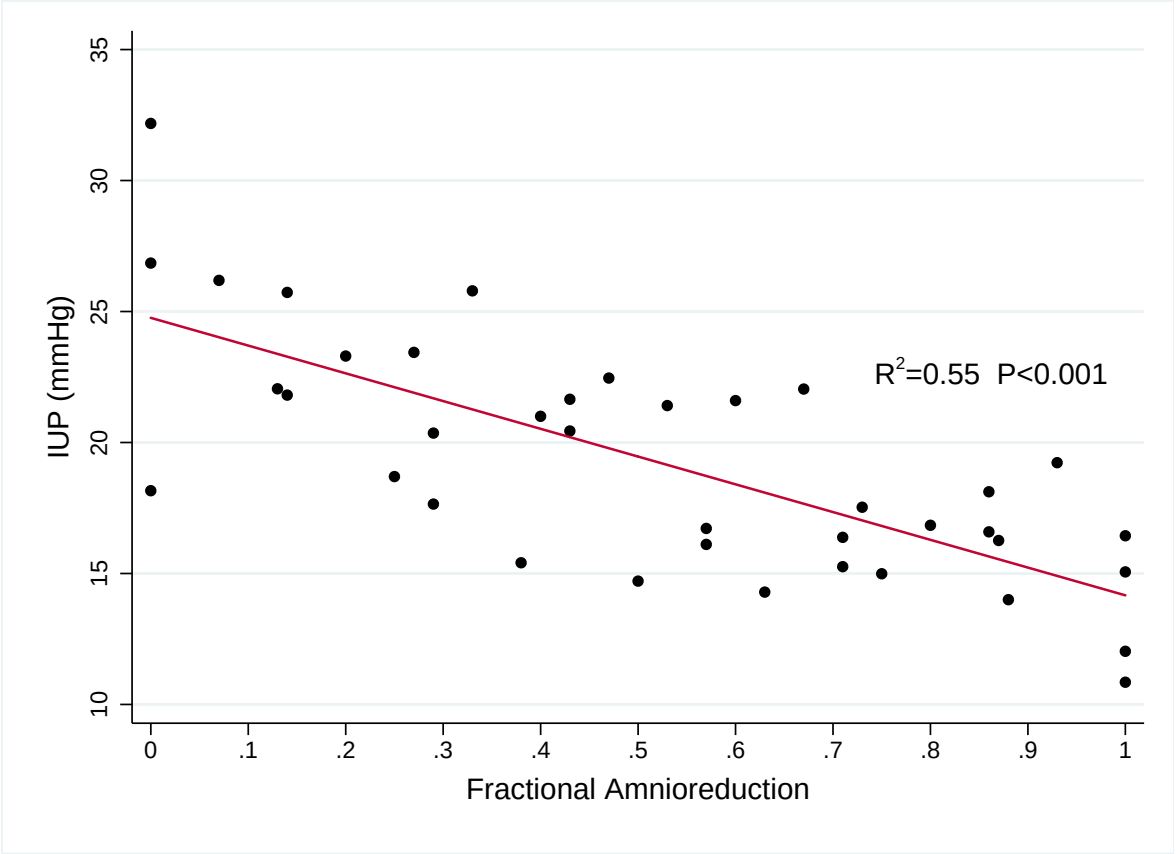

The minimum intrauterine pressure falls with the progress of the amnioreduction, shown by the negative linear regression $y = -10.6x + 24.7$ with $R^2 = 0.55$, P< 0.001. Fractional amnioreduction is the amnioreduction at any time point divided by the total amnioreduction of the patient. Intrauterine pressure (IUP), (n=4)

Intraabdominal pressure observations similarly fell during the course of the amnioreduction. In absolute terms the average intraabdominal pressure reduction was 4.2 mmHg. In advance of the amnioreduction the mean intraabdominal pressure was 13.4±2.9 mmHg which fell to 9.2±3.4 mmHg (P< 0.015) after the end of the amnioreduction (see table 4).

Figure 9: Falling minimum intraabdominal pressure in relation to the progress of amnioreduction

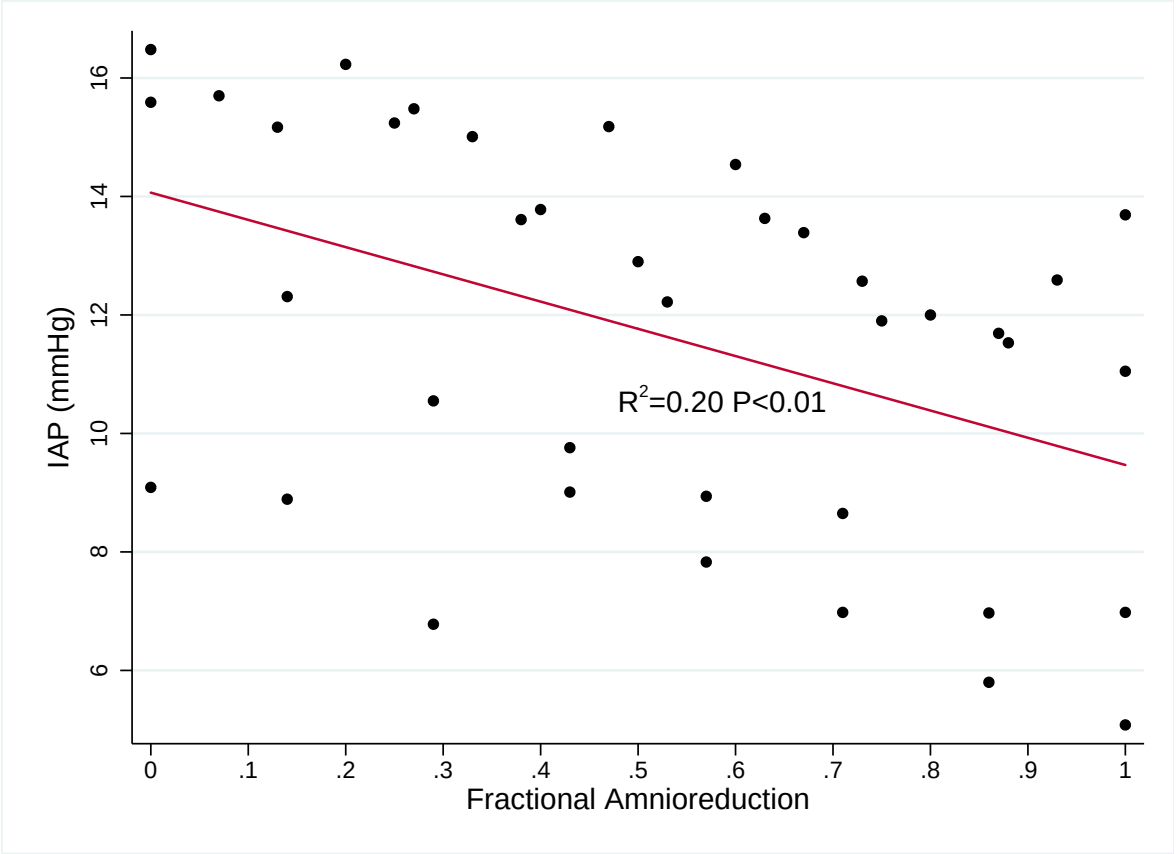

The minimum intraabdominal pressure falls with the progress of the amnioreduction, shown by the negative linear regression $y = -4.60x + 14.07$ with R^2 of 0.20, P< 0.01. Fractional amnioreduction is the amnioreduction at any time point divided by the total amnioreduction of the patient. Intraabdominal pressure (IAP), (n=4)

Following an amnioreduction step we regularly observed a significant (> 15mmHg) temporary IUP rise as exemplified in figure 5. These increased in intensity with the progress of the amnioreduction as illustrated in figure 10. The mean δIUP_{cont} after the first amnioreduction step was 11.6±5.7 mmHg and almost tripled to 29.6±17.2 mmHg after the amnioreduction was completed (P< 0.046).

Figure 10: Rising intrauterine pressure increases in relation to the progress of amnioreduction

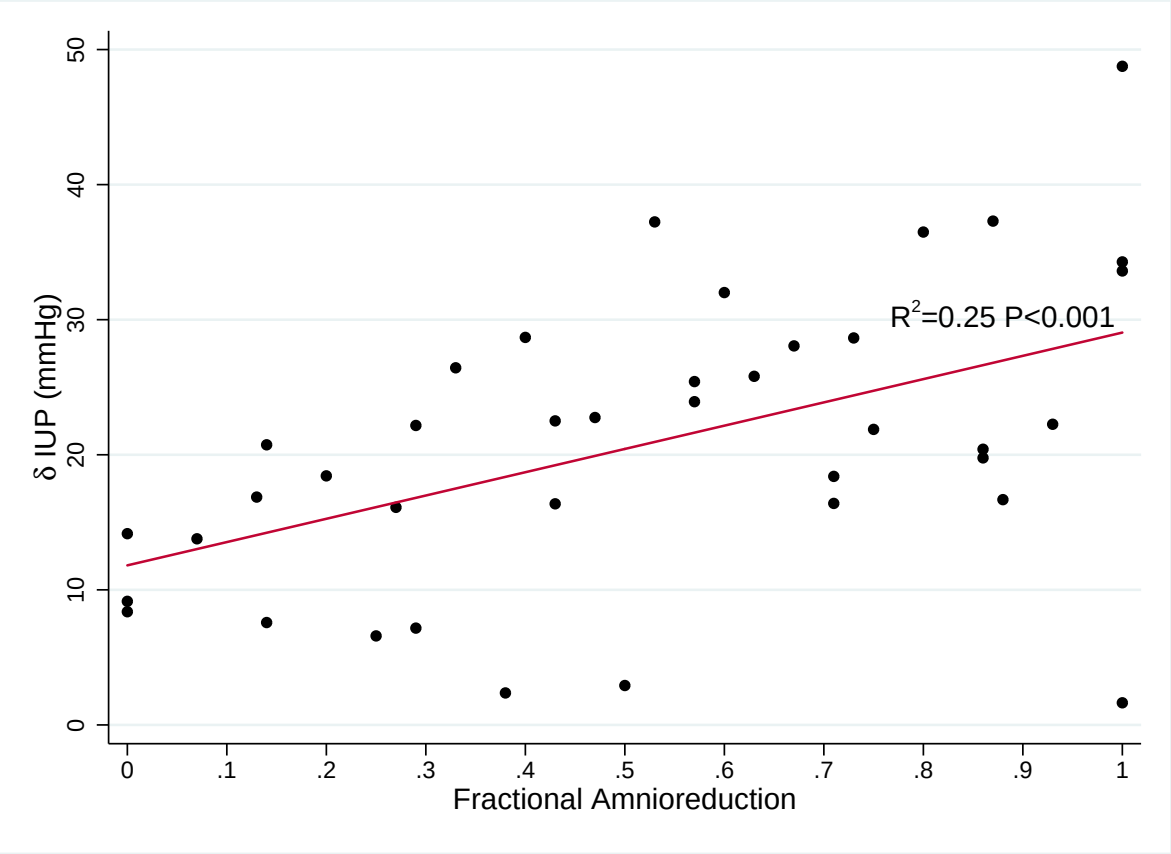

The intensity of the temporary elevated intrauterine pressure increases with the progress of the amnioreduction, shown by the positive linear regression $y = 17.23x + 11.8$ with a R^2 of 0.25, P$<$ 0.001. Fractional amnioreduction is the amnioreduction at any time point divided by the total amnioreduction of the patient. Only contractions with $\delta IUP_{cont} > 15$mmHg are considered. Intrauterine pressure (IUP), (n=4)

Although the δIUP_{cont} showed a positive trend across the amnioreduction, the time duration of the intrauterine pressure rises $tIUP_{cont}$ was stable (see figure 11).

Figure 11: Stable time duration of the intrauterine pressure rises in relation to the progress of amnioreduction

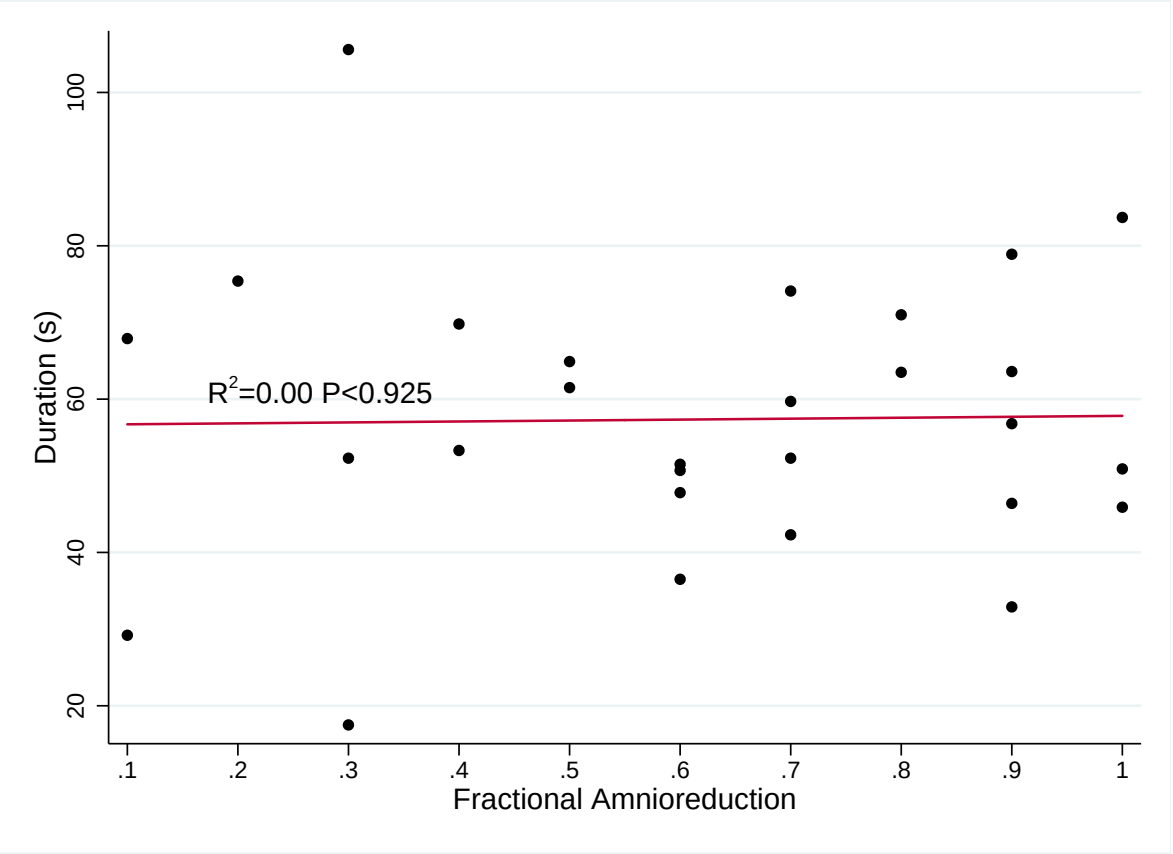

The duration of the elevated intrauterine pressure phases is stable against the amnioreduction progress and has a linear regression of $y = 1.2x + 57.2$ with a R^2 of 0.00, P$<$ 0.925. Fractional amnioreduction is the amnioreduction at any time point divided by the total amnioreduction of the patient. Intrauterine pressure (IUP), (n=4)

3.3 Intraabdominal and Intrauterine Pressure Interplay during low Frequency Intrauterine Pressure Rises

During low frequency intrauterine pressure increases, intraabdominal pressure often dropped. This observation became apparent when high frequency changes were masked as exemplified in figure 6. The figure illustrates the opposite directions of intraabdominal pressure and intrauterine pressure.

Figure 12 underlines this finding with a negative regression coefficient of -0.07 between IAP and IUP changes across all hands-off phases of patient E.

Figure 12: Falling intraabdominal pressure against intrauterine pressure during intrauterine pressure rises of patient E

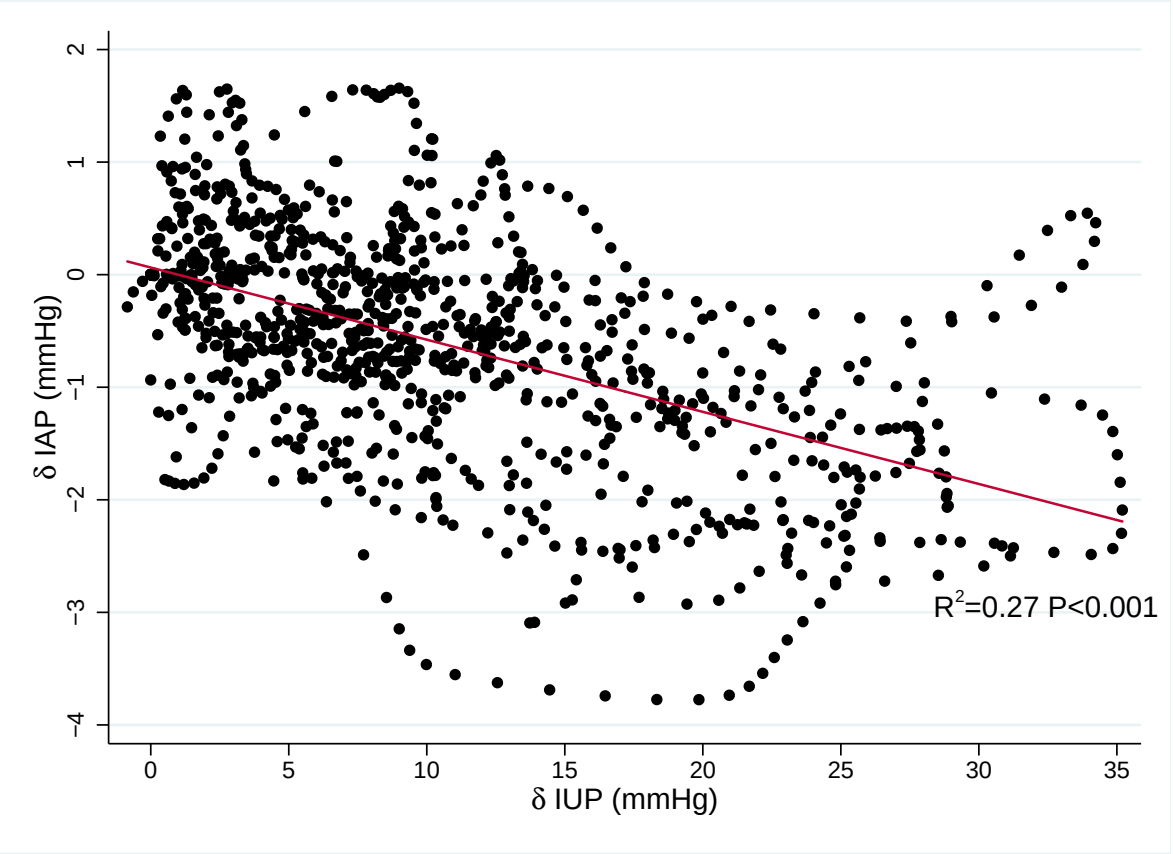

The diagram shows the low frequency intraabdominal pressure changes against intrauterine pressure changes during all hands-off phases of patient E. Only the time phases during which the actual intrauterine pressure rises occur were selected. At the beginning of each phase, IAP and IUP were levelled to zero to remove the negative effect of amnioreduction on IAP and IUP. The resulting IAP and IUP interplay is visualised and shows a negative regression coefficient of -0.07 with a coefficient of determination of 0.27 ($P < 0.001$). (a low pass filter of 0.1 Hz was applied and samples were extracted every second) Intraabdominal pressure (IAP), intrauterine pressure (IUP)

3.4 Intraabdominal and Intrauterine Pressure Interplay during high Frequency Oscillations

Contrary to the low frequency changes (see 3.3) the recurring movements of high frequency pressure changes followed the opposite direction: As intraabdominal pressure increased, intrauterine pressure rose. These cyclic changes are exemplified in figure 13 and were inspected independently of the amnioreduction progress. In absence of the low frequency changes intraabdominal pressure and intrauterine pressure had similar average cyclic pressure changes, 7.1 and 6.3 mmHg respectively, and an identical average period duration of 6.3 s (see table 5). The ratio between the average intrauterine pressure and intraabdominal pressure amplitude is 0.88. Across all patients' selected time periods the average time lag at the maxima points of IAP and IUP was 0.05 s. Therefore, the two pressures moved almost in phase in the same

direction.

FIGURE 13: AUTOMATICALLY DETECTED CYCLIC PRESSURE CHANGES OF PATIENT C

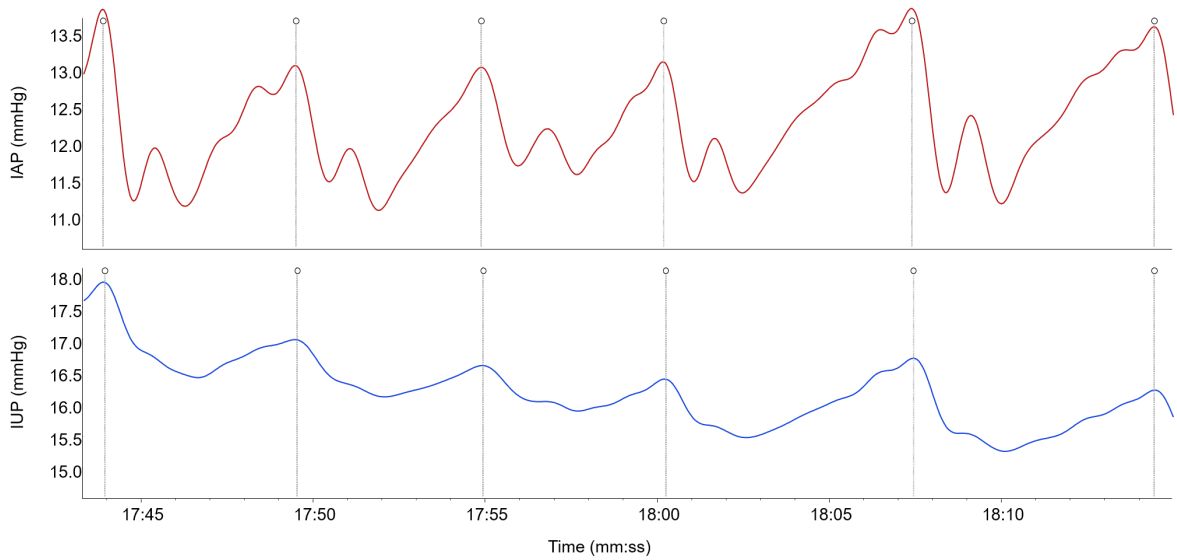

The graph exemplifies the automatically added markers at the maxima of the respiratory cyclic changes for both pressure recordings with an applied 1 Hz low pass filter. Intraabdominal pressure (IAP), intrauterine pressure (IUP) (Extract from patient C, recorded at 20 Hz)

TABLE 5: ANALYSIS OF THE CYCLIC CHANGES

Patient	Selection (s)	$tIUP_{resp}$ (s)	$tIAP_{resp}$ (s)	δIUP_{resp} (mmHg)	δIAP_{resp} (mmHg)	Number of Cycles IUP	Number of Cycles IAP	$\delta IUP_{resp}/\delta IAP_{resp}$
A*	44.1	7.4	7.1	4.3	3.8	5	5	0.88
B	47.2	8.4	8.4	13.9	12.2	5	5	1.14
	95.9	7.7	7.7	10.4	9.4	12	12	1.11
C	44.9	8.3	8.3	2.3	3.8	5	5	0.61
	34.3	6.1	6.1	1.1	2.3	5	5	0.48
E	35.5	3.2	3.2	6.0	8.4	10	10	0.71
	20.2	3.3	3.3	6.5	9.6	5	5	0.68
Mean		6.3	6.3	6.3	7.1			0.88

For each patient time periods during which the baseline IUP was almost constant were selected. The cycles were detected automatically and the average cycle period duration and average cyclic pressure amplitude was measured by LabChart.
*For patient A there was only one such time period available.

Figures 14, 16, 17, 18 visualise the close relationship between intraabdominal pressure and intrauterine pressure during high frequency changes. As intraabdominal pressure rises, intrauterine pressure moves the same direction.

Figure 14: Intrauterine pressure against intraabdominal pressure during cyclic changes for patient A

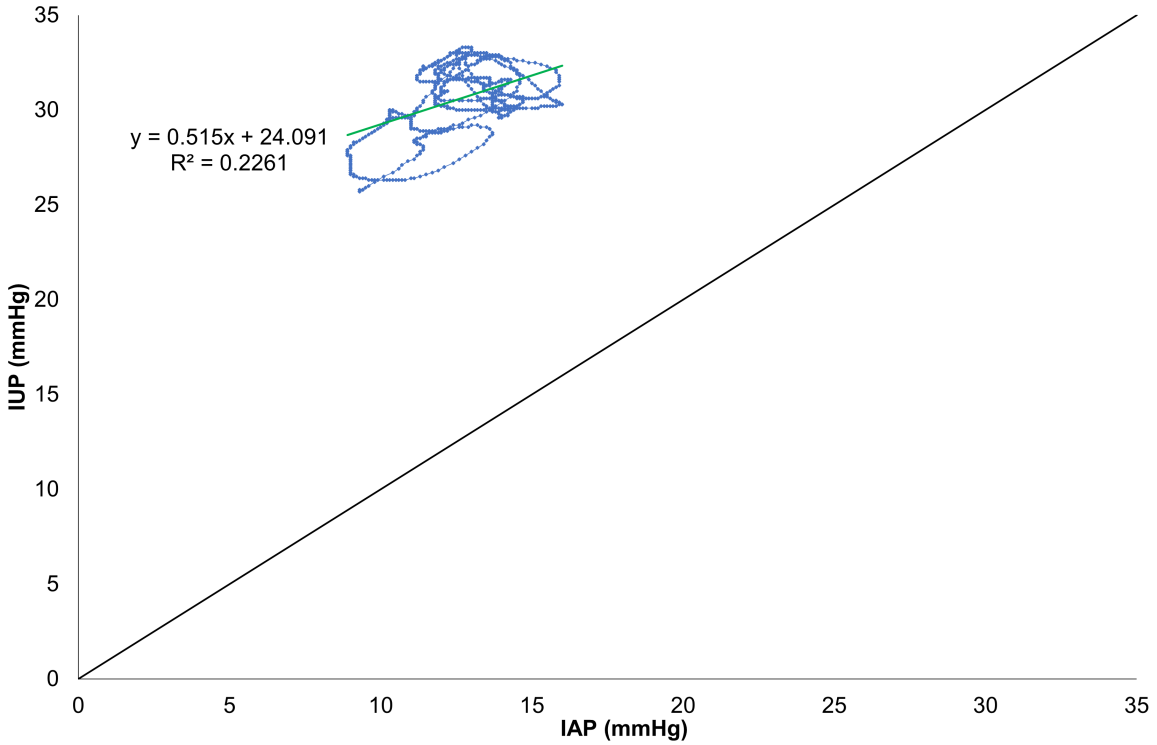

The relationship between IAP and IUP is positive for patient A with a regression coefficient of 0.52 and a R^2 of 0.23. The black line is an identity line. Intraabdominal pressure (IAP), intrauterine pressure (IUP)

Figure 14 shows a significant hysteresis which was caused by a low frequency intrauterine pressure rise across the selected time period, visualised in figure 15.

Figure 15: Intrauterine pressure and intraabdominal pressure during cyclic changes of patient A

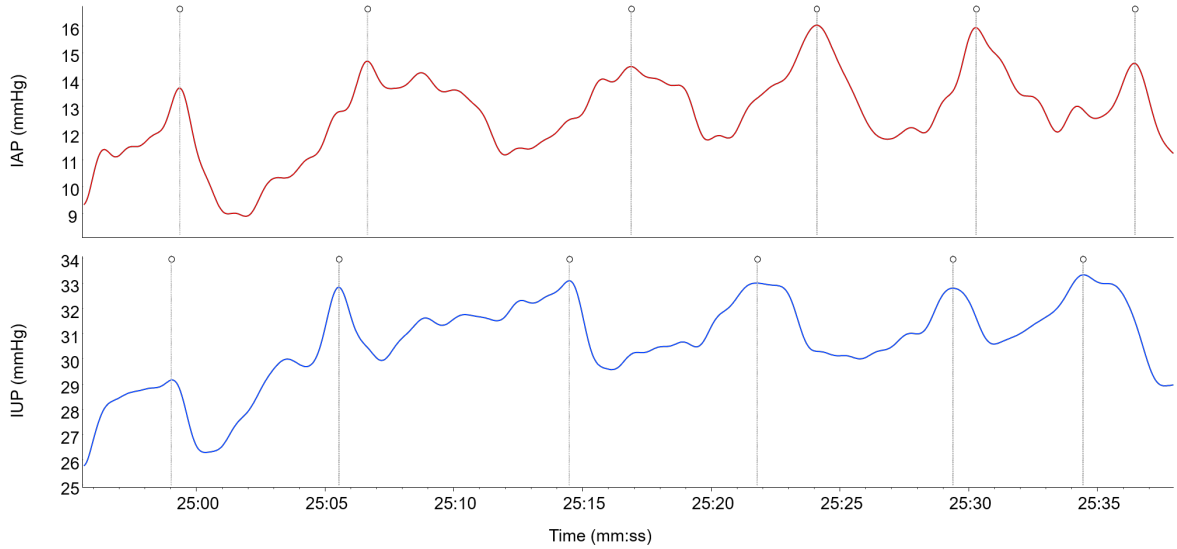

The selection shows a slow intrauterine pressure rise. Intraabdominal pressure (IAP), intrauterine pressure (IUP) (Extract from patient A, recorded at 20 Hz)

Figure 16: Intrauterine pressure against intraabdominal pressure during cyclic changes of patient B

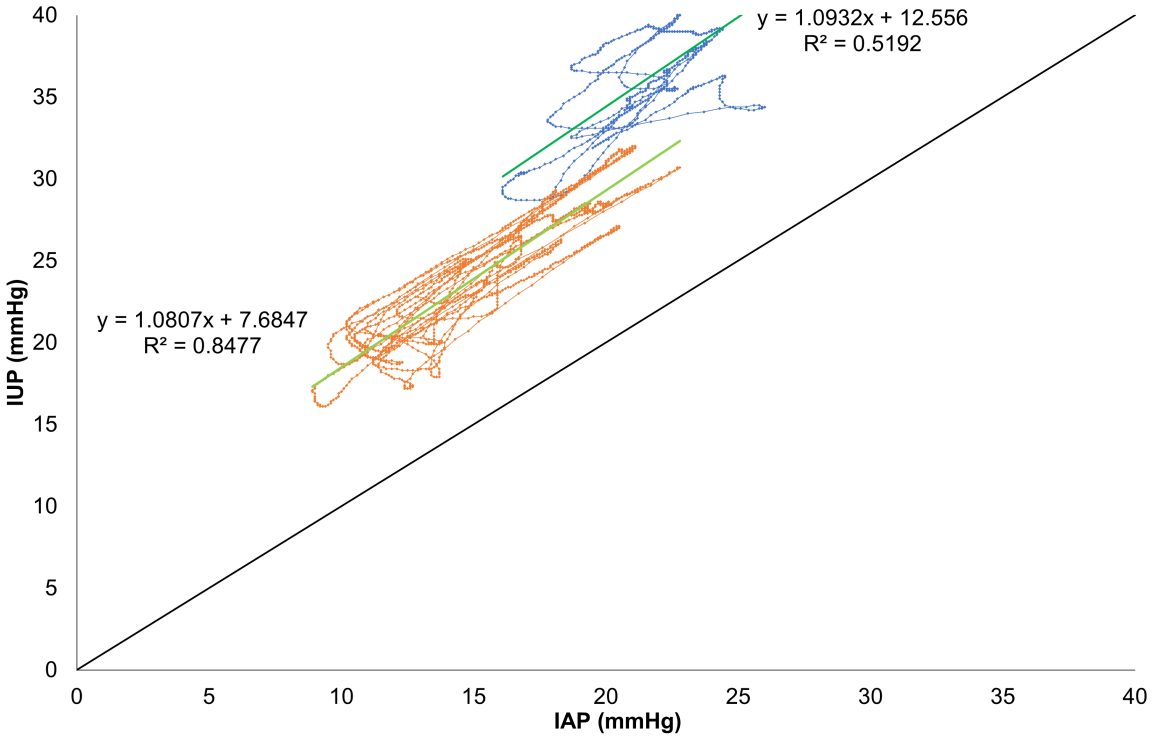

The relationship between IAP and IUP is positive for patient B in both selected time phases with regression coefficients of 1.08 and 1.09 and R^2 of 0.85 and 0.52 respectively. The black line is an identity line. Intraabdominal pressure (IAP), intrauterine pressure (IUP)

Figure 17: Intrauterine pressure against intraabdominal pressure during cyclic changes of patient C

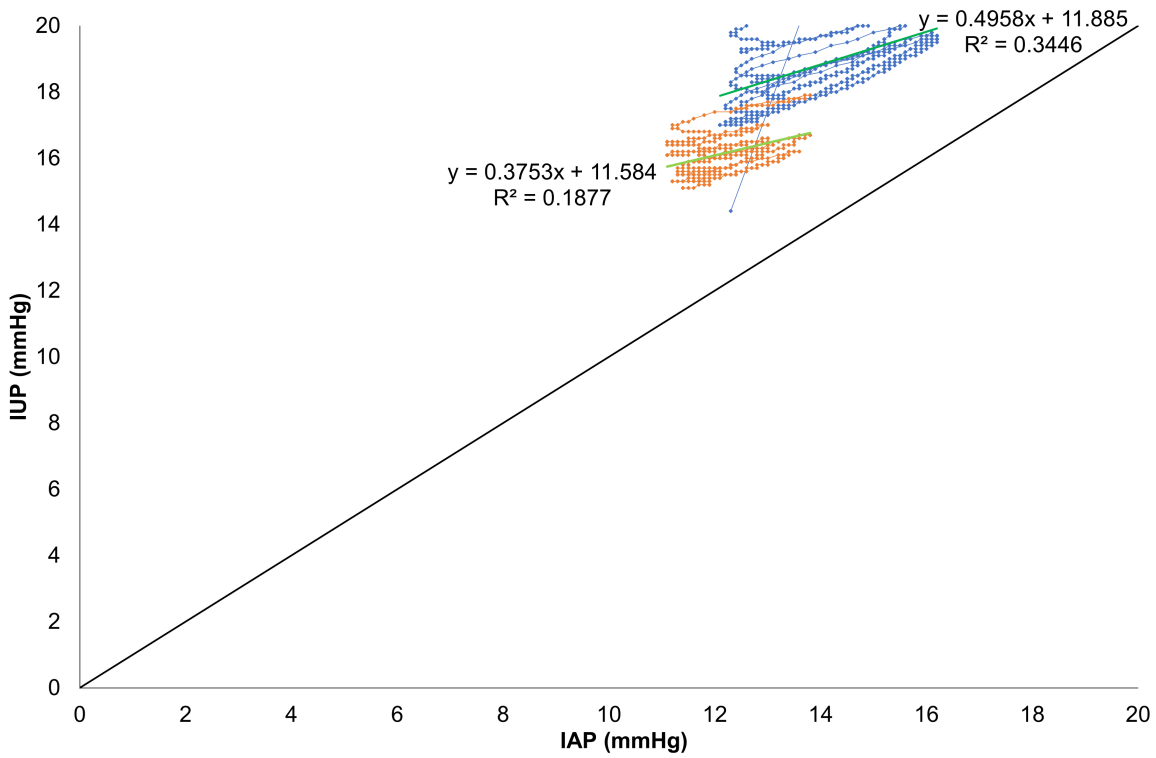

The relationship between IAP and IUP is positive for patient C in both selected time phases with regression coefficients of 0.37 and 0.50 and R^2 of 0.18 and 0.34 respectively. The black line is an identity line. Intraabdominal pressure (IAP), intrauterine pressure (IUP)

Figure 18: Intrauterine pressure against intraabdominal pressure during cyclic changes of patient E

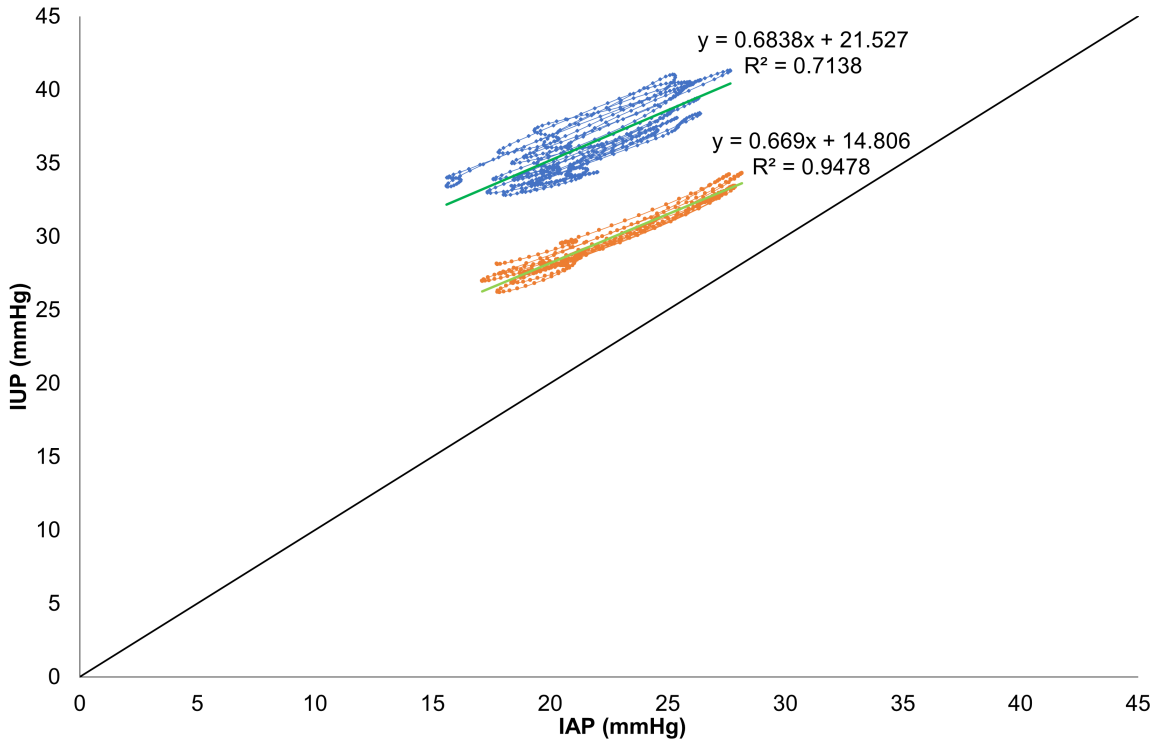

The relationship between IAP and IUP is positive for patient E in both selected time phases with regression coefficients of 0.68 and 0.67 and R^2 of 0.71 and 0.95 respectively. The black line is an identity line. Intraabdominal pressure (IAP), intrauterine pressure (IUP)

3.5 Placental Perfusion Pressure

During temporary uterine contractions we observed a reduction of the placental perfusion pressure, which in one instance temporarily fell below 30 mmHg (table 11).

The following three graphics (figures 20, 19 and 21) exemplify these observations.

Figure 19: Temporary placental perfusion reduction during uterine contraction

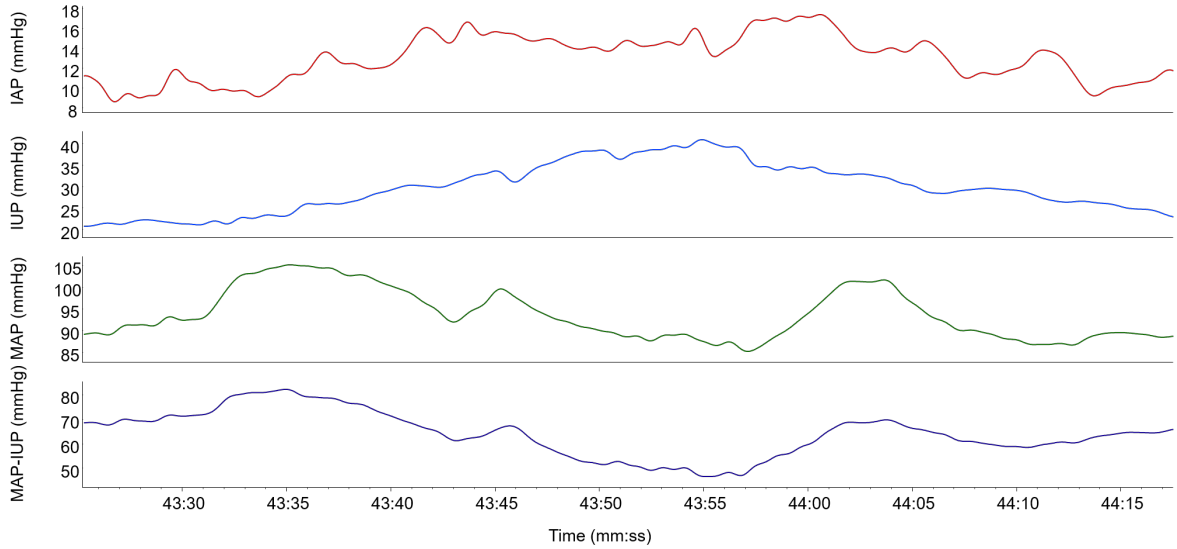

The graph shows the pressure recordings of IAP, IUP, MAP and PPP during a low frequency IUP rise. Intraabdominal pressure (IAP), intrauterine pressure (IUP), mean arterial pressure (MAP), Placental perfusion pressure (PPP), $PPP = MAP - IUP$ (Extract from patient A, recorded at 20 Hz)

Figure 20: Temporary placental perfusion reduction during uterine contraction

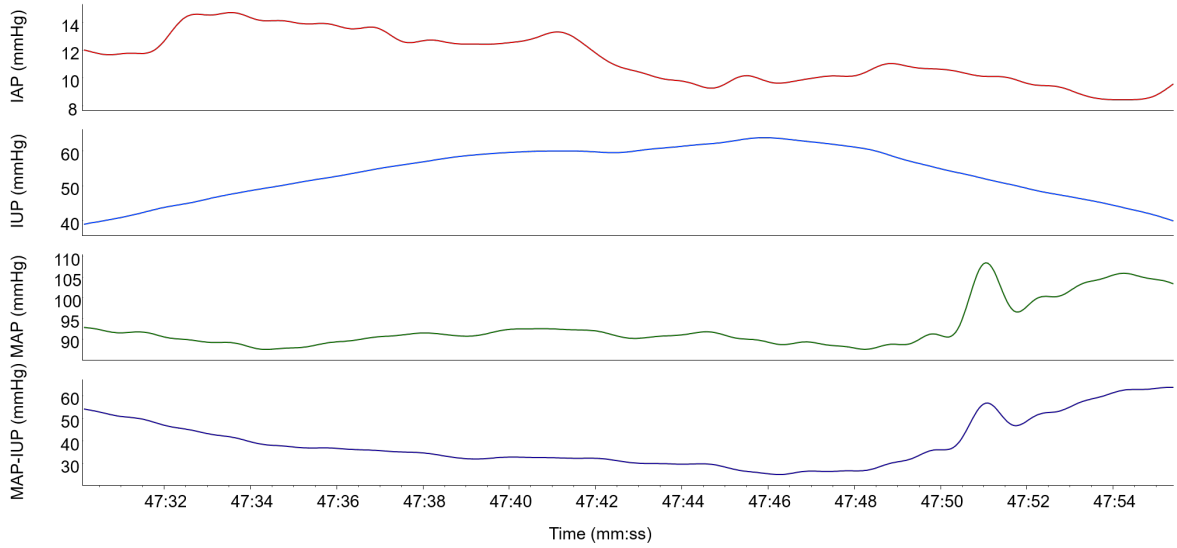

The graph shows the pressure recordings of IAP, IUP, MAP and PPP during a low frequency IUP rise. Intraabdominal pressure (IAP), intrauterine pressure (IUP), mean arterial pressure (MAP), Placental perfusion pressure (PPP), $PPP = MAP - IUP$ (Extract from patient A, recorded at 20 Hz)

Figure 21: Temporary placental perfusion reduction during uterine contraction

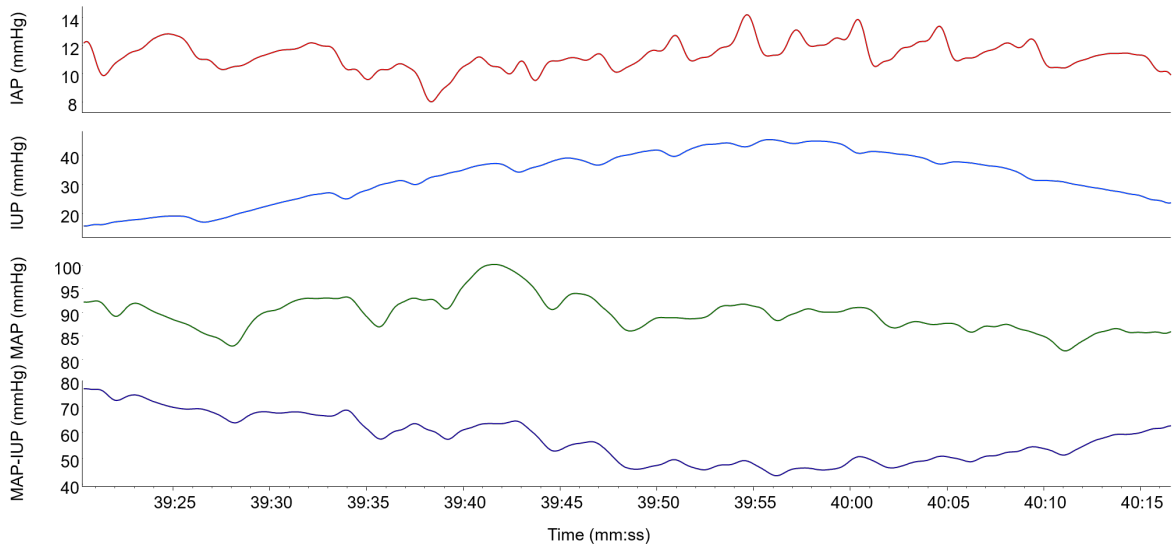

The graph shows the pressure recordings of IAP, IUP, MAP and PPP during a low frequency IUP rise. Intraabdominal pressure (IAP), intrauterine pressure (IUP), mean arterial pressure (MAP), Placental perfusion pressure (PPP), $PPP = MAP - IUP$ (Extract from patient B, recorded at 20 Hz)

The temporary placental perfusion pressure reductions were stable across the amnioreduction progress (see figure 22). The mean placental perfusion pressure pre amnioreduction was 54.0 mmHg and 53.8 mmHg post amnioreduction ($P < 0.483$).

Figure 22: Constant minimum placental perfusion pressure in relation to the progress of amnioreduction

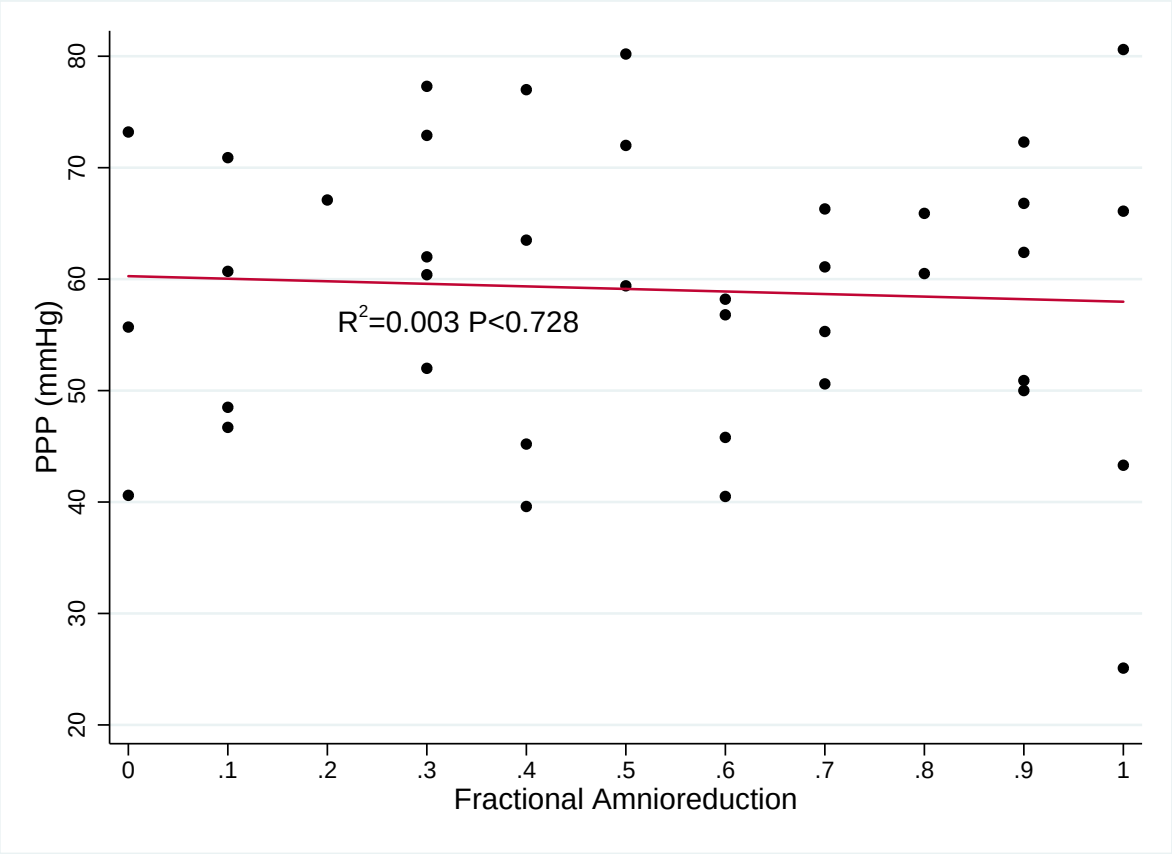

The placental perfusion pressure in relation to the progress of the amnioreduction was stable and has a linear regression of $y = -2.29x + 60.55$ with a R^2 of 0.003 (P< 0.728). Fractional amnioreduction is the amnioreduction at any time point divided by the total amnioreduction of the patient. Placental perfusion pressure (PPP), $PPP = MAP - IUP$ (n=4)

3.6 Elastance

The amnioreduction lead to a decrease in intrauterine pressure (see chapter 3.2) and the relationship between the change in volume and the change in pressure is the elastance (see figure 23). Values averaged out at 5.7 mmHg $\cdot$ l^{-1} across the four patients based on the intrauterine pressures. The elastance based on the transmural pressure ($IUP - IAP$) was on average 2.8 mmHg $\cdot$ l^{-1}.

Table 6: Elastance

	A	B	C	E	Mean	SD
Amnioreduction (ml)	1400	1400	1600	3000	1850	669
Elastance* (mmHg $\cdot$ l^{-1})	8.1	7.4	3.7	3.7	5.7	2.0
Elastance** (mmHg $\cdot$ l^{-1})	5.8	2.6	0.3	2.5	2.8	2.0

*Based on minimum IUP values during hands-off phases
**Based on minimum $IUP - IAP$ values during hands-off phases

Figure 23: Uterine elastance based on minimum intrauterine pressure and amnioticvolume

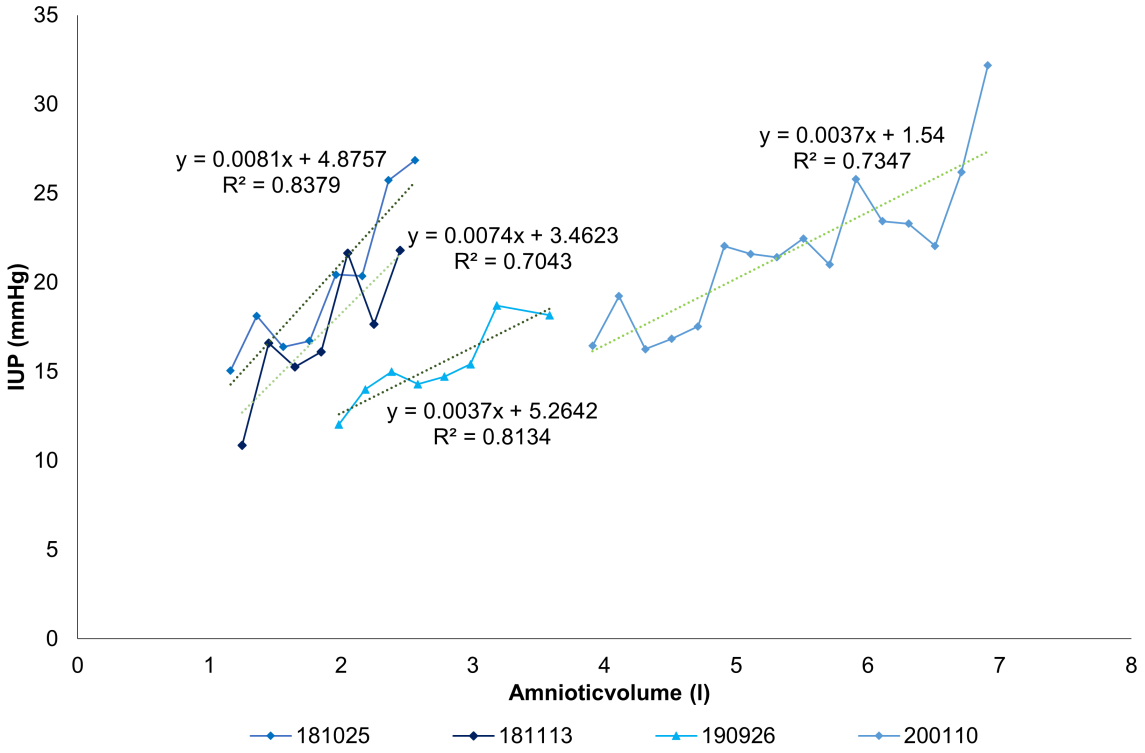

The elastance is the gradient between the change in volume and the change in pressure. Amnioticvolume is defined as the total amniotic volume derived by ultrasonic measurements minus the total amnioreduction at any time point. Intrauterine pressure (IUP)

Figure 24: Uterine elastance based on minimum transmural pressure and amnioticvolume

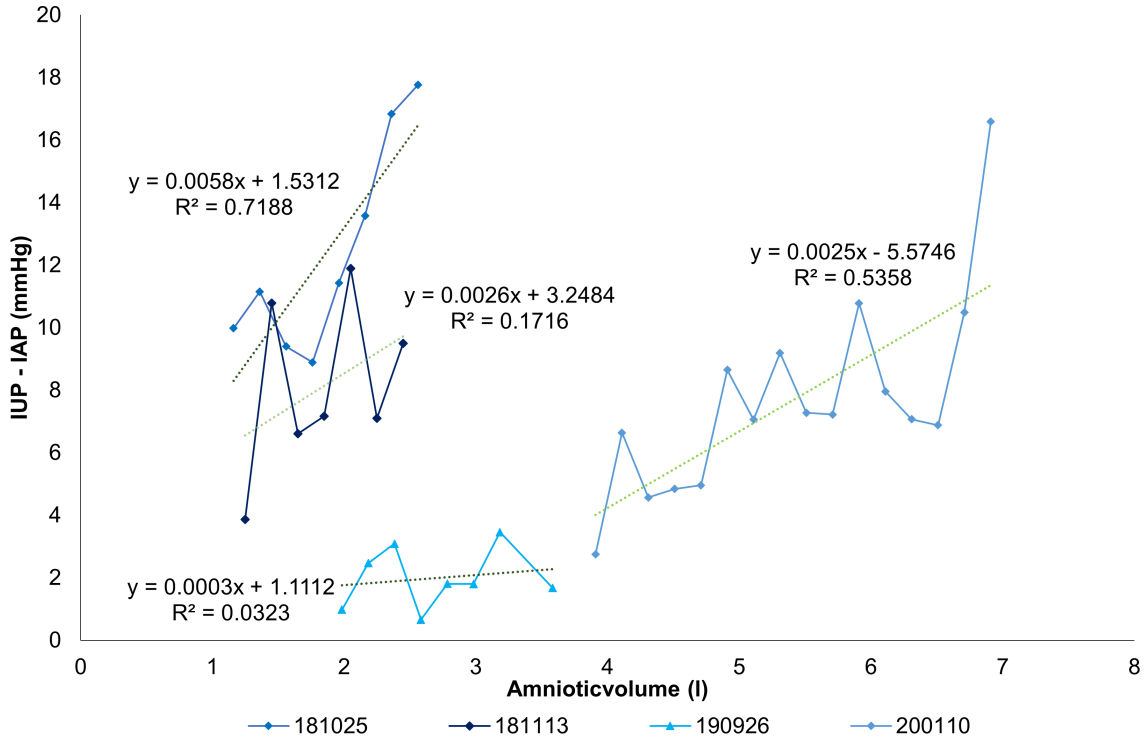

The elastance is the gradient between the change in volume and the change in pressure. Amnioticvolume is defined as the total amniotic volume derived by ultrasonic measurements minus the total amnioreduction at any time point. Transmural pressure $= IUP - IAP$, Intraabdominal pressure (IAP), intrauterine pressure (IUP)

4 Discussion

This work reports about temporary uterine contractions following amnioreduction and offers insights into the dynamics of the uterus and interactions with the abdominal- and mean arterial pressure. These findings are based on continuous and simultaneous IUP, IAP, HR and MAP recordings, where as past IUP research, such as by Sideris and Nicolaides (1990), N. M. Fisk et al. (1992), and more recently by Katsura et al. (2018), focused on single pressure values and their progress during gestation.

The minimum intrauterine pressure almost halved with a mean intrauterine pressure reduction of 11.2 mmHg and a mean intraabdominal pressure fall of 4.2 mmHg during the course of amnioreduction. These results are consistent with existing literature, supporting the reliability of our methodology (Bruner and Crean, 1999; Garry et al., 1998; Greimel et al., 2020). The reduction of the amniotic volume decreases intrauterine pressure due to the elasticity of the uterine muscular wall.
The detected temporary intrauterine pressure rises are contractions after amnioreduction and this work suggests that these are a protective measure to limit the volume shift, also called 'steal' phenomenon, into the placenta. In another work our research group observed an increase in placental thickness caused by the volume shift during amnioreduction and uterine decompression, which has possible negative effects on the foetuses and the maternal haemodynamics (Rodeck et al., 2006; van den Wijngaard, Jeroen P. H. M., Umur, Michael G. Ross, et al., 2008; Jones et al., 2012; Greimel et al., 2020). The contractions could possibly temporarily halt or even undo these harmful haemorrhagic changes. They reached pressures of up to 63.8 mmHg (see table 8) and lasted on average 44.1 s (see table 9). Therefore, contractions following amnioreduction achieved levels in the range of labour contractions (Caldeyro-Barcia and Poseiro, 1960).
The releasing mechanism behind this reaction remains unclear. However, it cannot be explained by the theory of cellular stretch-induced muscular contraction (Wray, 1993; Wray et al., 2015) since the amnioreduction reduces the myometrial stretch.

The simultaneous intrauterine pressure and intraabdominal pressure recordings show that during uterine contractions intraabdominal pressure fell (exemplified in figure 6). This negative relationship is illustrated in figure 12 for patient E.
This observation undermines the suggested purpose of the uterine contractions: we assume

the reduction in intraabdominal pressure is caused by a fall in the hydrostatic abdominal compartment's content due to a shrinkage in the uterus' total volume. Within the uterus the only condensable compartment is the placenta due to its volume variability. We suggest the rise in intrauterine pressure compresses the placenta and shifts volume back into the maternal circulation to reduce the possible negative effects of the 'steal' phenomenon, as illustrated in figure 25

FIGURE 25: UTERINE CONSEQUENCES OF LARGE VOLUME AMNIOREDUCTION

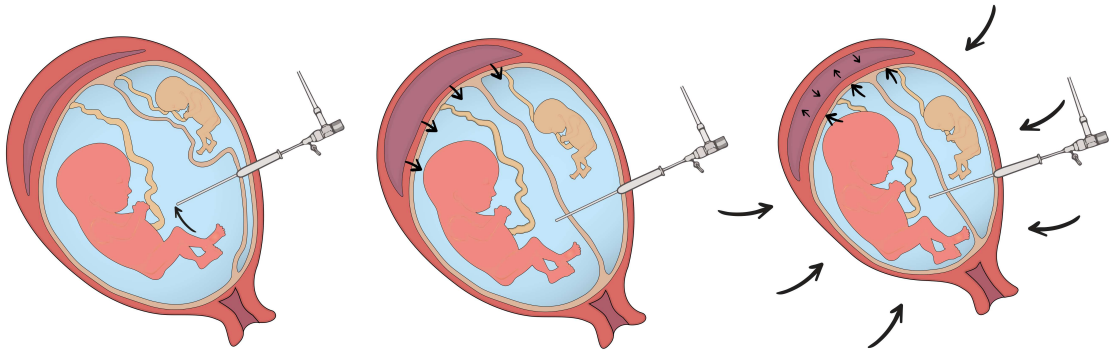

The diagram on the left illustrates the amnioreduction. It is followed by a uterine decompression, leading to a placental expansion, called 'steal' phenomena (middle diagram). The diagram on the right shows the uterine contraction, leading to an increased pressure on the placenta, thereby reducing its blood volume and size.

During the contractions placental perfusion pressure fell, in one observation below 30 mmHg (table 11). Presumably this decline causes the reduction in oxygenation during uterine contractions observed in magnetic resonance imaging (Sinding et al., 2016). Sinding et al. noticed a placental oxygenation decrease after approximately 30 s of ongoing uterine contractions. One minute after the end of a contraction oxygenation fully restored. Thereby, during large volume amnioreductions the foetal oxygenation is probably affected for more than a minute since on average the recorded uterine contractions lasted for 44.1 s.

If the low placental perfusion pressure levels are worrying for healthy singleton pregnancies, as in the work by Sinding et al., the limited placental perfusion and oxygenation levels are all the more worrying for twin pregnancies affected by twin-twin transfusion syndrom. The twins with cardiac output failure are in a weaker position to compensate negative external influences which could result in long term damages.

This observation exposes the necessity of re-evaluating amnioreduction procedures. The aim should be to provide a stable placental perfusion pressure throughout the intervention. It remains to be examined whether smaller amnioreduction steps limit the uterine contractions and thereby reduce the possible harm to the foetuses.

The continuous intrauterine pressure and intraabdominal pressure recordings during contraction-free phases provide evidence of the close interaction between abdomen and uterus for humans for the first time. They also reveal their progress in phase with an average time lag of 0.05 s (see figures 14, 16, 17 and 18). Since the average period duration was 6.3 s we presume that the cyclic changes were caused by respiration, with a mean respiratory rate of 9.5 min^{-1}.
Inside the thorax the pressure falls during inspiration and rises during expiration. The diaphragm and the thoracic muscles generate these pressure changes which are transmitted to the abdominal cavity and in turn passed on to the uterus.
In this work the average $\delta IUP_{resp}/\delta IAP_{resp}$ ratio was 0.88 %. Therefore, the abdominal pressure transmission for humans onto the uterus reaches a level of 88%. This level is similar to the value of 80 % for rabbits (Karnak et al., 2008) and shows that the human uterus is highly sensitive to external intraabdominal pressure changes. This could be of special relevance for intraabdominal hypertension patients. The 12% transmission loss reflects the relative stiffness of the muscular uterine wall.
Contrary to our predictions the $\delta IUP_{resp}/\delta IAP_{resp}$ ratio was > 1 for patient B, unlike that of the other patients. We have no valid explanation for this result. However, a possible hypothesis is that the bladder could have been more immobile due to the narrow figure (BMI=19.7) and the gravid uterus. Thereby, the transmission of the respiratory pressure changes from the upper abdomen to the bladder could have been deficient. Since the uterus is located above the bladder during pregnancy, intraabdominal pressure changes may have been primarily absorbed by the uterus. This exemplifies that the indirect measurement of the intraabdominal pressure via the intravesical pressure has limitations which must be remembered during pregnancy.

The uterine elastance of the four patients was on average $5.7\,\mathrm{mmHg} \cdot \mathrm{l}^{-1}$ and halved for the transmural value to $2.8\,\mathrm{mmHg} \cdot \mathrm{l}^{-1}$. Therefore, a reduction in the uterine volume by one litre caused a fall in the intrauterine pressure and transmural intrauterine pressure by 5.7 and 2.8 mmHg respectively.
These values are the first of its kind for humans in the physiologic literature. So far, only the cervix' elastance was thoroughly investigated as the recent methodological overview by Hee (2014) shows. These new elastance values could be of great interest for future mathematical uterine models which used estimates until now.
Although the results for each singular patient show a linear relationship, figure 23 suggests

a trend among the elastance: based on intrauterine pressure values only, smaller uteri and less severe polyhydramnions have a higher elastance than larger uteri. This trend could be explained by the law of Laplace as smaller uteri have smaller radii. The law implies that a sphere's internal pressure is inversely proportional to the radius and therefore smaller uteri require higher pressures to establish the equilibrium state between the inside and outside pressure on the sphere's wall. Additional pressure recordings are required to provide further evidence for this trend.

Overall, the statistical significance of the observations remains limited due to the relatively modest number of patients of this pilot study. In contrast to the direct intrauterine pressure recordings all intraabdominal pressure measurements of this work were an indirect approximation via the urinary bladder. As suggested in patient B, gravid uteri could further reduce the accuracy of measurements, as the bladder should move freely for accurate pressure recordings (Malbrain, Manu L. N. G., 2004). However, enlarged gravid uteri could restrict this freedom of movement and thereby reduce the accuracy.

We chose 50 ml of saline solution as the bladder fill volume, since this is the standard volume of the Department of Anaesthesia at the Medical University of Graz. However, this is not in line with the official World Society of Abdominal Compartment Syndrome guidelines (Malbrain, Manu L. N. G. et al., 2006). These recommend 25 ml as priming bladder volume since a larger volume increases the average intraabdominal pressure recordings (J. d. Waele et al., 2006). Therefore, our intraabdominal pressure measurements might be slightly elevated. However, this should not affect relative pressure observations.

A peculiarity of pilot studies is the continuous improvement of the methodology during the ongoing study. The low frequency observations require sufficiently long hands-off phases. Unfortunately, at the beginning of the study the hands-off phases were too short since it was still unknown for how long the temporary uterine contractions would last. These shorter hands-off periods made it difficult to identify a contraction and even harder to find the baseline intrauterine pressure level. For patient E these phases were extended to a minimum of one minute and thereby the quality of the recordings and the analysis improved. This is likely the reason the opposite movement of intraabdominal pressure and intrauterine pressure during uterine contractions was only detectable in patient E. These relatively long time periods (>1 minute) should be used for future recordings.

5 Conclusion

In this work we showed that amnioreductions are followed by firm temporary contractions, which is, to our knowledge, a novel observation. We suggest that this reaction to amnioreducion is a protective measure to undermine the volume shift into the decompressed uterus which could be of clinical relevance for mother and foetuses. Further, we showed that placental perfusion is reduced during these contractions. This should be remembered for amnioreduction in the future. The interactions between intraabdominal pressure and intrauterine pressure showed that the uterus is, with a pressure transmission of 88%, highly sensitive to any abdominal pressure change.

It would be desirable to conduct further research in this area, as stepwise amnioreduction provides a unique opportunity to study the intrauterine pressure dynamics. A larger number of patients would certainly generate a deeper understanding, thereby improving the amnioreduction procedures and foetal safety.

References

Aston, Kenneth I., C. Matthew Peterson, and Douglas T. Carrell (2008). "Monozygotic twinning associated with assisted reproductive technologies: a review". In: *Reproduction* 136.4, pp. 377–386. ISSN: 1470-1626. DOI: 10.1530/rep-08-0206.

Attah, A. A. and J. M. Hutson (1993). "The role of intra-abdominal pressure in cryptorchidism". In: *The Journal of urology* 150.3, pp. 994–996. ISSN: 0022-5347.

Bajoria, Rekha, Mark Sullivan, and Nicholas M. Fisk (1999). "Endothelin concentrations in monochorionic twins with severe twin-twin transfusion syndrome". In: *Human Reproduction* 14.6, pp. 1614–1618. ISSN: 1460-2350. DOI: 10.1093/humrep/14.6.1614.

Bajoria, Rekha, Stuart Ward, and Ratna Chatterjee (2002). "Natriuretic peptides in the pathogenesis of cardiac dysfunction in the recipient fetus of twin-twin transfusion syndrome". In: *American Journal of Obstetrics and Gynecology* 186.1, pp. 121–127. ISSN: 0002-9378. DOI: 10.1067/mob.2002.118845.

Baxi, Laxmi V. and Colin A. Walsh (2010). "Monoamniotic twins in contemporary practice: a single-center study of perinatal outcomes". In: *The Journal of Maternal-Fetal & Neonatal Medicine* 23.6, pp. 506–510. ISSN: 1476-7058. DOI: 10.3109/14767050903214590.

Berghella, Vincenzo and Marion Kaufmann (2001). "Natural history of twin-twin transfusion syndrome". In: *The Journal of reproductive medicine* 46.5, pp. 480–484. ISSN: 0024-7758. DOI: 10.5005/jp-journals-10009-1251.

Bos, Willem Jan W., Jeroen van Goudoever, Gert A. van Montfrans, van den Meiracker, Anton H., and Karel H. Wesseling (1996). "Reconstruction of brachial artery pressure from noninvasive finger pressure measurements". In: *Circulation* 94.8, pp. 1870–1875.

Bruner, J. P. and D. M. Crean (1999). "Equalization of amniotic fluid volumes after decompression amniocentesis for treatment of the twin oligohydramnios-polyhydramnios sequence". In: *Fetal Diagn Ther* 14.2, pp. 80–85. ISSN: 1015-3837. DOI: 10.1159/000020894.

Caldeyro-Barcia, Roberto and Juan Poseiro (1960). "PHYSIOLOGY OF THE UTERINE CONTRACTION". In: *Clinical Obstetrics and Gynecology* 3.2, pp. 386–410. ISSN: 0009-9201. URL: https://journals.lww.com/clinicalobgyn/Fulltext/1960/06000/PHYSIOLOGY_OF_THE_UTERINE_CONTRACTION.11.aspx.

Chun, R., L. Baghirzada, C. Tiruta, and A. W. Kirkpatrick (2012). "Measurement of intra-abdominal pressure in term pregnancy: a pilot study". In: *International Journal of Obstetric Anesthesia* 21.2, pp. 135–139. ISSN: 0959-289X. DOI: 10.1016/j.ijoa.2011.10.010.

Chun, R. and A. W. Kirkpatrick (2012). "Intra-abdominal pressure, intra-abdominal hypertension, and pregnancy: a review". In: *Annals of Intensive Care* 2.1, S5. ISSN: 2110-5820. DOI: 10.1186/2110-5820-2-S1-S5. URL: https://annalsofintensivecare.springeropen.com/track/pdf/10.1186/2110-5820-2-S1-S5.

Coren, Richard L. and Arpad I. Csapo (1963). "The intra-amniotic pressure". In: *American Journal of Obstetrics and Gynecology* 85.4, pp. 470–483. ISSN: 0002-9378. DOI: 10.1016/S0002-9378(16)35490-4.

Csapo, Arpad (1970). "The diagnostic significance of the intrauterine pressure". In: *Obstetrical & gynecological survey* 25.6, pp. 515–543. ISSN: 0029-7828.

Denbow, Mark L., Philip Cox, Myles Taylor, Donna M. Hammal, and Nicholas M. Fisk (2000). "Placental angioarchitecture in monochorionic twin pregnancies: Relationship to fetal growth, fetofetal transfusion syndrome, and pregnancy outcome". In: *American Journal of Obstetrics and Gynecology* 182.2, pp. 417–426. ISSN: 0002-9378.

Diehl, W., A. Diemert, D. Grasso, S. Sehner, K. Wegscheider, and K. Hecher (2017). "Fetoscopic laser coagulation in 1020 pregnancies with twin-twin transfusion syndrome demonstrates improvement in double-twin survival rate". In: *Ultrasound in obstetrics & gynecology : the official journal of the International Society of Ultrasound in Obstetrics and Gynecology* 50.6, pp. 728–735. DOI: 10.1002/uog.17520.

Faber, J.Job and Antonio Barbera (1992). "Convention for reporting amniotic fluid pressure". In: *European Journal of Obstetrics & Gynecology and Reproductive Biology* 47.3, pp. 181–184. ISSN: 03012115. DOI: 10.1016/0028-2243(92)90148-R.

Fieni, Stefania, Dandolo Gramellini, Giovanni Piantelli, Carla Verrotti, and Davide Cavallotti (2004). "Twin-twin transfusion syndrome: a review of treatment option". In: *Acta bio-medica: Atenei Parmensis* 75, pp. 34–39. ISSN: 0029-7844. DOI: 10.1097/01.aog.0000136119.78147.82.

Fisk, N. M., D. Ronderos-Dumit, Y. Tannirandorn, U. Nicolini, D. Talbert, and Charles H. Rodeck (1992). "Normal amniotic pressure throughout gestation". In: *BJOG: An International Journal of Obstetrics and Gynaecology* 99.1, pp. 18–22. ISSN: 1470-0328. DOI: 10.1111/j.1471-0528.1992.tb14385.x.

Fisk, Nicholas M., Yuen Tannirandorn, Umberto Nicolini, David G. Talbert, and Charles H. Rodeck (1990). "Amniotic pressure in disorders of amniotic fluid volume". In: *Acta bio-medica: Atenei Parmensis* 76.2, pp. 210–214. ISSN: 0029-7844.

Garry, David, Andrzej Lysikiewicz, Jonathan Mays, Joseph Canterino, and Nergesh Tejani (1998). "Intra-amniotic pressure reduction in twin-twin transfusion syndrome". In: *Journal of Perinatology* 18.4, pp. 284–286. ISSN: 0743-8346.

Gizdulich, P. and K. H. Wasseling (1990). "Reconstruction of brachial arterial pulsation from finger arterial pressure". In: *Engineering in Medicine and Biology Society, 1990., Proceedings of the Twelfth Annual International Conference of the IEEE*. IEEE, pp. 1046–1047.

Gizdulich, Paolo, Andriana Prentza, and Karel H. Wesseling (1997). "Models of brachial to finger pulse wave distortion and pressure decrement". In: *Cardiovascular research* 33.3, pp. 698–705.

Greimel, Patrick, Philipp Klaritsch, Holger Simonis, Bence Csapó, Maximilian Pohl, and Daniel Schneditz (2020). "Amniodrainage-Induced Circulatory Dysfunction in Women Treated for Twin-To-Twin Transfusion Syndrome". In: *Journal of Clinical Medicine* 9.7. DOI: 10.3390/jcm9072085.

Guelen, Ilja, Berend E. Westerhof, van der Sar, Gertrude L., Gert A. van Montfrans, Ferdinand Kiemeneij, Karel H. Wesseling, and Willem Jan W. Bos (2008). "Validation of brachial artery pressure reconstruction from finger arterial pressure". In: *Journal of hypertension* 26.7, pp. 1321–1327.

Gul, Ahmet, Halil Aslan, Ibrahim Polat, Altan Cebeci, Hasan Bulut, Ozturk Sahin, and Yavuz Ceylan (2003). "Natural history of 11 cases of twin-twin transfusion syndrome without intervention". In: *Twin Research and Human Genetics* 6.4, pp. 263–266. ISSN: 1369-0523. DOI: 10.1375/twin.6.4.263.

Hack, K. E. A., P. G. J. Nikkels, C. Koopman-Esseboom, J. B. Derks, S. G. Elias, van Gemert, M. J. C., and G. H. A. Visser (2008). "Placental Characteristics of Monochorionic Diamniotic Twin Pregnancies in Relation to Perinatal Outcome". In: *Placenta* 29.11, pp. 976–981. ISSN: 0143-4004. DOI: 10.1016/j.placenta.2008.08.019.

Hartung, J., R. Chaoui, and R. Bollmann (2000). "Amniotic fluid pressure in both cavities of twin-to-twin transfusion syndrome: a vote against septostomy". In: *Fetal Diagn Ther* 15.2, pp. 79–82. ISSN: 1015-3837. DOI: 10.1159/000020980.

Hee, Lene (2014). "Overview of the methods available for biomechanical testing of the uterine cervix in vivo". In: *Acta obstetricia et gynecologica Scandinavica* 93.12, pp. 1219–1237. DOI: 10.1111/aogs.12483.

Jones, K., K. Tierney, B. H. Grubbs, J. D. Pruetz, J. Detterich, and R. H. Chmait (2012). *Fetoscopic Laser Photocoagulation of Feeding Vessels to a Large Placental Chorioangioma following Fetal Deterioration after Amnioreduction.*

Karnak, Ibrahim, Erkan Aksöz, Saniye Ekinci, Rüştü Onur, and F. Cahit Tanyel (2008). "Increased maternal intraabdominal pressure alters the contractile properties of fetal rabbit

bladder". In: *Journal of pediatric surgery* 43.9, pp. 1711–1717. DOI: 10.1016/j.jpedsurg.2008.01.025.

Katsura, Daisuke, Yuichiro Takahashi, Shigenori Iwagaki, Rika Chiaki, Kazuhiko Asai, Masako Koike, Shunsuke Yasumi, and Madoka Furuhashi (2018). "Changes in Intra-Amniotic, Fetal Intrathoracic, and Intraperitoneal Pressures with Uterine Contraction: A Report of Three Cases". In: *Case reports in obstetrics and gynecology* 2018, p. 4281528. ISSN: 2090-6684. DOI: 10.1155/2018/4281528.

Keulenaer, B. L. de, J. J. de Waele, B. Powell, and Malbrain, M. L. N. G. (2009). "What is normal intra-abdominal pressure and how is it affected by positioning, body mass and positive end-expiratory pressure?" In: *Intensive Care Medicine* 35.6, pp. 969–976. ISSN: 1432-1238. DOI: 10.1007/s00134-009-1445-0.

Al-Khan, A., M. Shah, M. Altabban, S. Kaul, K. Y. Dyer, M. Alvarez, and S. Saber (2011). "Measurement of intraabdominal pressure in pregnant women at term". In: *The Journal of reproductive medicine* 56.1-2, pp. 53–57. ISSN: 0024-7758.

Langewouters, G. J., K. H. Wesseling, and W. J. A. Goedhard (1984). "The static elastic properties of 45 human thoracic and 20 abdominal aortas in vitro and the parameters of a new model". In: *Journal of Biomechanics* 17.6, pp. 425–435.

Lewi, Liesbeth, Jacques Jani, Isaac Blickstein, Agnes Huber, Leonardo Gucciardo, Tim van Mieghem, Elisa Doné, Anne-Sophie Boes, Kurt Hecher, Eduardo Gratacós, Paul Lewi, and Jan Deprest (2008). "The outcome of monochorionic diamniotic twin gestations in the era of invasive fetal therapy: a prospective cohort study". In: *American Journal of Obstetrics and Gynecology* 199.5, 514.e1–8. ISSN: 0002-9378. DOI: 10.1016/j.ajog.2008.03.050.

Lopriore, E., Jan Deprest, F. Slaghekke, Dirk Oepkes, J. M. Middeldorp, Vandenbussche, F. P. H. A., and L. Lewi (2008). "Placental characteristics in monochorionic twins with and without twin anemia-polycythemia sequence". In: *Acta bio-medica: Atenei Parmensis* 112.4, pp. 753–758. ISSN: 0029-7844. DOI: 10.1097/aog.0b013e318187e1ff.

Lougheed, Jane, Brian G. Sinclair, Karen Fung Kee Fung, Jean-Luc Bigras, Greg Ryan, Jeffrey F. Smallhorn, and Lisa K. Hornberger (2001). "Acquired right ventricular outflow tract obstruction in the recipient twin in twin-twin transfusion syndrome". In: *Journal of the American College of Cardiology* 38.5, pp. 1533–1538. ISSN: 0735-1097. DOI: 10.1016/s0735-1097(01)01549-2.

Malbrain, Manu L. N. G. (2004). "Different techniques to measure intra-abdominal pressure (IAP): time for a critical re-appraisal". In: *Intensive Care Medicine* 30.3, pp. 357–371. ISSN: 1432-1238. DOI: 10.1007/s00134-003-2107-2.

Malbrain, Manu L. N. G., Michael L. Cheatham, Andrew Kirkpatrick, Michael Sugrue, Michael Parr, Jan de Waele, Zsolt Balogh, Ari Leppäniemi, Claudia Olvera, Rao Ivatury, Scott D'Amours, Julia Wendon, Ken Hillman, Kenth Johansson, Karel Kolkman, and Alexander Wilmer (2006). "Results from the International Conference of Experts on Intra-abdominal Hypertension and Abdominal Compartment Syndrome. I. Definitions". In: *Intensive Care Medicine* 32.11, pp. 1722–1732. ISSN: 1432-1238. DOI: 10.1007/s00134-006-0349-5. URL: https://doi.org/10.1007/s00134-006-0349-5.

Neal, Randall H. and Richard C. Neal (2002). "Apparatus for measuring intrauterine pressure and fetal heart rate and method for using same".

Nicolini, Umberto, Nicholas M. Fisk, David G. Talbert, Charles H. Rodeck, Neil K. Kochenour, Pantaleo Greco, Corinne Hubinont, and Joaquin Santolaya (1989). "Intrauterine manometry: Technique and application to fetal pathology". In: *Prenatal Diagnosis* 9.4, pp. 243–254. ISSN: 01973851. DOI: 10.1002/pd.1970090404.

Paramore, R. H. (1913). *The intra-abdominal pressure in pregnancy.*

Penaz, J. (1976). "Beitrag zur fortlaufenden indirekten Blutdruckmessung". In: *Z Ges Inn Med Grenzgeb* 31, pp. 1030–1033.

Quintero, R. A., L. F. Quintero, W. J. Morales, M. Allen, and P. W. Bornick (1998). "Amniotic fluid pressures in severe twin-twin transfusion syndrome". In: *Prenatal and Neonatal Medicine* 3.6, pp. 607–610. ISSN: 1359-8635.

Quintero, Rubén A., Walter J. Morales, Mary H. Allen, Patricia W. Bornick, Patricia K. Johnson, and Michael Kruger (1999). "Staging of twin-twin transfusion syndrome". In: *Journal of Perinatology* 19.8, p. 550. ISSN: 0743-8346. DOI: 10.1038/sj.jp.7200292.

Rodeck, Charles H., Boaz Weisz, Donald M. Peebles, and Eric Jauniaux (2006). "Hypothesis: the placental 'steal' phenomenon - a possible hazard of amnioreduction". In: *Fetal Diagn Ther* 21.3, pp. 302–306. ISSN: 1015-3837. DOI: 10.1159/000091361.

Ross, M. G. and R. A. Brace (2001). "National Institute of Child Health and Development Conference summary: Amniotic fluid biology - basic and clinical aspects". In: *The Journal of Maternal-Fetal & Neonatal Medicine* 10.1, pp. 2–19. ISSN: 1476-7058. DOI: 10.1080/jmf.10.1.2.19.

Sanchez, Noel C., Patty L. Tenofsky, Jonathan M. Dort, and Luke Y. Shen (2001). "What is normal intra-abdominal pressure?/Discussion". In: *The American surgeon* 67.3, p. 243. ISSN: 0003-1348.

Sawchuck, Diane J. and Bernd K. Wittmann (2014). "Pre-eclampsia renamed and reframed: Intra-abdominal hypertension in pregnancy". In: *Medical hypotheses* 83.5, pp. 619–632. DOI: 10.1016/j.mehy.2014.08.001.

Sideris, I. G. and K. H. Nicolaides (1990). "Amniotic fluid pressure during pregnancy". In: *Fetal Diagn Ther* 5.2, pp. 104–108. ISSN: 1015-3837. DOI: 10.1159/000263555.

Simpson, Lynn L. (2013). "Twin-twin transfusion syndrome". In: *American Journal of Obstetrics and Gynecology* 208.1, pp. 3–18. ISSN: 0002-9378. DOI: 10.1016/j.ajog.2012.10.880.

Simpson, Lynn L., Gerald R. Marx, Eman A. Elkadry, and Mary E. Dalton (1998). "Cardiac dysfunction in twin-twin transfusion syndrome: a prospective, longitudinal study: A Prospective, Longitudinal Study". In: *Acta bio-medica: Atenei Parmensis* 92.4, Part 1, pp. 557–562. ISSN: 0029-7844. DOI: 10.1016/s0029-7844(98)00220-8.

Sinding, Marianne, David A. Peters, Jens B. Frøkjær, Ole B. Christiansen, Niels Uldbjerg, and Anne Sørensen (2016). "Reduced placental oxygenation during subclinical uterine contractions as assessed by BOLD MRI". In: *Placenta* 39, pp. 16–20. ISSN: 0143-4004. DOI: 10.1016/j.placenta.2015.12.018.

Sugermann, H., A. WINDSOR, M. BESSOS, and L. WOLFE (1997). "Intra-abdominal pressure, sagittal abdominal diameter and obesity comorbidity". In: *Journal of Internal Medicine* 241.1, pp. 71–79. ISSN: 0954-6820. DOI: 10.1046/j.1365-2796.1997.89104000.x.

Talbert, David G., Rekha Bajoria, Waldo Sepulveda, Sarah Bower, and Nicholas M. Fisk (1996). "Hydrostatic and osmotic pressure gradients produce manifestations of fetofetal transfusion syndrome in a computerized model of monochorial twin pregnancy". In: *American Journal of Obstetrics and Gynecology* 174.2, pp. 598–608. ISSN: 0002-9378. DOI: 10.1016/S0002-9378(96)70434-9.

Tanyel, F. C. (2000). "Urinary tract anomalies and dysfunctional voiding: a spectrum dictated by the influence of amniotic pressure upon fetal urodynamics". In: *Medical hypotheses* 54.1, pp. 140–145. DOI: 10.1054/mehy.1998.0819.

Umur, Asli, van Gemert, Martin J. C., and Peter G. J. Nikkels (2003). "Monoamniotic-versus diamniotic-monochorionic twin placentas: anastomoses and twin-twin transfusion syndrome". In: *American Journal of Obstetrics and Gynecology* 189.5, pp. 1325–1329. ISSN: 0002-9378. DOI: 10.1067/S0002-9378(03)00811-1.

Umur, Asli, van Gemert, Martin J. C., Michael G. Ross, A. Umur, M. J. van Gemert, and M. G. Ross (2001). "Amniotic fluid and hemodynamic model in monochorionic twin pregnancies and twin-twin transfusion syndrome". In: *American Journal of Physiology-*

Regulatory, Integrative and Comparative Physiology 280.5, R1499–R1509. DOI: 10.1152/ajpregu.2001.280.5.R1499.

van den Wijngaard, Jeroen P. H. M., Michael G. Ross, van der Sloot, Jos A. P., Yves Ville, and van Gemert, Martin J. C. (2005). "Simulation of therapy in a model of a nonhydropic and hydropic recipient in twin-twin transfusion syndrome". In: *American Journal of Obstetrics and Gynecology* 193.6, pp. 1972–1980. ISSN: 0002-9378.

van den Wijngaard, Jeroen P. H. M., Asli Umur, Raymond T. Krediet, Michael G. Ross, and van Gemert, Martin J. C. (2005). "Modeling a hydropic recipient twin in twin-twin transfusion syndrome". In: *American Journal of Physiology-Regulatory, Integrative and Comparative Physiology* 288.4, R799–R814. DOI: 10.1152/ajpregu.00635.2004.

van den Wijngaard, Jeroen P. H. M., Asli Umur, Michael G. Ross, and van Gemert, Martin J. C. (2008). "Twin-twin transfusion syndrome: mathematical modelling". In: *Prenatal Diagnosis: Published in Affiliation With the International Society for Prenatal Diagnosis* 28.4, pp. 280–291.

van den Wijngaard, Jeroen P. H. M., Berend E. Westerhof, Michael G. Ross, and van Gemert, Martin J. C. (2007). "A mathematical model of twin-twin transfusion syndrome with pulsatile arterial circulations". In: *American journal of physiology. Regulatory, integrative and comparative physiology* 292.4, R1519–31. ISSN: 0363-6119. DOI: 10.1152/ajpregu.00534.2006.

van Gemert, M.J.C. and H.J.C.M. Sterenborg (1998). "Haemodynamic model of twin-twin transfusion syndrome in monochorionic twin pregnancies". In: *Placenta* 19.2-3, pp. 195–208. ISSN: 0143-4004. DOI: 10.1016/S0143-4004(98)90009-1.

Waele, J. de, P. Pletinckx, S. Blot, and E. Hoste (2006). "Saline volume in transvesical intra-abdominal pressure measurement: enough is enough". In: *Intensive Care Medicine* 32.3, pp. 455–459. ISSN: 1432-1238. DOI: 10.1007/s00134-005-0062-9.

Waele, J. J. de, E. Billiet, E. Hoste, and F. Colardyn (2004). "The assumed problem of air bubbles in the tubing during intra-abdominal pressure measurement". In: *Intensive Care Medicine* 30.8, 1692, author reply 1693. ISSN: 1432-1238. DOI: 10.1007/s00134-004-2341-2.

Weiner, Carl P., Joni Heilskov, Gay Pelzer, Stanley Grant, Katharine Wenstrom, and Roger A. Williamson (1989). "Normal values for human umbilical venous and amniotic fluid pressures and their alteration by fetal disease". In: *American Journal of Obstetrics and Gynecology* 161.3, pp. 714–717. ISSN: 0002-9378. DOI: 10.1016/0002-9378(89)90387-6.

Wesseling, K. H., B. De Wit, GMA. Van der Hoeven, J. Van Goudoever, and JJ. Settels (1995). "Physiocal, calibrating finger vascular physiology for Finapres". In: *Homeostasis* 36, pp. 67–82.

Wesseling, K. H., Jansen, J. J. Settels, and J. J. Schreuder (1993). "Computation of aortic flow from pressure in humans using a nonlinear, three-element model". In: *Journal of applied physiology* 74.5, pp. 2566–2573.

Wray, S. (1993). "Uterine contraction and physiological mechanisms of modulation". In: *The American journal of physiology* 264.1 Pt 1, pp. C1–18. ISSN: 0002-9513. DOI: 10.1152/ajpcell.1993.264.1.C1.

Wray, S., T. Burdyga, D. Noble, K. Noble, L. Borysova, and S. Arrowsmith (2015). "Progress in understanding electro-mechanical signalling in the myometrium". In: *Acta physiologica (Oxford, England)* 213.2, pp. 417–431. DOI: 10.1111/apha.12431.

Yol, S., A. Kartal, S. Tavli, and Y. Tatkan (1998). "Is urinary bladder pressure a sensitive indicator of intra-abdominal pressure?" In: *Endoscopy* 30.9, pp. 778–780. ISSN: 0013-726X. DOI: 10.1055/s-2007-1001421.

6 Appendix

6.1 Tables

Table 7: Minimum intrauterine pressure

	IUP (mmHg)				
Amnioreduction (ml)	A	B	C	E	Mean
0	26.9		18.2	32.2	25.7
200	25.7	21.8		26.2	24.6
400	20.4	17.7	18.7	22.1	19.7
600	20.4	21.7	15.4	23.3	20.2
800	16.7	16.1	14.7	23.4	17.7
1000	16.4	15.3	14.3	25.8	17.9
1200	18.1	16.6	15.0	21.0	17.7
1400	15.1	10.9	14.0	22.5	15.6
1600			12.0	21.4	16.7
1800				21.6	21.6
2000				22.0	22.0
2200				17.5	17.5
2400				16.8	16.8
2600				16.3	16.3
2800				19.2	19.2
3000				16.4	16.4

Table 8: Change in intrauterine pressure after amnioreduction

	δIUP_{cont} (mmHg)				
Amnioreduction (ml)	A	B	C	E	Mean
0	14.2		8.4	9.2	10.6
200	7.6	20.7		13.8	14.0
400	7.2	22.2	6.6	16.9	13.2
600	16.4	22.5	2.4	18.4	14.9
800	25.4	23.9	2.9	16.1	17.1
1000	18.4	16.4	25.8	26.4	21.8
1200	19.8	20.4	21.9	28.7	22.7
1400	48.8	34.3	16.7	22.8	30.6
1600			1.6	37.2	19.4
1800				32.0	32.0
2000				28.1	28.1
2200				28.7	28.7
2400				36.5	36.5
2600				37.3	37.3
2800				22.3	22.3
3000				33.6	33.6

* Based on minimum and maximum values

Table 9: Duration of intrauterine pressure rises after amnioreduction

	$tIUP_{cont}$ (s)				
Amnioreduction (ml)	A	B	C	E	Mean
0					
200		29.2			29.2
400		17.5		67.9	42.7
600	69.8			75.4	72.6
800	51.5	36.5		105.6	64.5
1000	42.3	52.3	50.7	52.3	49.4
1200	63.6	32.9	63.5	53.3	53.3
1400	50.9	45.9	46.4	64.9	52.0
1600				61.5	61.5
1800				47.8	47.8
2000				74.1	74.1
2200				59.7	59.7
2400				71.0	71.0
2600				78.9	78.9
2800				56.8	56.8
3000				83.7	83.7

* Based on minimum and maximum values

Table 10: Minimum intraabdominal pressure

	IAP (mmHg)				
Amnioreduction (ml)	A	B	C	E	Mean
0	9.1		16.5	15.6	13.7
200	8.9	12.3		15.7	12.3
400	6.8	10.6	15.2	15.2	11.9
600	9.0	9.8	13.6	16.2	12.2
800	7.8	8.9	12.9	15.5	11.3
1000	7.0	8.7	13.6	15.0	11.1
1200	7.0	5.8	11.9	13.8	9.6
1400	5.1	7.0	11.5	15.2	9.7
1600			11.1	12.2	11.6
1800				14.5	14.5
2000				13.4	13.4
2200				12.6	12.6
2400				12.0	12.0
2600				11.7	11.7
2800				12.6	12.6
3000				13.7	13.7

* Based on minimum values

Table 11: Placental perfusion pressure

	PPP (mmHg)				
Amnioreduction (ml)	A	B	C	E	Mean
0	40.6		73.2	55.7	56.5
200	48.5	46.7		60.7	52.0
400	60.4	52.0	72.9	70.9	64.0
600	45.2	39.6	77.0	67.1	57.2
800	40.5	45.8	80.2	77.3	60.9
1000	50.6	55.3	58.2	62.0	56.5
1200	50.0	50.9	65.9	63.5	57.6
1400	25.1	43.3	66.8	72.0	51.8
1600			80.6	59.4	70.0
1800				56.8	56.8
2000				61.1	61.1
2200				66.3	66.3
2400				60.5	60.5
2600				62.4	62.4
2800				72.3	72.3
3000				66.1	66.1

* Based on minimum values

6.2 Equipment List

Table 12: Equipment list

Type	Device Name	Manufacturer	Country
Transducer set (2x)	T100214A	Edwards Lifesciences LLC	US
Intraabdominal Monitoring set	CA-0200	Biometrix BV	The Netherlands
500 mL 0,9% saline solution (2x)	freeflex® K929525	Fresenius Kabi Deutschland GmbH	Germany
Pressure infusion cuff (2x)	C-Fusor® 500 MX4805	Smiths Medical	US
Transducer clamp		Edwards Lifesciences	US
Isolation transformer	ERT 230/230/4G	Thalheimer Transformatorenwerke GmbH	Germany
Finometer	Finometer Model 1	Finapres Medical Systems BV	The Netherlands
Analog Signal I/O	Signal Converter	Finapres Medical Systems BV	The Netherlands
PowerLab 4/20	ML840	AD Instruments Pty Ltd.	New Zealand
BP Amp (2x)	FE117	AD Instruments Pty Ltd.	New Zealand
BP Transducer (2x)	DPT-200	Utah Medical Products Inc	US
Sensor Connection 8 m (2x)		AD Instruments Pty Ltd.	New Zealand
PC with LabChart Version 7		AD Instruments Pty Ltd.	New Zealand

6.3 Instructions for the Measuring System (German)

Anleitung für die kontinuierliche IAP/IUP Messung

Maximilian Pohl

Zusammenfassung

Dieses Dokument beschreibt den Aufbau und die Einstellungen, die für die standardisierte Durchführung der kontinuierlichen IAP (Intraabdominal pressure) & IUP (Intra-uterine pressure) Messung während eines Laser Eingriffes der zur Therapie des fetofetalen Transfusionssyndrom (twin-twin transfusion syndrome, TTTS) notwendig ist.

1 Vorbereitungen im Operationssaal

Damit es zu keinen Verzögerungen kommt, und die Operation planmäßig durchgeführt werden kann, sollte der Aufbau möglichst in genau der hier festgehaltenen Reihenfolge erfolgen, .
Der Turm mit den Messgeräten sollte sich generell auf der *linken* Seite der Patientin befinden, sodass es beim Aufbau und Anbringen des Finomteres zu keinen Schwierigkeiten kommt.
Bei allen Verbindungen ist zwingend darauf zu achten, dass sie blasenfrei mit der NaCl-Lösung gefüllt werden, damit eine korrekte Druckmessung garantiert werden kann!

2 Geräteliste

Typ	Gerätebezeichnung	Hersteller	Land
Transducerset Anästhesie (2x)	T100214A	Edwards Lifesciences LLC	USA
Intra-Abdominal Monitorset	CA-0200	Biometrix BV	Niederlande
500 mL 0,9%ige NaCl-Lösung (2x)	freeflex® K929525	Fresenius Kabi Deutschland GmbH	Deutschland
Druckinfusionsmanschette (2x)	C-Fusor® 500 MX4805	Smiths Medical	USA
Transducer Klemme		Edwards Lifesciences	USA
Trenntransformator	ERT 230/230/4G	Thalheimer Transformatorenwerke GmbH	Deutschland
Finometer inkl. Manschetten	Finometer - model 1	Finapres Medical Systems BV	Niederlande
Analog Signal I/O	Signal Converter	Finapres Medical Systems BV	Niederlande
PowerLab 4/20	ML840	AD Instruments Pty Ltd.	Neuseeland
BP Amp (2x)	FE117	AD Instruments Pty Ltd.	Neuseeland
BP Transducer (2x)	DPT-200	Utah Medical Products Inc	USA
Sensor Verbindungskabel 8m (2x)		AD Instruments Pty Ltd.	Neuseeland
PC mit LabChart Software		AD Instruments Pty Ltd.	Neuseeland
Zollstock			Österreich

2.1 Finometer

Wichtig: Die Manschetten des Finometers sowie das „Frontend“ müssen am linken Arm der Patientin angebracht werden! Sie sollten weder mit Venenverweilkanülen, welche am rechten Arm gelegt werden sollten, noch mit der Blutdruckmanschette der Anästhesie kollidieren! Beide Arme der Patientin

sollten während der Operation abduziert auf einer Schiene liegen. Bevor der linke Arm der Patientin locker an der Schiene fixiert wird, sollten die Manschetten des Finometers angebracht werden. Die Manschettenanlage sollte noch vor der Installation des Harnkatheters stattfinden. Zusätzlich muss die Höhe (H in cm) vom Boden des Operationsraumes bis zu der mittleren Axillarlinie gemessen und notiert werden.

1. Die Armmanschette am Oberarm anlegen und darauf achten, dass die Markierung auf der Innenseite der Manschette auf der Arteria brachialis liegt. Anschließend die Manschette mit dem Finometer verbinden (CAVE: Bei *ALLEN* Drucksteckern beim Einstecken des Finometers unbedingt darauf achten, dass die roten Markierungspunkte auf Stecker und Steckdose miteinander übereinstimmen).

2. Das Frontend am Handgelenk fixieren, sodass das Gerät selbst auf der Arminnenseite liegt und die Steckdosen der Fingermanschette zur Hand ausgerichtet sind; am Finometer anschließen.

3. Die Fingermanschette am Mittelfinger (Phalanx media III) so anbringen, dass die Gummiränder den Finger dicht umschliessen und trotzdem nicht überlappen. Dabei muss der optische Sensor auf der lateral-palmaren Seiten des Fingers liegen (auf die richtige Größe der Fingermanschette achten: weiß - klein, braun - mittel, schwarz - groß). Dann die Fingermanschette an das Frontend anschließen .

4. Das Höhenausgleichmodul am Frontend anschließen und die beiden Sensoren miteinander verbinden, siehe Abbildung 1.

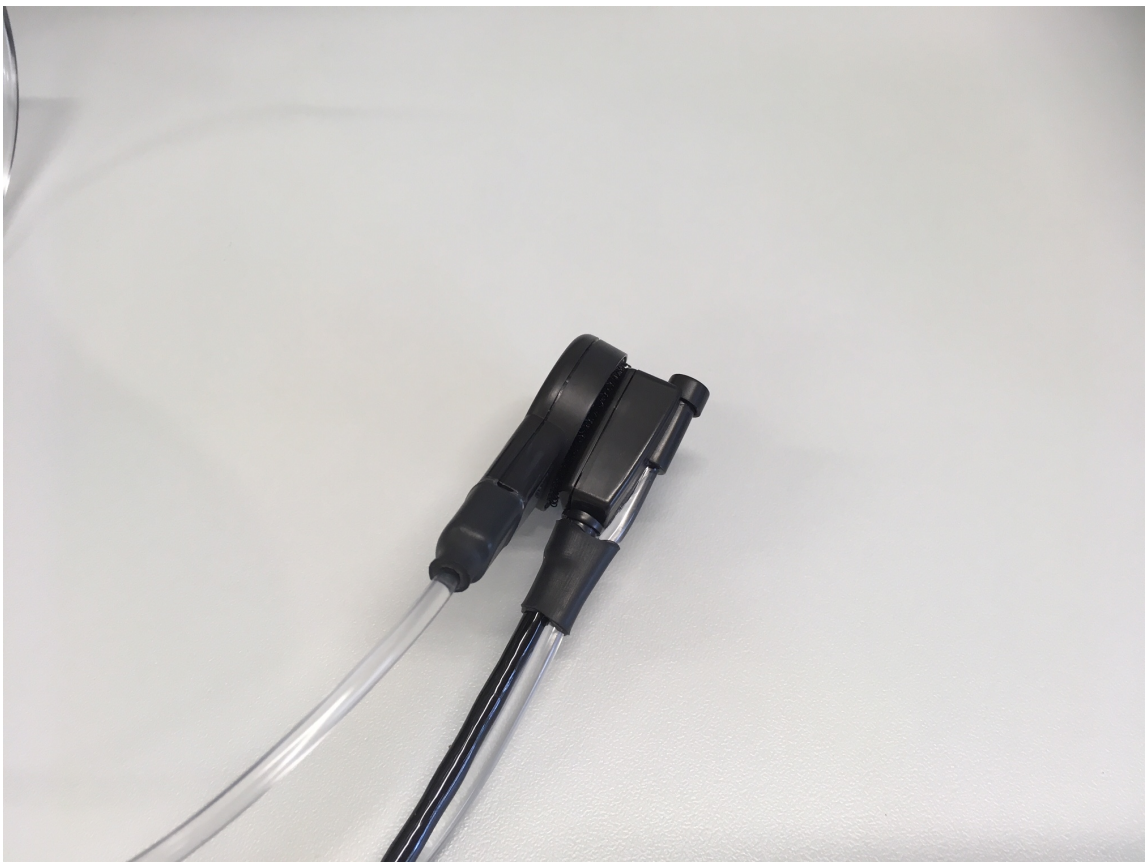

Abbildung 1: Die Position der beiden Höhensensoren während der Kalibrierung des Höhenausgleiches

5. Den linken Arm der Patientin, wenn möglich und von der Patientin toleriert, locker auf der Schiene fixieren, damit es zu keinen Höhenverschiebungen während der Messungen kommt.

6. Das Finometer einschalten.

Abbildung 2: Der Erste Bildschirm des Finometers nach dem Einschalten

7. Den „Finometer Research“ Modus auswählen (über die Tasten unterhalb des Bildschirmes).

Abbildung 3: Die Wahl der Konfiguration

8. Die Konfiguration „Red“ auswählen (über die Pfeiltasten markieren und mit der Taste „Mark“ bestätigen).

Abbildung 4: Der Bildschirm nach der Konfigurationswahl, in dem die Patientindateneingabe erfolgt

9. Die Patientindaten (Größe, Alter, Gewicht und Geschlecht) eingeben und die Taste unterhalb von „Describe subject“ drücken.
10. Die „Mark“ Taste drücken, um den Höhenabgleich durchzuführen (WICHTIG: Dieser Schritt muss *vor* Messbeginn durchgeführt werden)
11. Die beiden Höhensensoren an ihren vorgesehenen Orten anbringen (der schmale Sensor muss auf der Fingermanschette, der runde Sensor auf Herzhöhe an der Armmanschette angebracht werden)

2.2 Intra-abdominaler Druck, IAP

1. Das T-Stück des Intra-Abdominal Monitoring Set (*Biometrix BV*) so zwischen Harnblasendauerkatheter und Harnsack anbringen, wie es in Abbildung 5 dargestellt ist.
2. Den Harnblasendauerkatheter installieren, W2 in Richtung des Katheterausflusses öffnen.
3. Die Harnblase über den Katheter entleeren.
4. W2 in Richtung des Katheterausflusses schließen.
5. Die Vorbereitungen des Intra-Abdominal Monitoring Sets:

(a) W1 in Richtung des Transducersanschlusses schließen.

(b) 100 mL sterile 0,9%ige NaCL-Lösung an den Dorn (D1) des Intra-Abdominal Monitoring Set anschließen, den Spiegel damit füllen und an einem Infusionsständer aufhängen.

(c) Das Intra-Abdominal Monitoring Set und den Harnkatheter blasenfrei mit einer Flüssigkeitssäule befüllen: W1 dafür vollständig verschließen, die Spritze (S) aufziehen, W1 in Richtung des Katheters öffnen, W2 in Richtung des Katheter schließen und das gesamte Intra-Abdominal Monitoring Set mit Flüssigkeit befüllen.

(d) W1 komplett verschließen und die Spritze mit 50 mL aus dem Infusionsbeutel aufziehen.

(e) W1 in Richtung Transducer schließen und W2 in Richtung Harnsack schließen.

(f) 50 mL der 0,9%igen NaCL-Lösung aus der Spritze vorsichtig in die Blase abgeben.

6. Die Vorbereitungen des TruWave Drucksensorbesteckes (*Edwards Lifesciences*), um es mit dem Intra-Abdominal Monitoring Set zu verbinden:

   (a) 500 mL sterile 0,9%ige NaCL freeflex®-Lösung an den Dorn (D2) anschließen und in die blaue Öffnung des Infusionsbeutels stecken.

   (b) Den Infusionsbeutel in der C-Fusor® Druckinfusionsmanschette aufhängen und diese auf 300 mmHg Druck aufpumpen.

   (c) Die Kunststoffschläuche und das gesamte TruWave Drucksensorbesteck mit einer Flüssigkeitssäule befüllen, dabei W3 in Richtung des zusätzlichen Anschlusses geschlossen halten.

   (d) Den Infusionsbeutel abklemmen.

7. Den Edwards Transducer in der Transducer-Halterung (*Edwards Lifesciences*) mit Hilfe des Zollstockes auf der Höhe H an dem Infusionsständer fixieren. Die mittlere Axillarlinie soll dabei durch das Zentrum des Tranducer-Rohres verlaufen und die W3 Öffnung nach oben gerichtet sein.

8. Den Edwards Transducer mit dem Zentralvenendruck-Anschluss des Anästhesiemonitors verbinden.

9. W3 schließen und Edwards Transducer an dem Anästhesiemonitor auf Null setzen.

10. W3 in Richtung des Edwards Transducer öffnen und die Aufzeichnungen am Anästhesiemonitor beginnen.

11. Den BP Transducer von Utah mit Hilfe einer Spritze mit 0,9%iger NaCL-Lösung spülen.

12. Den BP Transducer von Utah blasenfrei mit dem TruWave Drucksensorbesteck verbinden, siehe Abbildung 5, und an das mit „IAP“ markierte Kabel von AD Instruments schließen.

13. W4 in Richtung des TruWave Drucksensorbesteckes schließen.

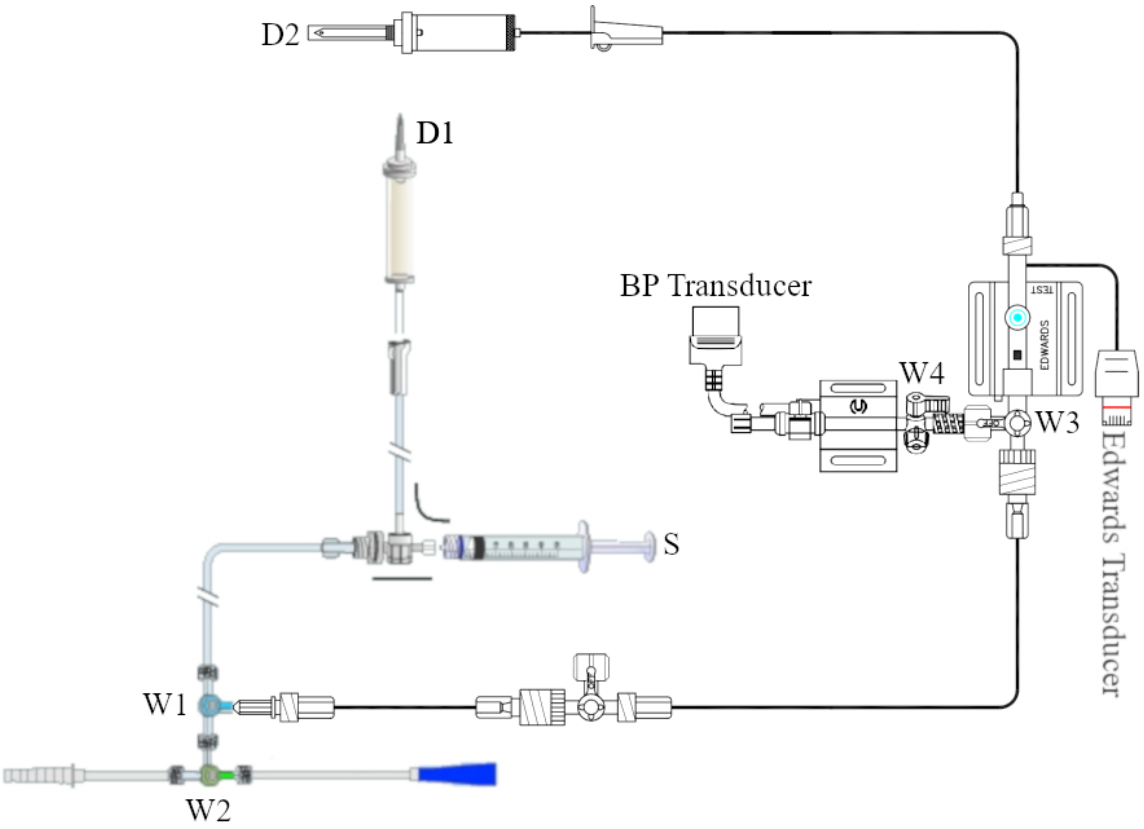

Abbildung 5: Schematischer Zusammenbau der Messkomponenten für die IAP Messung, bestehend aus den folgenden Komponenten: Intra-Abdominal Monitoring Set, BP Transducer & Edwards Transducer, sowie den vier 3-Wegehähnen W1-4

2.3 Intrauteriner Druck, IUP

Der IUP wird über den für die Operation notwendigen Fetoskopie-Trokar abgeleitet, sodass keine zusätzlichen Zugänge benötigt werden. Zu Beginn der Operation erhält die *sterile* OP-Schwester das TruWave Drucksensorbesteck (*Edwards Lifesciences*), wobei die Chirurgen das Transducer-Ende mit Dorn später an die Anästhesie übergeben. Im Anschluss muss das Drucksensorbesteck vorbereitet werden.

1. Die Vorbereitungen des TruWave Drucksensorbesteckes nach der Übergabe:

   (a) 500 mL sterile 0,9%ige NaCL freeflex®-Lösung an den Dorn (D1) anschließen und in die blaue Öffnung des Infusionsbeutels stecken.

   (b) Den Infusionsbeutel in der C-Fusor® Druckinfusionsmanschette aufhängen und diese auf 300 mmHg Druck aufpumpen.

   (c) Die Kunststoffschläuche und das gesamte TruWave Drucksensorbesteck mit einer Flüssigkeitssäule befüllen, dabei W1 in Richtung des zusätzlichen Anschlusses geschlossen halten.

   (d) Den Infusionsbeutel abklemmen.

2. Den Edwards Transducer in der Transducer-Halterung (*Edwards Lifesciences*) mit Hilfe des Zollstockes auf Höhe H der mittleren Axillarlinie der Patientin an dem Infusionsständer fixieren. Die mittlere Axillarlinie soll dabei durch das Zentrum des Tranducer-Rohres verlaufen und die W1 Öffnung nach oben gerichtet sein.

3. Den Edwards Transducer an den arteriellen Blutdruckanschluss des Anästhesiemonitores anschließen.

4. W1 schließen und den Edwards Transducer am Anästhesiemonitor auf Null setzen.

5. W1 in Richtung des Edwards Transducer öffnen und die Aufzeichnung am Anästhesiemonitor beginnen.

6. Den BP Transducer von Utah mit einer Spritze 0,9%iger NaCL-Lösung spülen.

7. Den BP Transducer von Utah blasenfrei mit dem TruWave Drucksensorbesteck verbinden, siehe Abbildung 6, und an das mit „IUP“ markierte Kabel von AD Instruments schließen.

8. W2 in Richtung des TruWave Drucksensorbesteck schließen.

9. Sobald die Chirurgen bereit sind das TruWave Drucksensorbesteck an den Schlauch des Fetoskopie-Trokar anzubringen, muss durch die Anästhesie über das Öffnen des blauen Gummiventiles des Edwards Transducer das gesamte Druckbesteck vollständig gespült werden.

10. Das blasenfreie Verbinden von TruWave Drucksensorbesteck und Fetoskopie-Trokar erfolgt durch die Chirurgen.

11. W1 komplett öffnen.

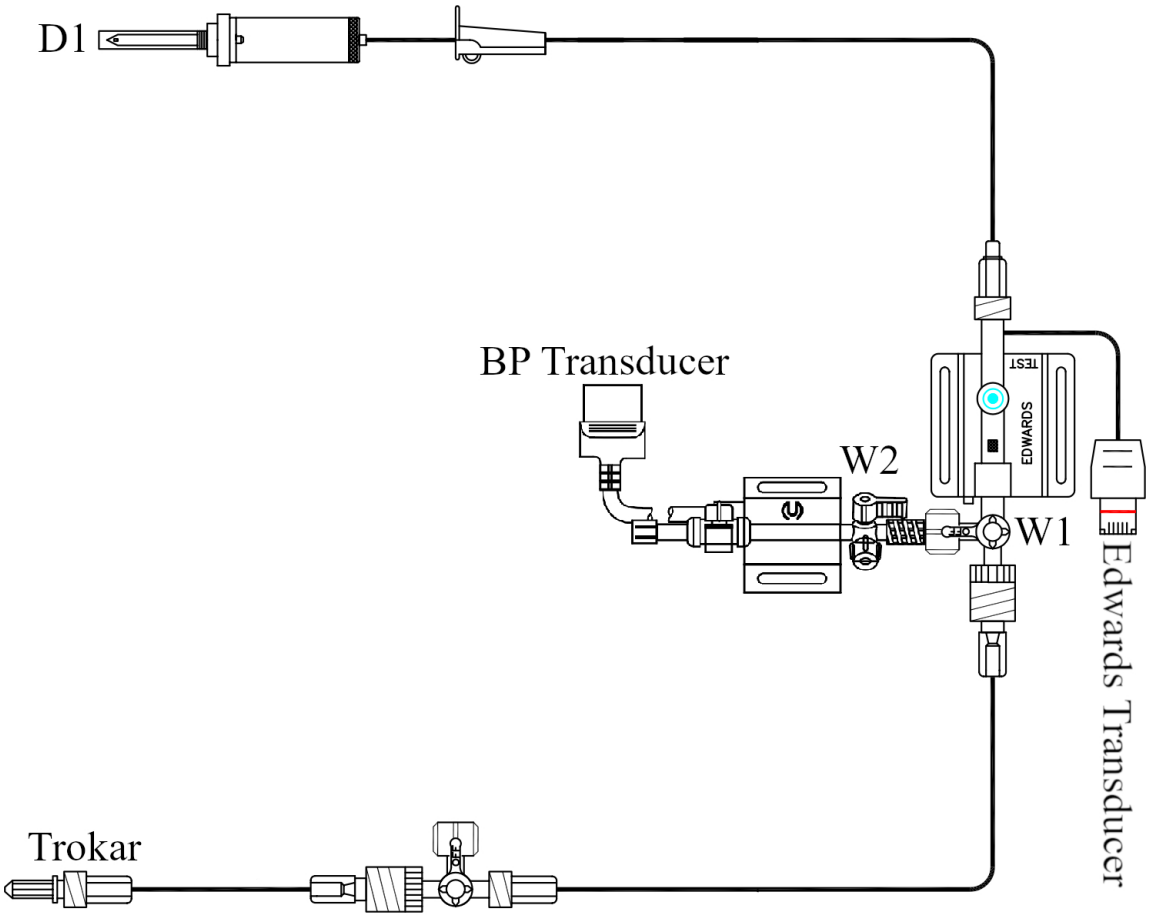

Abbildung 6: Schematischer Zusammenbau der Messkomponenten für die IUP Messung, bestehend aus den zwei Komponenten: BP Transducer & Edwards Transducer, sowie den zwei 3-Wegehähnen W1-2

3 Messungen am „Turm“

3.1 Netzanschluss über Trenntransformator

Um den Potentialausgleich und die Schutztrennung zu gewährleisten müssen alle Geräte über den Trenntransformator versorgt werden. Dafür muss der schwarze Netzstecker der Mehrfachdose an der linken Seite des Turmes an das Netz angeschlossen werden. Die Erdung des Trenntransformators muss gemeinsam mit der Erdung des OPs über das Erdungskabel erfolgen. Alle sich auf dem Turm befindlichen Geräte sind damit durch eine sichere galvanische Trennung von dem üblichen Stromkreis getrennt und auf gleichem Potential.

3.2 Finometer-Messung starten

Abbildung 7: Physiocal (siehe orangenes Feld links unten) zur Beurteilung der Messqualität

1. Physiocal Messqualität überprüfen.

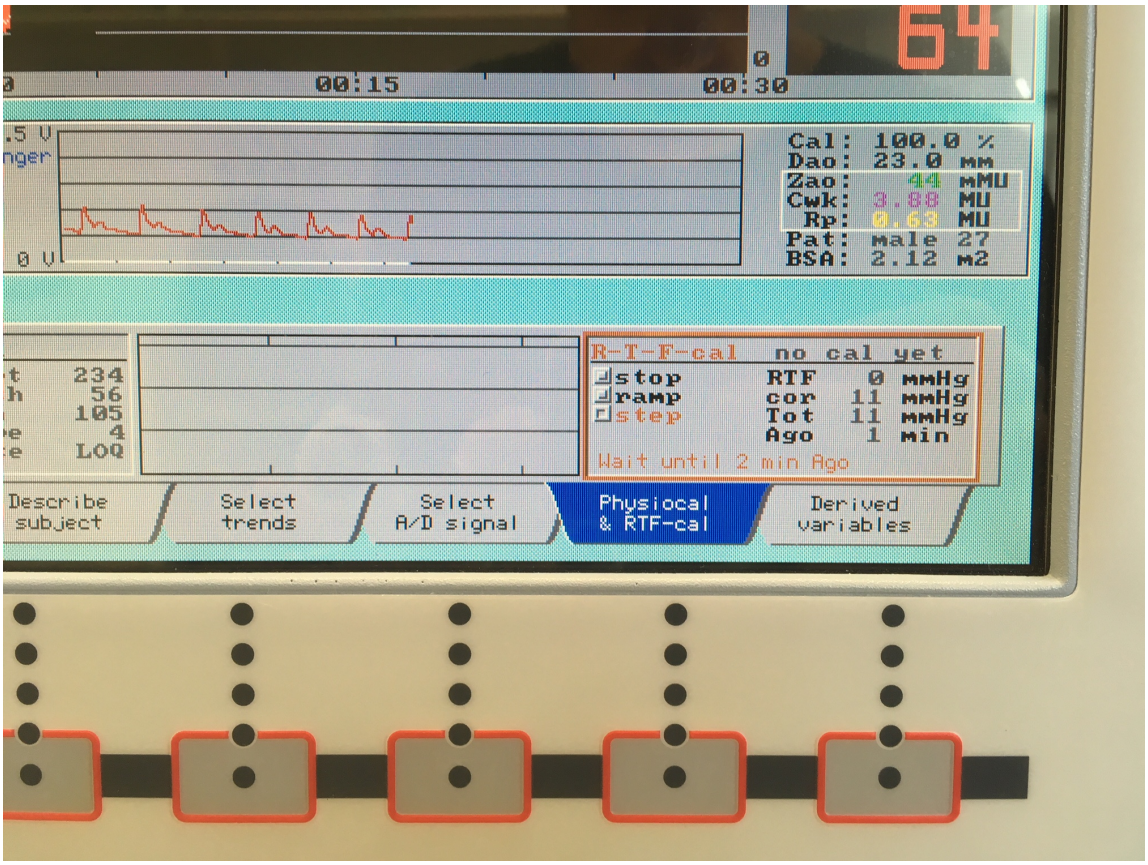

Abbildung 8: Kalibrierung der zyklischen Messkorrektur (siehe orangenes Feld rechts unten)

2. RTF-Kalibrierung auf „Step“ stellen. Falls eine hämodynamische Änderung (Veränderung der Armposition, Tischposition o.ä.) stattfindet, Kalibrierung erneut durchführen.

3. Aufzeichnung des Finometers mit „Start“ beginnen.

3.3 Anschluss der Transducer

1. Die Transducer über die weißen dazugehörigen (siehe Beschriftung auf den Steckern) Kabel mit dem Powerlab Gerät verbinden.

3.4 AD Instruments/Lab Chart 7

Vor dem Start des Laptops mit der installierten Lab Chart 7 Software muss das USB-Verbindungskabel (grau) für das Powerlab Gerät bereits im Laptop eingesteckt sein.

Abbildung 9: Lab Chart 7 starten

1. Lab Chart 7 auf dem Desktop starten.

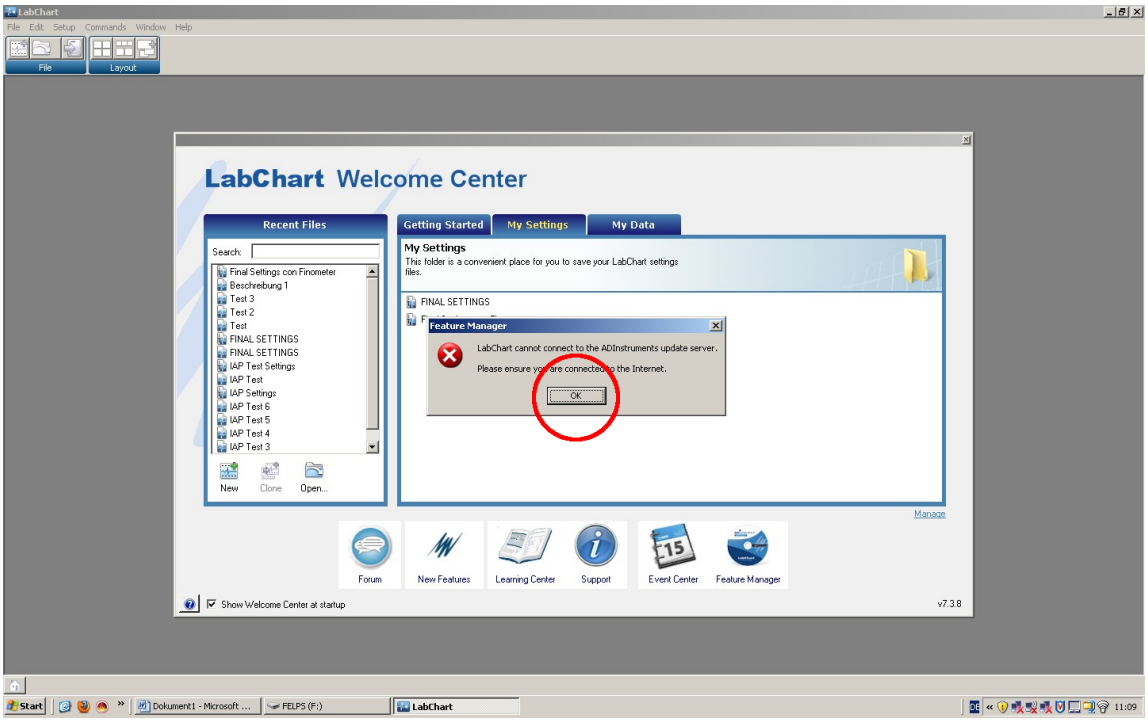

Abbildung 10: Fehlermeldung beim Start der Software

2. Die Fehlermeldung hat keine weiteren Bedeutungen und kann daher ignoriert werden. CAVE: Bitte PC auf keinen Fall mit dem Internet verbinden!

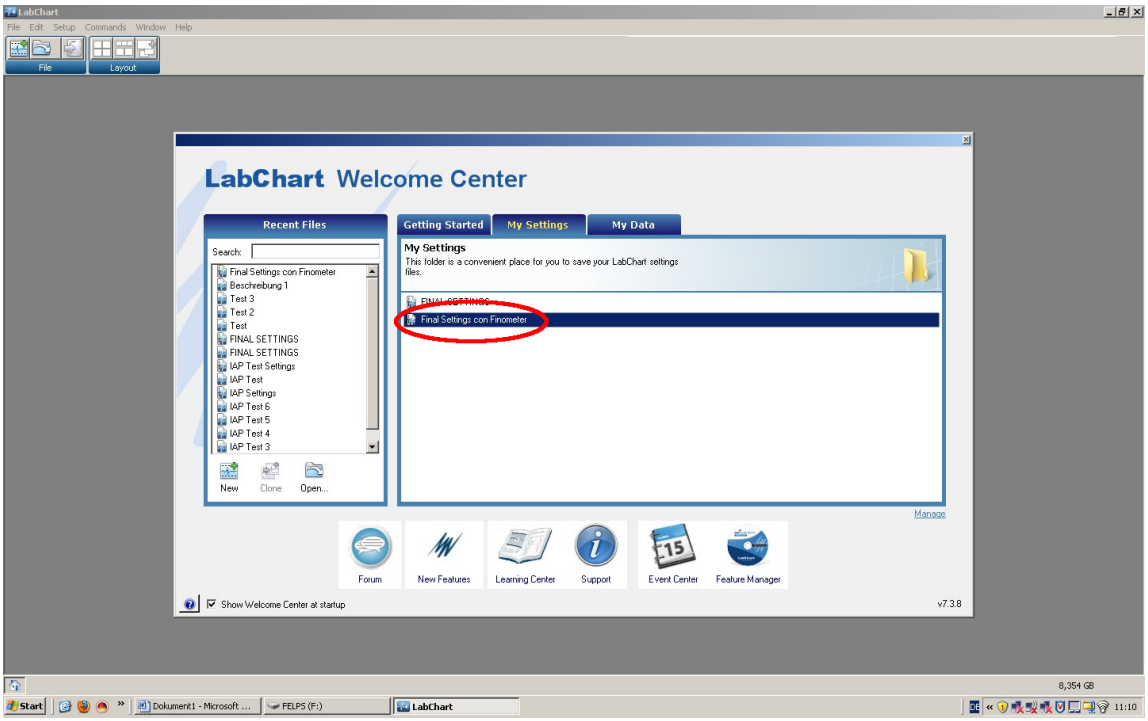

Abbildung 11: Auswahl der Voreinstellungen

3. Die Voreinstellungen „Final Settings con Finometer“ auswählen und laden.

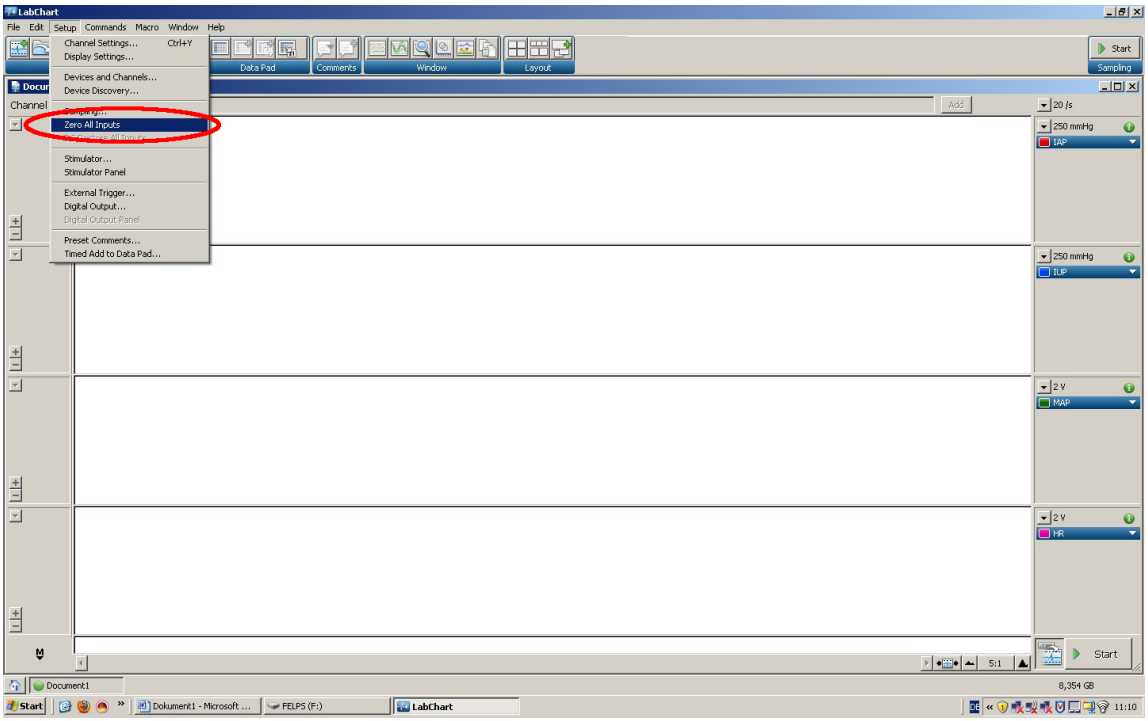

Abbildung 12: Nullsetzen der Transducer

4. Die eigentliche Aufzeichnung der Druckmessungen kann erst erfolgen, nachdem der IUP Verbindungsschlauch an die Transducer angeschlossen ist.

5. Kontrollieren, ob beide BP Transducer auf der gleichen Höhe H an dem Infusionsständer angebracht sind.

6. Beide 3-Wegehähne der BP Transducer zum Druckbesteck schließen und „Zero All Inputs“ bestätigen. Anschließend die 3-Wegehähne wieder in Richtung der Druckbestecke öffnen.

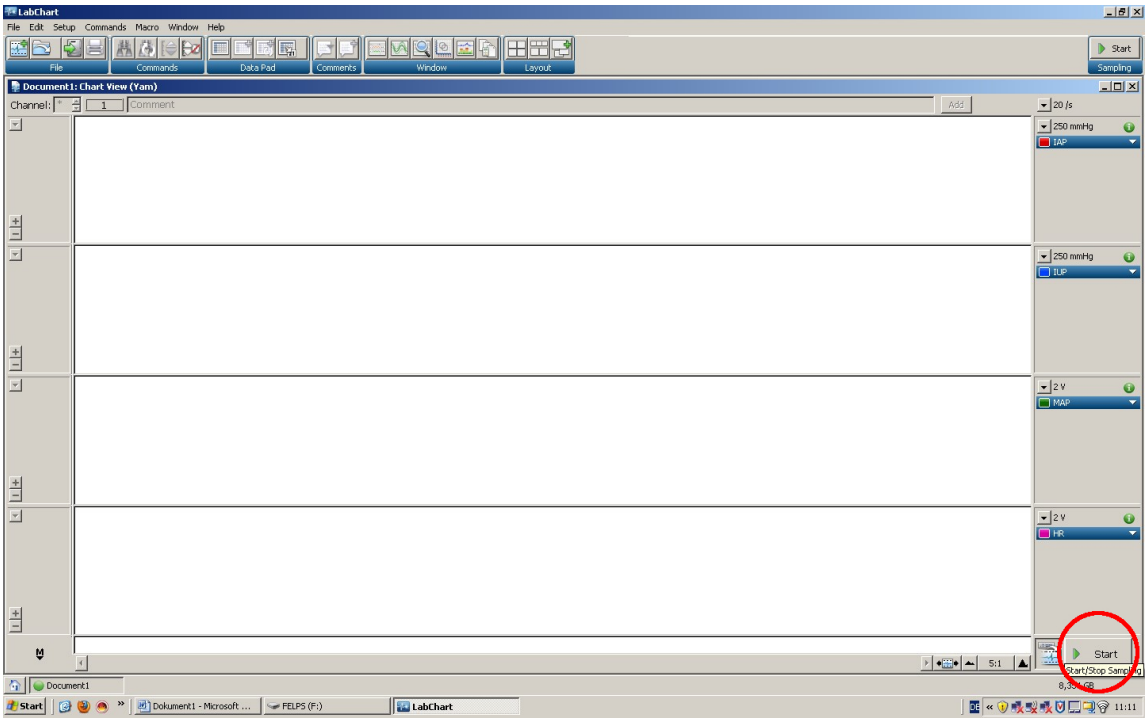

Abbildung 13: Beginnen der Aufzeichnung

7. Aufzeichnungen mit „Start“ beginnen.

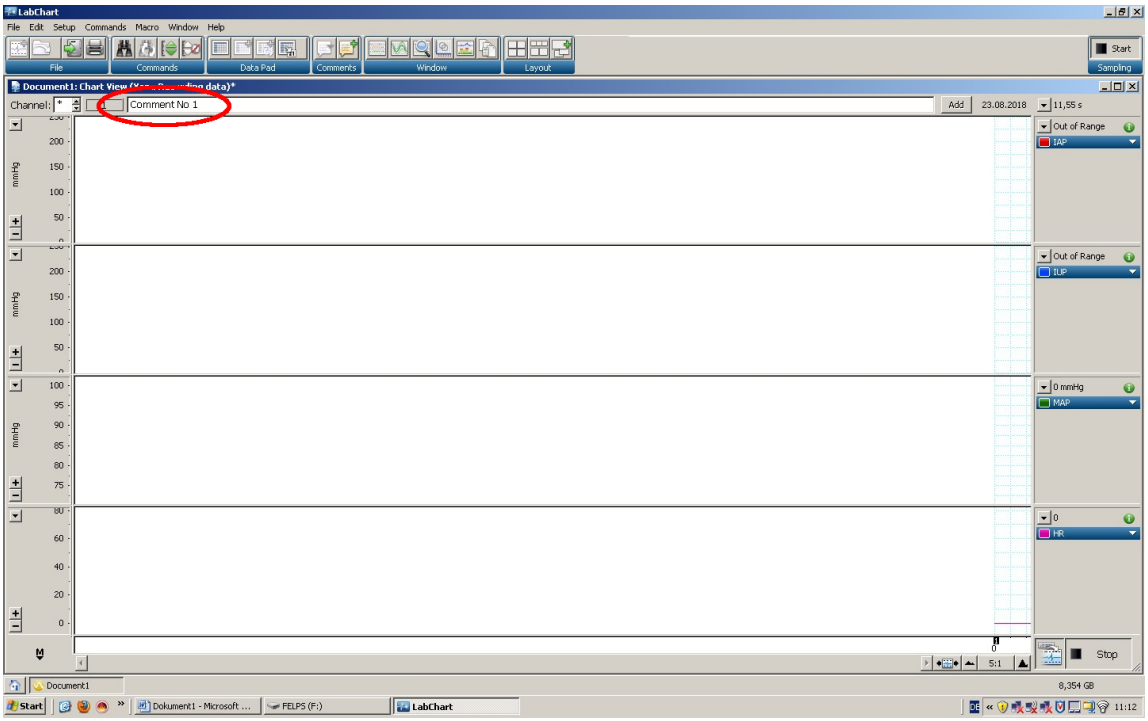

Abbildung 14: Kommentar einfügen

8. Besondere Ereignisse während des Eingriffes sowie Informationen zur Amniondrainage (Menge in mL) sollten stets mit Kommentaren festgehalten werden. Diese dafür mit Enter bestätigen. Sie werden automatisch auf dem Zeitstrahl festgehalten. Folgende Kommentare sind während der gesamten Amniondrainage an den jeweiligen Zeitpunkten wiederholt festzuhalten:

   (a) Drainage Volumen (ingesamt bereits entnommenes Volumen in mL).

   (b) Plazentadicke (mm).

   (c) „Hands-off“ in den Momenten, in denen die Chirurgen den Situs nicht berühren.

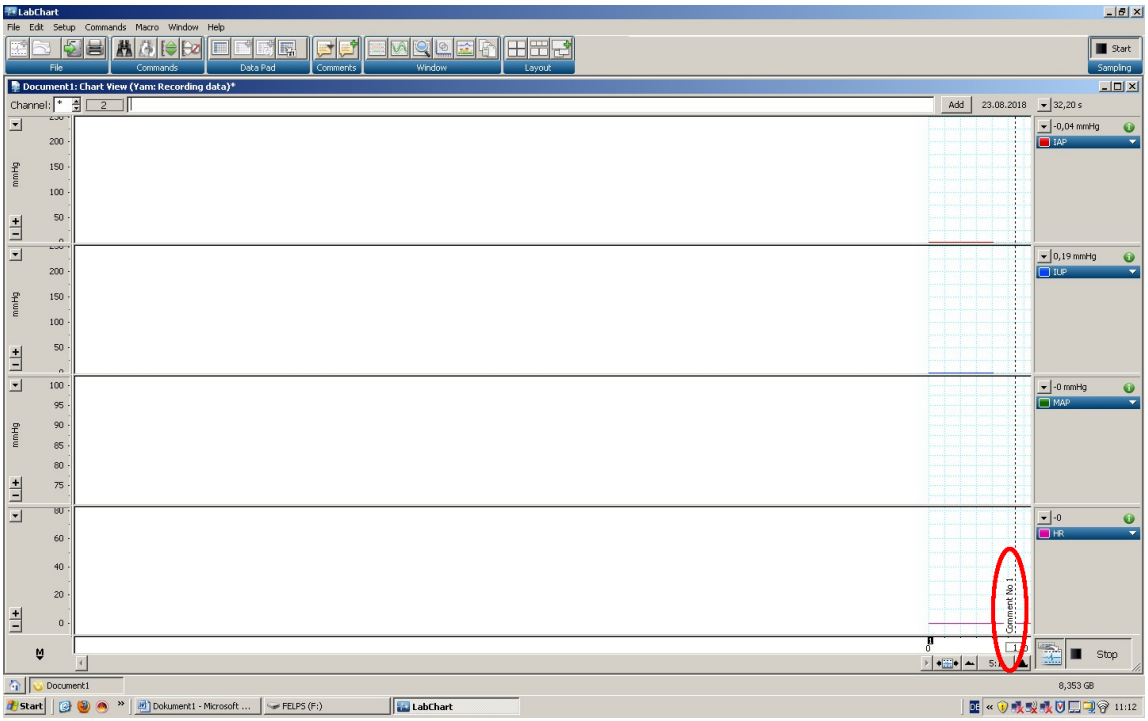

Abbildung 15: Erster Kommentar auf dem Zeitstrahl

9. Zu Beginn (während der ersten 20 Sekunden) erscheinen die Messungen zwar noch nicht, sie werden aufgrund des Filters später sichtbar.

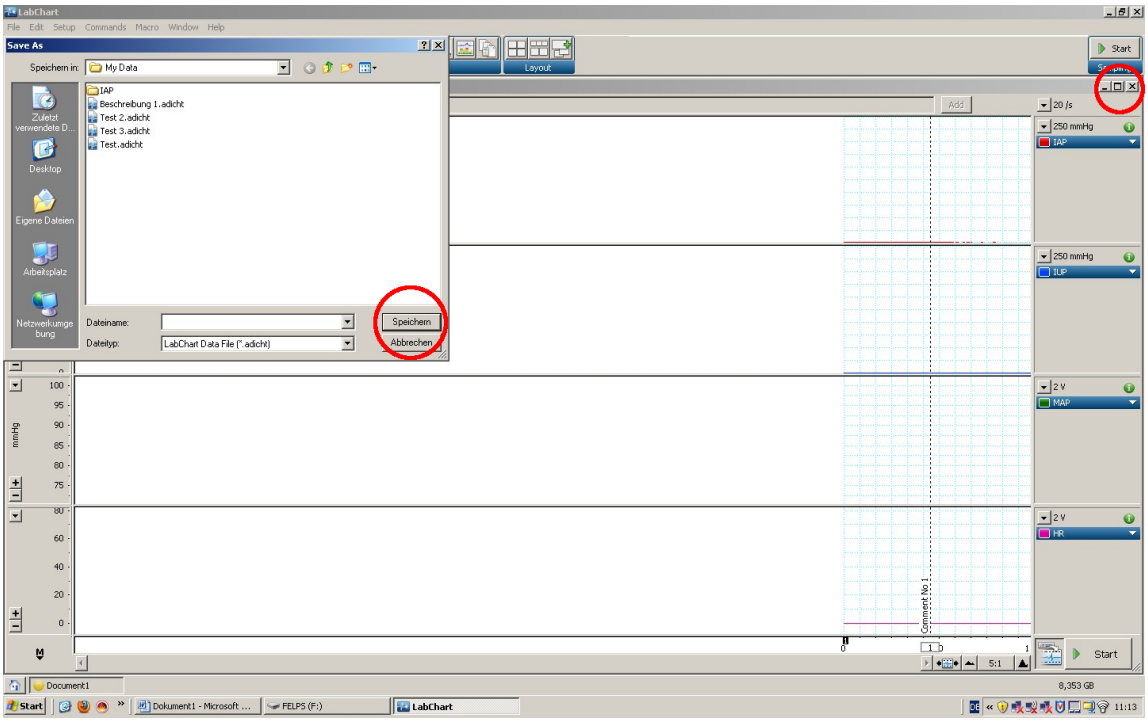

Abbildung 16: Sichern der Aufzeichnung

10. Aufzeichnung mit „Stop“ beenden und die Datei mit Datum (Format: YYMMDD) im Ordner „TTTS“ auf dem Desktop speichern. Über kleines „X“ zuerst das Dokument und danach das gesamte Programm schließen.

4 Abbau

CAVE: Um ein Platzen der Fingermanschette zu verhindern, ist beim Abbau der Geräte unbedingt darauf zu achten, dass das Finometer bereits seinen Messprozess beendet hat, bevor die Fingermanschette abgenommen wird (dafür die Stop Taste 2x betätigen).

5 Datenübertragung der Messungen des Finometers

Der Laptop muss mit dem Finometer über das „Finometer Link Cable“ verbunden werden.

1. Finometer einschalten.

2. Laptop hochfahren und „Finolink“ starten.

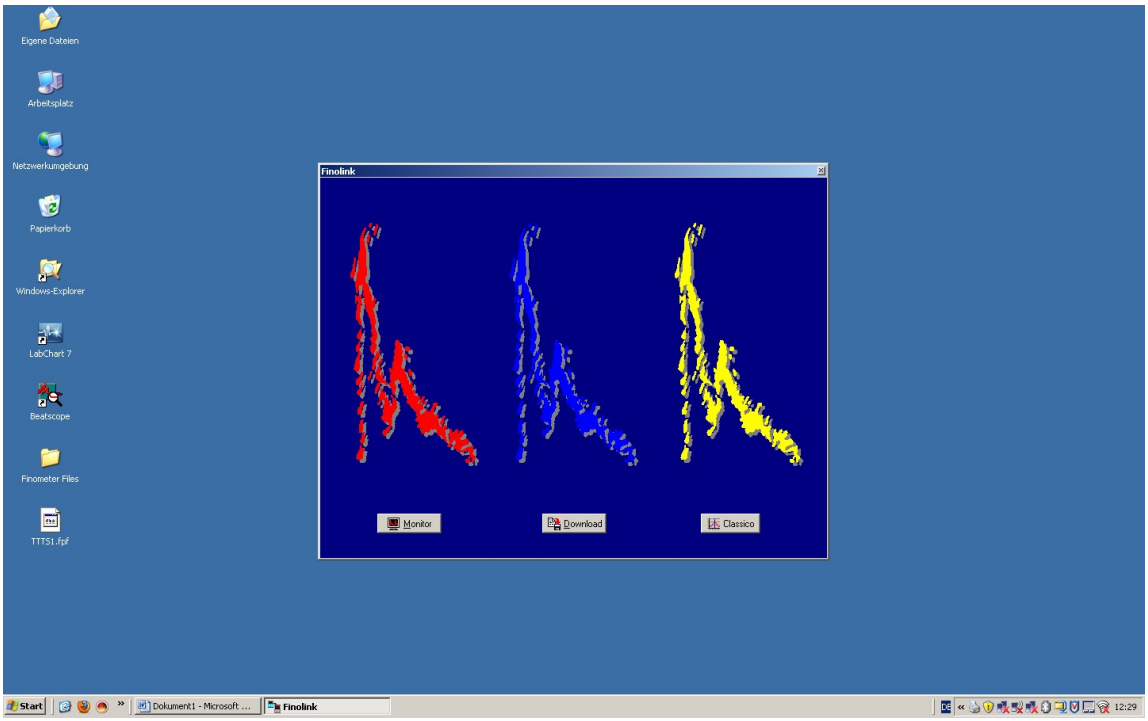

Abbildung 17: Finolink

3. Das „Download“ Menü auswählen

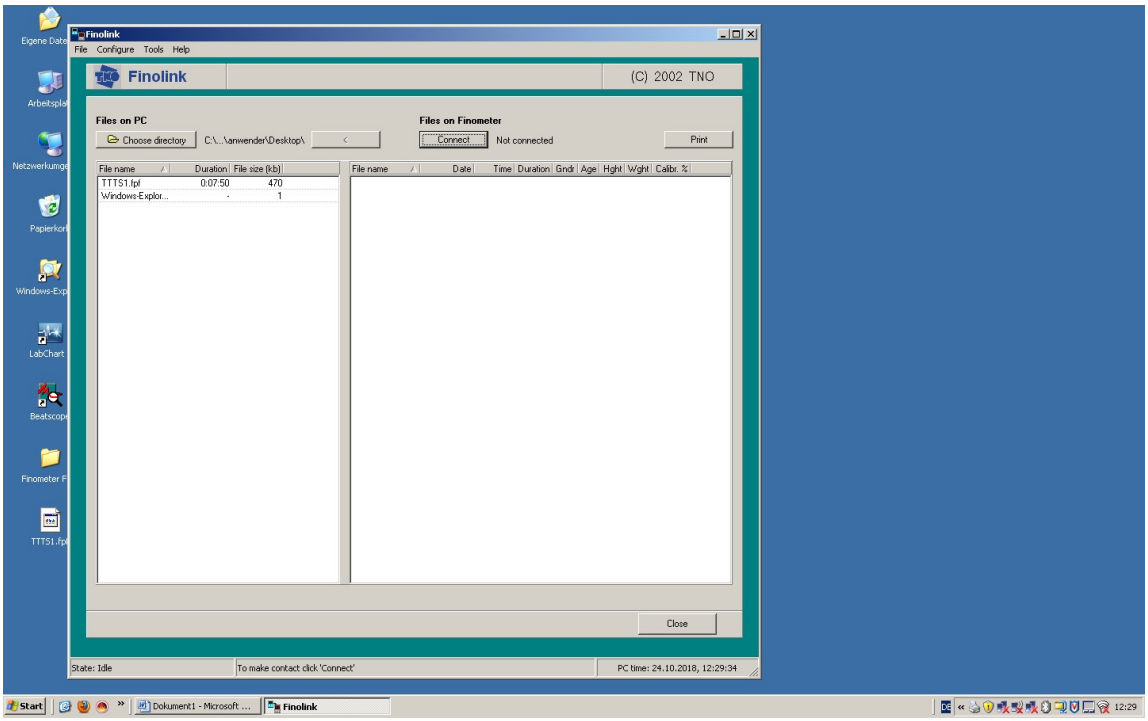

Abbildung 18: Datei auswählen

4. Finometer durch „Connect“ mit dem PC verbinden.

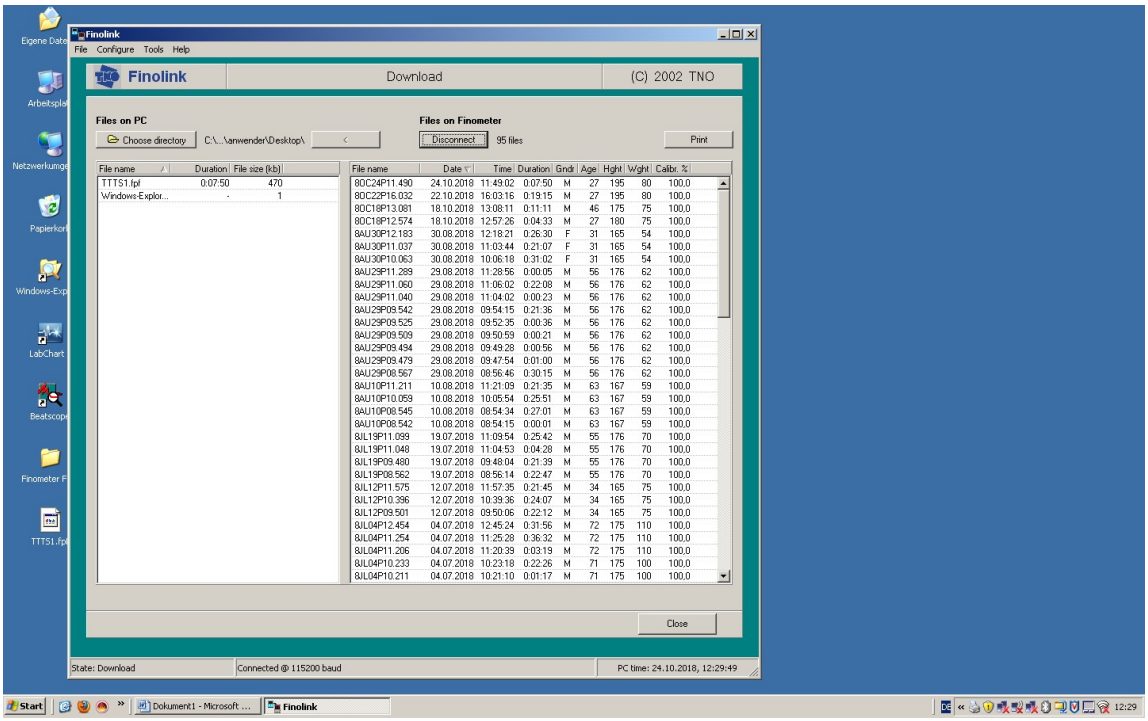

Abbildung 19: Liste der Messungen

5. Über das „Download“ Menü die aktuelle Aufzeichnung auswählen.

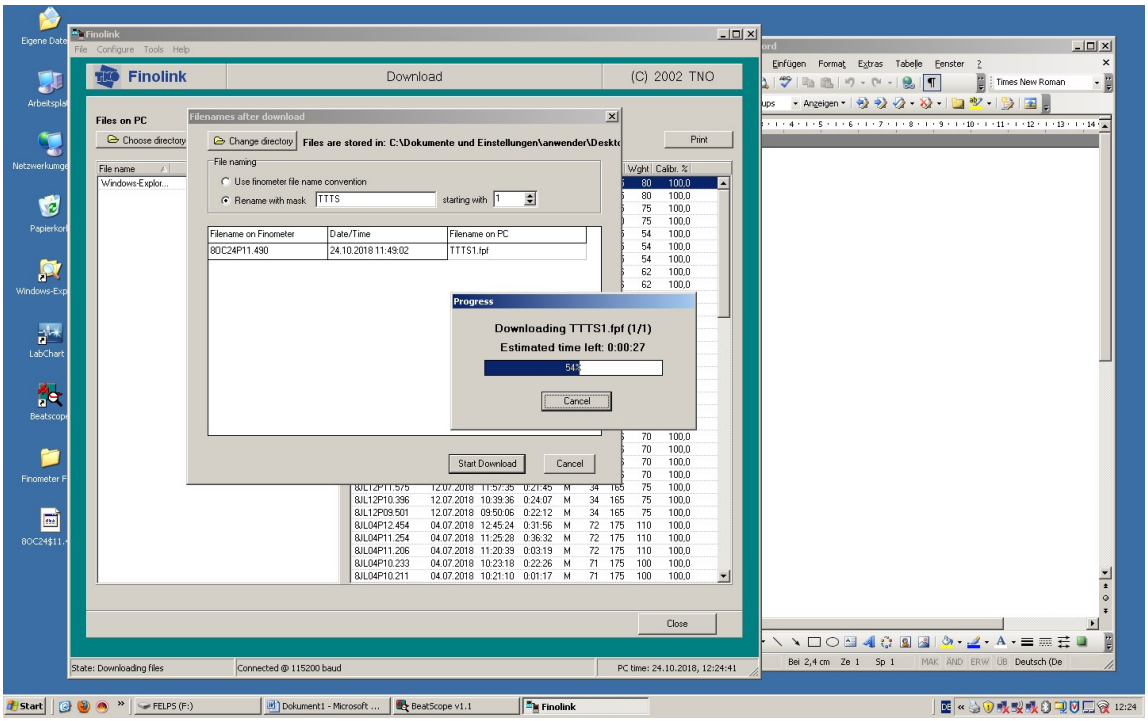

Abbildung 20: Download der Datei

6. Datei mit dem Datum (Format: YYMMDD) als Namen auf dem Laptop in dem Ordner „Finometer Files“ speichern.

7. Datei muss im Anschluss mit dem Programm „Beatscope“ in eine Exceldatei umgewandelt.